

CHARACTERIZATION OF THE MICROSECOND PULSED
GLOW DISCHARGE: A NOVEL SPECTROSCOPIC SOURCE

By

KRISTOFOR INGENERI

A DISSERTATION PRESENTED TO THE GRADUATE SCHOOL
OF THE UNIVERSITY OF FLORIDA IN PARTIAL FULFILLMENT
OF THE REQUIREMENTS FOR THE DEGREE OF
DOCTOR OF PHILOSOPHY

UNIVERSITY OF FLORIDA

2000

ACKNOWLEDGMENTS

I am deeply indebted to many individuals who have enriched my graduate experience and made this work possible. I have a deep respect for my advisor, Dr. W. W. Harrison. I am honored that I could work so closely with the laboratory of Dr. James D. Winefordner. These gentlemen have created a research atmosphere which has drawn me into contact with many brilliant individuals, many who are very highly regarded in their respective fields. Dr. Benjamin Smith is but one scholar who requires a special mention due to his active part in answering my incessant questions. I thank them.

This work would not have been possible if not for the efforts of several of my colleagues. Dr. Wei Hang was responsible for my training in glow discharge mass spectrometry and in graduate research as a whole. I would like to thank Dr. Xiaomei Yan and Dr. Chenglong Yang for contributing figures which supplemented my work and completed our characterization of the pulsed spectroscopic source. I would like to thank these three, not only for their efforts, but also for their friendship. I would also like to extend thanks to the members of the Harrison and Winefordner groups whom I have had the good fortune to meet. They have been an endless source of encouragement and amusement.

My family deserves a word of mention for shaping me into the person, and scientist, that I have become. The UF Aikido club served a pivotal role in keeping my

body fit and my mind agile. I would also like to thank my love, Dani Fallin, for holding my hand through all of this.

This work has been supported by the US Department of Energy, Basic Energy Sciences, Hewlett-Packard Laboratories, and LECO Corporation.

TABLE OF CONTENTS

	<u>page</u>
ACKNOWLEDGMENTS	ii
ABSTRACT	vii
 CHAPTERS	
1 INTRODUCTION.....	1
Solid Analysis Techniques	2
The Glow Discharge	4
The Microsecond Pulsed Glow Discharge	6
Overview	6
Summary.....	8
2 GLOW DISCHARGE PROCESSES	9
Glow Discharge Species	11
Glow Discharge Processes.....	11
Electrons	14
Argon	15
Sputtering	16
Sputtered Species.....	17
Spatial Zones in the Glow Discharge	20
The Cathode Glow Region	20
The Cathode Dark Space	21
The Negative Glow.....	22
3 POWERING THE GLOW DISCHARGE	26
Analytical Utility of the Glow Discharge.....	27
Atoms	27
Photons	29
Ions	30
Methods of Powering the Glow Discharge.....	31
Direct Current (dc) Glow Discharge.....	32

Radio Frequency (rf) Glow Discharge	34
Pulsed Glow Discharge	36
Advantages of the Microsecond Pulsed Glow Discharge.....	38
Enhanced Sputter Rates.....	38
Enhanced Atomic Emission	40
Enhanced Ionization	40
Temporal Resolution	40
Chemistry	41
Concluding Remarks	42
 4 EMISSION OF THE PULSED GLOW DISCHARGE	 43
Theory of Pulsing the Glow Discharge	43
Experimental	44
Temporal Considerations.....	48
Electrical Characteristics of the Pulsed Discharge	52
Parameter Studies of the Emission Signal.....	57
Additional Characteristics of the Pulsed Discharge	64
Frequency	64
Pulse Width	71
Results of Emission Studies	75
Enhancements in Emission Intensity.....	75
Temporal Effects	79
 5 PLASMA DIAGNOSTICS	 86
Absorption, Diffusion and Sputtering	86
Measurement of Rotational and Excitational Temperatures within the Plasma.....	99
Electrostatic Probe Measurements of the Glow Discharge Plasma.....	103
 6 MICROSECOND PULSED GLOW DISCHARGE TIME-OF-FLIGHT MASS SPECTROMETRY.....	 117
Introduction	117
Background	117
Experimental	119
Overview of Microsecond Pulsed GD TOFMS	122
Spectral Interferences	127
Temporal Resolution	127
Factors Affecting Temporal Resolution	129
Parameters Studied	133
Parameter Studies of the Pulsed GD TOFMS	137
Voltage Studies	139
Effect of Pressure.....	147
Summary of Parametric Study Results.....	153

Mass Spectral Results.....	155
Relative Sensitivity Factors.....	166
Isotope Ratios	170
Trace Analysis and Detection Limits	170
 7 INTRODUCTION TO LASER ABLATION SAMPLING INTO A PULSED GLOW DISCHARGE	 174
Laser Ablation and the Glow Discharge.....	177
Basics of Laser Induced Plasma Emission	179
 8 INTRODUCTION TO THE LASER ABLATION-GLOW DISCHARGE.....	203
 9 PARAMETRIC STUDY AND APPLICATIONS OF THE LASER ENHANCED GLOW DISCHARGE	 222
Parametric Study of the Laser-Enhanced Glow Discharge	222
Bulk Analysis	223
Minor and Trace Analysis	229
Insights into the Method of Excitation in the LEGD	234
Introduction	234
Ionization	238
Introduction to the Analysis of Non-conductors with the LEGD.....	240
Thin Layer Laser Deposition.....	248
Laser Sampled Non-conductive Material into a Pulsed Glow Discharge	257
 10 SUMMARY	274
 REFERENCES.....	277
 BIOGRAPHICAL SKETCH	281

Abstract of Dissertation Presented to the Graduate School
of the University of Florida in Partial Fulfillment of the
Requirements for the Degree of Doctor of Philosophy

CHARACTERIZATION OF THE MICROSECOND PULSED
GLOW DISCHARGE: A NOVEL SPECTROSCOPIC SOURCE

By

Kristofor Ingeneri

May 2000

Chair: Willard W. Harrison
Major Department: Chemistry

The focus of this dissertation is to study the pulsed glow discharge (GD) whereby a repetitive, short-duration ($10\ \mu\text{s}$), high-power pulse is used to drive the electrical discharge. Glow discharges generate a plasma that directly atomizes and ionizes a solid sample. The microsecond pulsed glow discharge creates intense, time-dependent signals that are useful for both fundamental studies and analytical applications. Therefore, the pulsed discharge has shown great potential as an ion source for atomic mass spectrometry and as a photon source for atomic emission spectroscopy.

We have constructed a reflectron mode time-of-flight mass spectrometer (TOFMS) incorporating a prototype microsecond pulsed GD ion source. The pulsed GD source generates greater signals than the dc source and has shown improved

detection limits. The transient nature of the source has allowed temporal separation between fill gas species and the sputtered analyte signal. This temporal separation is critical for the removal of isobaric interferences of important light elements, specifically when considering trace analysis. Diagnostic studies were performed to evaluate such parameters as applied voltage (1-2.5 kV), pressure (0.3 to 5 torr), pulse width (2-200 μ s), and frequency (10 Hz-5 kHz). Pulsing the discharge has resulted in up to three orders of magnitude greater signal intensity and in signal-to-noise. Emission plasma diagnostics were employed to characterize the same parameters with respect to emission spectroscopy, in addition to studying the diffusion of sputtered material and the rotational, excitational, and electronic temperatures within the plasma.

A combined laser ablation-pulsed GD source has been implemented in order to study laser – pulsed GD interactions. Using a laser to ablate non-conductive material into the vacuum chamber of a pulsed glow discharge is shown to be an effective means of determining the composition of ceramics, glasses and powders. The interaction of the laser and the GD has resulted in greater signal intensity (3 to 9 fold) and elemental sensitivity under certain experimental conditions than the pulsed GD itself.

A detailed characterization of the microsecond pulsed discharge, involving emission, TOF mass spectrometry, and laser interactions, has been used to improve our understanding and application of this novel spectroscopic source.

CHAPTER 1 INTRODUCTION

Mass spectrometry is an analytical technique in which ions are separated according to their mass to charge ratio. The technique was first described by J.J. Thompson in the early twentieth century,¹ but mass spectrometry was not widely practiced until the 1940s.² Its ability to analyze volatile organic material was useful in the petroleum industry and in searching for natural rubber alternatives for the war effort. Mass spectrometry has since developed from its modest beginnings to one of the most selective, sensitive and versatile modern analytical methods. Mass spectrometry continues to be a vital, exciting area of research. Advances in instrumentation have led to ion-trap spectrometers, high-resolution magnetic sector devices, and super-high resolution ion cyclotron resonance instruments. Increases in the speed and quality of electronics have allowed the reemergence of time-of-flight mass spectrometry as a versatile research tool. New methodologies such as combined MS-MS techniques have been developed as well.

Advancements in the methodology and technology of mass spectrometers have necessitated an equal demand for ion sources with improved performance as well. The development of electrospray, and the smaller nano-spray, ionization sources as well as the practice of matrix assisted laser desorption ionization (MALDI) have revolutionized research in the biological and pharmaceutical industries. While the pharmaceutical industry continues to fuel research in organic analysis, the use of mass

spectrometry for the analysis of inorganic solid materials is less prevalent due to the problems which arise when producing an atomic vapor and corresponding ion population from a solid matrix. However, the analysis of these materials is no less important, especially in the areas of geological and environmental research, as well as the metallurgical, materials, and semiconductor industries.

Certainly, solid samples can be crushed into a powder, dissolved into a solution, and analyzed by an appropriate method such as inductively coupled plasma (ICP) mass spectrometry. However, this is a task not always easily undertaken. High pressures, high temperatures and highly acidic conditions may be necessary to achieve dissolution. The expenditure of time, materials, and production of waste all add to the cost of performing analysis by solution-based methods. In addition, the dissolution procedures can lead to contamination of the sample and dilution, which reduces the sensitivity of analyses. Contamination and dilution are particularly problematic when performing trace elemental analysis. The comminuting and dissolving of the sample also precludes the option of surface analysis, for all information concerning the surface and the composition of layers of the material will be lost if a sample is physically altered.

Solid Analysis Techniques

Several techniques are capable of generating an ionic population directly from a solid, thereby avoiding the problems of contamination, dilution, and the loss of compositional data. These include thermal sources, laser ablation, secondary ion sputtering sources (SIMS), and arc/spark discharges. All are capable of generating ions directly from a sample and are effective means of bulk and trace solids analysis.

While each method has its particular advantages, it also has associated limitations and problems.

Thermal sources are very stable and have been used to analyze nearly every periodic element. However, the elemental sensitivity varies from 100% for the alkali metals to less than 0.2% for elements like uranium and the refractory elements.³

Thermal analysis also takes a considerable amount of time. A laser focused to sufficient irradiance, 10^8 W/cm^2 , will vaporize and ionize a sample as well. The laser plasma ionizes 100% of the sample and is capable of sensitive measurements with a high degree of spatial resolution. Unfortunately, the laser plasma interaction is not well understood at this time. Plasma processes and ion production are dependent on a number of parameters which are difficult to control, limiting the reproducibility and therefore the quantitative applications of the laser source. The large energy spread of the ions formed also complicates mass spectral analysis.

SIMS sources rely on the bombardment of the sample with a beam of positive ions with energies between 20 – 1000 eV. Material is sputtered from the source and some ions are produced (< 1%). The lateral and depth resolution of this technique are excellent. However, SIMS experiences strong matrix effects, fairly large differences in elemental sensitivities (up to three orders of magnitude) and has very stringent high vacuum requirements. A high vacuum, 10^{-5} to 10^{-8} torr, is a requirement of the spark source as well. The spark source generates a high current (100 A) discharge between two electrodes. One of the electrodes is the sample and it is vaporized by electron bombardment and heating. While sensitive (sub ppm detection) and possessing relatively stable elemental response, the arc discharge produces erratic and complex

spectral results. The ions produced also have a wide energy spread, making them difficult to focus.

The Glow Discharge

All of the solid sampling methods discussed thus far are expensive, complex and produce specific difficulties. Another alternative for solids analysis is the glow discharge (GD). The glow discharge is a simple, less expensive, yet proven ion and emission source for elemental spectrometry. The GD plasma suffers from only modest matrix effects, less than a factor of three, and generates a strong, stable signal capable of analyzing the bulk and trace composition of a solid with little or no sample preparation.

The glow discharge has been around for quite some time. Since its widespread acceptance as an analytical technique in the 1970's,⁴ the glow discharge has been used as source for atomic emission (GDAES),^{5,6} atomic absorption (GDAAS),^{7,8} atomic fluorescence (GDAFS),^{9,10} and for mass spectrometry (GDMS).¹¹ The glow discharge now plays a vital, stable role in the manufacturing and metallurgical industries, as well as research laboratories worldwide.

The glow discharge spectroscopic source consists of two electrodes immersed in a low pressure (1 to 10 torr) atmosphere, typically argon or another noble gas. The sample to be analyzed serves as the cathode. When a sufficient voltage is applied to the cathode, the gas breaks down dielectrically and forms a plasma (Figure 1-1).

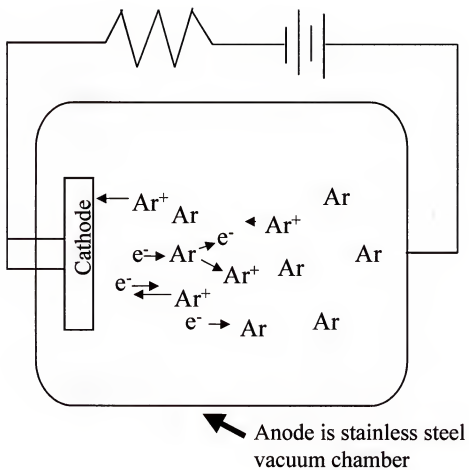


Figure 1-1. Simple illustration of a glow discharge. Electrons (e^-) flow away from the cathode toward the anode, while ions (Ar^+) move in the opposite direction.

Plasma processes give the discharge its characteristic glow and also sputter atoms from the surface of the cathode. Atoms liberated in this manner may be excited, leading to emission spectroscopy or ionized and sampled into a mass spectrometer.

The Microsecond Pulsed Glow Discharge

A recent development in the study of glow discharge spectroscopy is the microsecond-pulsed discharge. In the microsecond-pulsed GD, a short duration (10 microseconds), high voltage (up to 3.5 kV) pulse is applied to the sample at a frequency between 10 and 1000 Hz. Emission intensities and mass spectral signals in the pulsed discharge are increased by orders of magnitude when compared to the traditional continuous dc counterparts. Resulting improvements in signal to noise and detection limits have been encountered as well. However, virtually nothing is known about the operation of the pulsed source and only a handful of publications have appeared prior to our work.¹² Our research efforts have centered on the characterization of this spectroscopic source.

Overview

Since the pulsed discharge generates a transient ion signal, it is best fitted to a mass spectrometer that is capable of handling pulsed signals. Time-of-flight mass spectrometers, which have experienced a resurgence in the past several years due to the increased performance of computers and electronics, require pulsed injection of ions. We have therefore constructed a prototype microsecond pulsed glow discharge time-of-flight mass spectrometer.

This dissertation details work completed in three distinct but related areas. Our goal of improving our ability to perform the direct mass spectral analysis of solids has led to a renewal in our interest in optical spectroscopy due to the unique ability to perform plasma diagnostics. Therefore, the initial experiments use emission spectroscopy to investigate the pulsed glow discharge as an atom and ion source. Emphasis is placed on determining the spectroscopic response of the pulsed discharge with regard to its experimental parameters. Some fundamental properties, such as the removal and diffusion of cathode material, plasma temperature and electron temperature, are also reported.

The second experimental section details the construction and performance of the prototype pulsed GD TOFMS system. Parameter studies were performed in order to optimize the operation of the source as well as study the temporal effects observed in emission studies. The behavior of the source, as well as figures of merit, will be discussed.

The last experimental chapter details the construction and performance of an analytical source which uses a laser to ablate material into the fill gas of the discharge chamber for subsequent excitation and ionization by the pulsed discharge. In addition to studying the interaction of the two plasmas, some analytical utility resulted. The pulsed discharge uses an intermittent dc power generator, thus it can only characterize solids with a conductive or semi-conductive matrix. To analyze a non-conductive material, the material must be ground into a powder, mixed with a conductive matrix such as carbon or copper, and pressed into a pellet. Since a laser has no such restriction and can easily operate at the conditions dictated by the glow discharge, a

laser could be used to sample non-conductive material into the pulsed discharge. A combined laser ablation - glow discharge source was designed and tested to investigate the efficacy of non-conductor analysis and to study laser ablation – glow discharge interactions.

In order to provide a framework for the reader, two background chapters have been added prior to the experimental sections. The first chapter reviews the major species within the discharge, their function and their formation. Different spatial zones of the plasma are formed by these processes and will be discussed because they can affect the experimental configuration. The second section discusses the three primary modes of powering the discharge: continuous dc, continuous rf and the microsecond pulsed dc modes, and includes a justification for the use of the pulsed mode.

Summary

It was stated earlier that improvements in mass spectrometry have demanded equal performance from the sources used to generate ions. The pulsed glow discharge, with its greater peak signals and greater sensitivity, represents such an improvement. Increased signal to noise ratios result in lower detection limits. Moreover, the additional dimension of time, due to the transient nature of pulsed operation, aids in the diagnostic study of the plasma as kinetics may be more clearly revealed. The purpose of this work is to detail the characterization of this novel spectroscopic source, to study its fundamental processes, and to apply its use to solve real analytical challenges.

CHAPTER 2

GLOW DISCHARGE PROCESSES

The glow discharge, regardless of its configuration, consists of two electrodes immersed in a low pressure gas, most often argon. In the diode configuration (otherwise known as the coaxial), the sample to be analyzed is the cathode and the anode is the vacuum chamber. The gas, in its normal state, is an insulator. However, when a sufficiently high voltage is applied between the two electrodes, atoms of the gas will break down electrically, forming ion-electron pairs. These charged particles permit current to flow through the system. The gas has now become an effective conductor. This phenomenon is referred to as an “electrical discharge” or “gas discharge.”

The dielectric breakdown, the splitting of the gas atoms into ions and electrons, initiates the discharge and begins a cascade of events that produces the glow discharge plasma. When formed, the positive ions are accelerated toward the cathode due to its negative potential. Likewise the electrons are accelerated toward the anode by the potential difference across the discharge chamber. When gas ions hit the surface of the cathode, they have enough energy to release secondary electrons. These electrons are accelerated by the electric field and are capable of ionization collisions with the gas atoms. These atoms form into new ion-electron pairs, thus propagating the self-sustaining plasma. Atoms of the cathode may also be released by ion bombardment in

a process called sputtering. The sputtered atoms enter the discharge and are subject to the same ion, atom, and electron collisions as the fill gas.

The two most important types of collisions lead to ionization and excitation of the fill gas and the sputtered atoms. The light given off from the relaxing of these excited atoms and ions is what gives the discharge its characteristic glow – hence the term “glow discharge.” The excitation and ionization of the sputtered particles allow the glow discharge utility as an analytical technique. In this manner, the glow discharge generates an atom reservoir directly from the solid sample. This atomic population is excited by collisions within the plasma and the light given off can be used for analysis by atomic emission. The ions formed can be sampled into a mass spectrometer resulting in mass spectral analysis of the sample. Furthermore, this atomic population can be probed with an external light source leading to atomic fluorescence and absorption spectroscopy. Figure 2-1 illustrates the variety of analytical methods that can be used to investigate the glow discharge.

There is an art to the investigation of the glow discharge. Assuming a pure copper cathode and pure argon fill gas, a more simple chemical system is difficult to imagine. Copper can be formed in high purity with a precise crystal structure. Argon is chemically inert. However, application of a voltage to the electrode and subsequent ionization of the argon gas turns this static, well-understood system into a cauldron within a microsecond. Understanding this cauldron and making sense out of the resulting chaos within the newly formed plasma has been the goal of researchers for the better part of three decades.

Glow Discharge Species

The glow discharge is a complex, chaotic mix of a number of different species of varying energy. To better understand the discharge and its processes, it is important to know what these species are and how they are formed. The rest of this chapter will be dedicated to discussing the mechanisms within the glow discharge. This subject can be divided into two parts. The first part will describe the major plasma species and the processes responsible for their generation. The formation of charged and excited species establishes various zones within the discharge, which will be discussed in the second section.

Most diagnostic work has been performed using a copper cathode due to its high conductivity, high purity and availability. For simplicity, the plasma processes will be described in relation to this model, consisting of a copper cathode in a 1 torr argon atmosphere. The most important plasma species, the electron, will be discussed first. Next, processes involving argon, the most abundant species, will be covered. Finally, the formation, excitation and ionization of sputtered atoms will be described.

Glow Discharge Processes

A systematic overview of the basic plasma processes within the glow discharge will be beneficial to a better understanding of the experimental results in the following chapters. In reality, a complete coverage of the GD processes would be much more complex, involving sputtered clusters, multi-body collisions and the formation of negative ions. These species will not be discussed in favor of covering the major processes and their influence on the behavior of the glow discharge.

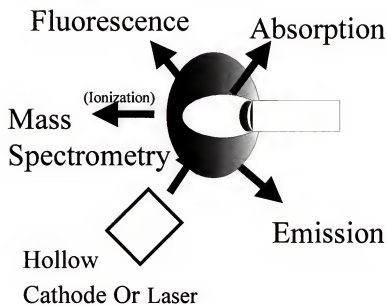


Figure 2-1. Spectroscopy of the glow discharge.

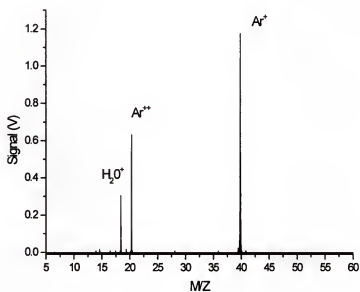


Figure 2-2. Mass spectrum showing gas ions. Conditions: 2 kV, 1 torr Ar, 10 μs delay.

There are several reviews and publications which cover the glow discharge process in much greater detail.^{4,13,14}

The majority of all processes within the glow discharge are due to collisions between discharge species. Therefore the pressure of the discharge cell exhibits great influence on the performance of the discharge. There are two types of collisions within the glow discharge, elastic and inelastic. Elastic collisions do not change the internal energy of the bodies involved. Only kinetic energy is transferred in an elastic collision. As such, elastic collisions are not responsible for the formation of plasma species. However, the frequency of these collisions, about 2×10^6 collisions/second at 1 torr nitrogen and 293 K, within the glow discharge warrants mentioning. While lacking the energy to transform an atom into one of the other species, elastic collisions serve to redistribute the kinetic energy within the plasma, leading to thermalization of the plasma. It is important to note that collisions between two particles of equal or near equal mass such as Ar-Ar or Ar-Cu, are much more efficient at transferring energy than those of disparate masses such as Ar-electron collisions.⁴

Inelastic collisions are responsible for the formation of species of analytical interest, as well as allowing the glow discharge to be a self-sustaining plasma. Due to the importance of these collisional processes, their description has been separated into three sections to be discussed. First, inelastic collisions with electrons will be detailed. This includes electron impact excitation and ionization in which excited atoms and ions are formed. Second, several reactions involving argon will be described. These include excitation and ionization by fast argon atoms and ions, metastable atom ionization, and several other processes such as thermal and

photoionization. Third, important reactions involving the excitation and ionization of sputtered species will be covered. This includes impact with the previously mentioned species in addition to Penning ionization and asymmetric charge transfer.

Electrons

Electrons formed from collisions within the discharge, or from impact with the cathode are accelerated by the potential difference between the cathode and anode. The electric field imparts a vast amount of energy to the electrons, quickly accelerating them. Electrons lose their energy by imparting it to other species upon collision. These collisions are able to raise the internal energy of atoms to an excited state. The relaxation of these excited species releases photons that can be detected by optical devices. Electrons accelerated by the potential field can impact with enough energy to ionize atoms in the discharge. Argon, which has an ionization potential of 15.76 eV, is primarily ionized by electron impact.

This is one of the most important and most studied processes within the glow discharge because it is essential in sustaining the plasma. Electrons formed by impact ionization may be accelerated by the electric field and then excite or ionize more atoms. Mass spectral analysis has shown that Ar^{2+} , with an ionization potential of 27.63 eV, is formed as well (Figure 2-2). The only plasma species capable of imparting that much energy are the electrons. There are two processes which limit the energy of electrons (potentially 2000 eV in the 2 kV electric field of a pulsed discharge). First, even at low pressures the number densities and collision rates are very high, even for electrons. Due to the differences in mass, electrons that undergo

collisions lose all their energy and so must be accelerated again. Second, the transfer of energy from a light mass to a greater mass, such as electron-Ar interactions, is very low. While 2000 eV electrons may be present, their collisional cross-section, and ability to transfer energy would be small.

Argon

While the energy transfer from electrons to atoms is frequent but fairly inefficient, collisions between two like masses, such as Ar-Ar and Ar-Cu, transfer energy more effectively. Argon atoms are primarily involved in elastic collisions, thermalizing the plasma. However, like electron impact, argon ions and atoms of sufficient kinetic energy can collide inelastically with other species. These collisions result in excited atoms and ion species. Due to their higher masses, ions are accelerated more slowly than electrons. Therefore, collisions with fast argon species will occur close to the cathode after the ion has been accelerated by the potential field. Likewise, greater applied voltage will result in a greater acceleration of the argon ions.

One specific species of argon that deserves a special mention is the argon metastable atom. Argon has two long-lived excited states with 11.55 and 11.72 eV of energy respectively. The lifetime of these two energy states is on the order of a millisecond.⁴ If any two metastable atoms were to collide, together they have enough energy to free an electron from one of the atoms. However, this mechanism of ionization is of only minor importance when compared with electron impact ionization.¹⁵

There are several other minor mechanisms of excitation and ionization that play a small role in the glow discharge plasma. These minor processes form ions and excited species by thermal processes or by absorbing photons. Ions and excited species of both atoms and ions can be generated by any form of energy input. Therefore, if enough kinetic energy is absorbed by a particle, or if the particle absorbs photons of sufficient energy, an excited state or ion may be formed. However, the glow discharge is a cool plasma having temperatures between 300 K to 700 K which corresponds to an average energy of less than 0.05 eV. Likewise, photo-ionization is possible since 15.8 eV corresponds to a wavelength of 80 nm, which is in the deep ultra-violet range. However, Bogaerts and Gijbels¹⁴ have suggested that this mechanism is still considerably less important than collisions with electrons and fast argon species.

Sputtering

During the lifetime of the plasma, ions and fast atoms will bombard the surface of the cathode. A number of different events can result, including the reflection or implantation of the bombarding particle. Alternatively, secondary electrons may be released and accelerated by the electric field into the plasma. Bombardment can also result in the ejection of a surface atom. This process of atom removal by particle bombardment is known as sputtering. The sputter rate is the measure of weight loss with respect to time. To sputter-remove material, an impacting particle must transfer enough energy to an atom to overcome the binding of its lattice structure. The sputtering rate is therefore dependent upon the nature of the bombarding species, the

matrix of the cathode, the mass of the atom sputtered, and experimental conditions such as pressure, current, and applied voltage. If the experimental conditions and identity of the fill gas are kept the same, the sputtering rate will be most influenced by the cathode matrix and identity of the atom to be sputtered. Relative sputtering rates of most elements vary by only a factor of three to five. Marcus¹³ has indicated that the sputtering rate follows the same trend as when a pure metal is subjected to bombardment of a 400 eV argon ion beam. Figure 2-3 indicates the expected trends in the sputtering rate of several elements. Fractionation, a result of different boiling points of the constituents causing differential sampling, is problematic in thermal ionization sources. While the rate of sputtering is slightly different for each matrix, sputtering affects the surface of the cathode equally and fractionation for most materials is not observed. However, there is a small amount of heating due to the bombardment process and therefore some fractionation from elements with very low vapor pressures, such as mercury, has been evidenced.

Sputtered Species

The same processes responsible for excitation and ionization of the argon atoms are also applicable to the excitation and ionization of the sputtered species. However, little is known about the effect of each mechanism on sputtered material.¹⁸ No mechanism stands out as a primary means of exciting the sputtered atoms. However, the three most important processes of ionization will be discussed in further detail.

Electron impact ionization is capable of ionizing helium, which has an ionization potential of 24.59 eV. Therefore, this mechanism has more than enough energy to ionize any element. An additional advantage of this process is that it is essentially unselective. The cross-section curve for electron impact ionization is relatively the same shape and magnitude for all elements.^{17,18} Therefore, the contribution of this mechanism will be based upon the number density distribution and not the chemistry of the sputtered atoms.

Penning ionization is another important mechanism within the discharge. Penning ionization consists of a collision involving an argon metastable atom and a sputtered particle. Because the argon metastable atoms have energies of 11.55 and 11.72 respectively, they have enough energy to ionize most elements. Only H, N, O, F, Cl, Br and the noble gases have higher ionization potentials. For elements with a lower ionization energy than the metastable state, the Penning process is unselective. Factors such as the number density, mass, and radius of an atom may affect its collision rate with metastable atoms. This process is particularly important in low pressure plasmas such as the glow discharge. It has been suggested that Penning ionization is the dominant ionization process within the glow discharge.^{19,20}

Asymmetric charge transfer is the last suggested process for ionization of sputtered species. Unlike electron impact and Penning ionization, asymmetric charge transfer is a selective mechanism for ionization of certain elements. Asymmetric charge transfer occurs when an electron is transferred from a sputtered atom to an argon atom, thus producing an analyte ion and an argon atom. This will occur if the difference in the energy between the atom and ion is very small.

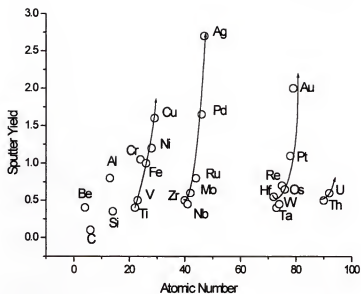


Figure 2-3. Sputter yields for various elements under bombardment of 400 eV Ar ions.¹⁶

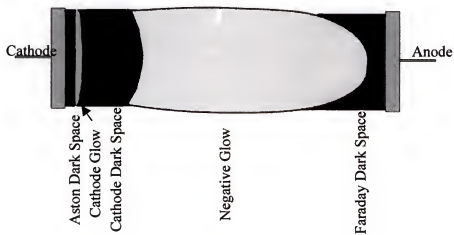


Figure 2-4. Spatial zones of the glow discharge.

Therefore, asymmetric charge transfer will only occur between specific energy levels. Steers and coworkers have demonstrated the occurrence of asymmetric charge transfer between Ar^+ and Cu, Fe, and Ti.^{21,22,23} However, the relative importance of this ionization process compared to Penning ionization is still a controversial subject.

Spatial Zones in the Glow Discharge

The processes within the glow discharge plasma cause several distinct spatial regions to be formed (Figure 2-4). The various regions differ in terms of luminosity, potential and electrical field distribution, current density, space charge density, and degree of ionization. The position and size of these areas depend upon experimental parameters such as applied voltage and pressure, as well as the distance from the cathode to the anode. The composition of the gas affects this distribution as well.

At longer cathode to anode distances, there are several different regions within the discharge. However, most analytical work involves the use of smaller discharge cells and only contains three regions. These include the cathode glow region, the cathode dark space and the negative glow region. There are excellent reviews which summarize the different zones of the plasma and refer to research pertaining to them.^{4,13,17} However, in the interest of brevity, only a short description of the three spatial zones of the analytical glow discharge will be discussed.

The Cathode Glow Region

The cathode glow consists of two regions. The Aston dark space, which appears above the surface of the cathode, and the cathode glow which appears just

beyond the Aston dark space. Atoms bombarding the surface of the cathode can release secondary electrons as well as sputter atoms from the surface. Electrons released in this manner are accelerated toward the anode due to the potential field. Just above the cathode is the Aston dark space. In the Aston dark space, the electrons have not gained enough energy to excite or ionize any discharge species, so the region appears dark to the observer. Immediately beyond this point a thin, luminous band appears. This region is the cathode glow and actually consists of a series of light and dark bands that are not distinguishable by the eye. Electrons released from the cathode quickly gain the energy to excite and even ionize species within the vacuum chamber. After passing through the Aston dark space, some electrons collide with atoms in the GD chamber and excite them resulting in the luminous cathode glow while others pass through continuing to accelerate. Those electrons that have experienced inelastic collisions with gas species lose their energy. The constant cycle of acceleration, collision and loss of energy, and re-acceleration gives rise to the alternating layers of the cathode glow region.

The Cathode Dark Space

Beyond the cathode glow appears a region of relatively low luminosity. It is called the cathode dark space. The cathode dark space is characterized by a large potential difference. Due to the space charge effects within the glow discharge, almost the entire potential difference between the cathode and anode is experienced in the region of the cathode dark space. Figure 2-5 shows the voltage potential as a function of distance with relationship to the regions of the glow discharge. Because the

potential “falls off” quickly in this region, it is also called the cathode fall. The large potential difference in the small region of the discharge gives rise to the high electric field. Electrons in the discharge, even those that collided with atoms in the cathode glow region, are rapidly accelerated by the strong potential field. Quickly, the energy of these electrons becomes too high for efficient excitation reactions. A resulting dip in the electron impact excitation cross section appears at higher energy.^{17,24,25}

Therefore, the region of the cathode dark space shows little light because the electrons have too little energy to ionize species and too much energy to effectively excite atoms. Any ions formed in the negative glow region are attracted to the cathode. However, due to their greater mass, ions accelerate much more slowly than electrons and have not obtained enough energy to excite other species in the cathode dark space.

The cathode dark space is the most important region of the discharge because it is the distance necessary to accelerate electrons to the energy needed to ionize the fill gas. These ionizing collisions form more electrons and ions. The electrons are capable of being accelerated and forming other ions, while the ions formed are attracted toward the cathode. This continuous cycle of secondary emission of electrons by ion bombardment and acceleration of electrons in order to form ions ensures the self-sustaining nature of the discharge.

The Negative Glow

The negative glow is the most prominent region of the glow discharge to the casual observer. It is a large, bright region just beyond the cathode dark space and is of the most importance to analytical applications. Two types of electrons enter the

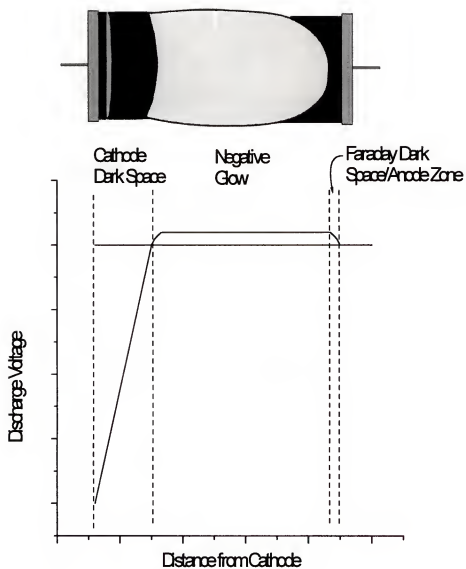


Figure 2-5. Potential Distribution Across the Glow Discharge.¹⁷

negative glow region: fast electrons, which traveled through the cathode dark space uninhibited, and slow electrons, which experienced a loss of energy when exciting atoms in the cathode glow region. The fast electrons are only capable of ionizing collisions. The slow electrons may excite atoms or ionize an already excited atom.

Electron impact ionization events result in electron multiplication. The ionization events slow down the electrons. The combination of ions and slow electrons causes the negative glow region to be field free. Since this region is equipotential, electrons are no longer accelerated. This large number of slow electrons have energies much more suitable for excitation collisions. Therefore, the negative glow is noted for its bright emission. The color of the discharge is determined by the fill gas. Argon produces a bluish purple color. The length of the negative glow region is determined by two factors. The pressure of the discharge serves to increase collisions and compress the spatial zones. The range of electron energies before thermalization also extends the diffuse negative glow region. Since the electrons are not re-accelerated after collisions in this region, the greatest emission intensity will be observed at the beginning of the negative glow and will fade as it stretches toward the anode. Therefore, the onset of the negative glow region is where optical spectroscopic techniques focus due to the greater emission intensity. Likewise, mass spectrometers are set to sample the largest population of ions, which will correspond to front of the negative glow region when the electrons have energies capable of ionization.

Electrons exiting the negative glow region have lost most of their energy and are considered more or less thermalized. This region of low luminosity is referred to as the Faraday dark space. At shorter cathode-anode distances, the anode comes into

contact with the negative glow region and the Faraday dark space is no longer observed. Most analytical discharges have short cell dimensions and therefore constrain the discharge. The plasma will still be maintained because the only critical region for sustaining the plasma is the cathode dark space. Thus the majority of analytical glow discharge cells consist only of the cathode glow, cathode fall and negative glow regions.

CHAPTER 3 POWERING THE GLOW DISCHARGE

The greatest advantage of the glow discharge lies in its operational simplicity. One must only apply to the cathode (sample) a sufficient voltage and current to establish a discharge. This discharge atomizes and excites the sample, and a number of spectroscopic techniques may be used to investigate the plasma. Why then would one wish to complicate this system by applying an intermittent voltage pulse to the cathode? Rather than a continuous, stable signal, the pulsed mode will require additional equipment to synchronize and collect the transient signal. A number of additional experimental parameters such as frequency and duty cycle also need to be factored into optimizing experiments as well. The only reason to pulse the glow discharge would be if there were some analytical advantage to be gained. Our results indicate that an analytical advantage can be obtained from pulsing the discharge. Also, an intermittent pulsed discharge allows a number of fundamental processes to be studied by allowing the initiation and decay of the plasma to be probed.

To understand the differences, advantages, and disadvantages of the pulsed mode, one must first understand the character and operation of the different modes of the glow discharge.²⁶ The glow discharge may be powered by direct current (dc), radio frequency (rf) and pulsed power sources. Each of these modes has some specific

advantages and disadvantages. A discussion of the different modes will provide the background for our decision to investigate the pulsed glow discharge.

Analytical Utility of the Glow Discharge

The analytical utility of the glow discharge arises from the fundamental processes involving sputtering, excitation and ionization that were discussed in the last chapter. The glow discharge has held the research interests of analytical chemists due to its ability to convert a solid analyte directly into the atomic state, thus providing a pool of atoms representative of the sample composition that can be investigated by a number of different spectroscopic means. The primary uses of the glow discharge are thus as a source for atoms, ions and photons.

Atoms

The process of sputtering is responsible for the atomization of the sample. As discussed in the preceding chapter, sputtering results when ions and fast atoms bombard the surface of the cathode. If the energy transferred by the incident particle is sufficient to overcome the binding energy of the lattice of the sample matrix, atoms on the surface will be dislodged. The bombarding particle penetrates only a few atomic layers²⁸ and the entire impact energy transfer, sputter removal, and lattice relaxation process takes on the order of 10^{-12} seconds.⁴ Though a billion or more surface collisions take place in the span of one second, each event takes so little time that they can be considered discrete. Sputtering produces few dimers, and some

polyatomic and molecular species have also been observed. However, single atoms and secondary electrons are the overwhelming predominant species produced.

Because sputtering relies on collisions, rather than thermal processes to ablate material from the sample surface, the negative effects of thermal based ablation methods are avoided. The main disadvantage of the thermal methods such as arc discharges and thermal vaporization sources is the selective vaporization and matrix effects due to the composition of the sample. These thermal effects can cause differences of orders of magnitude in elemental sensitivities. The low energy, cool glow discharge plasma responsible for the sputtering process is relatively free of thermal effects. Eventually, the sputtering process raises the temperature of the sample. As the temperature rises, the atoms on the surface are less tightly bound and a net increase in the sputtering rate, referred to as the thermal sputtering rate, is observed. Therefore, thermal effects have been encountered with the lower melting point elements such as zinc. Most glow discharge sources have some form of cooling to remove this effect.

Bulk analysis is performed by qualitative and quantitative determination of the sputtered atoms. Due to the non-selectivity of the sputter process and the lack of thermal effects, what is obtained is an atom population representative of the bulk composition. Furthermore, because the plasma samples the entire area of the cathode, the resulting atom population represents the bulk composition integrated over the entire surface. Therefore, the glow discharge does an excellent job at both bulk and even trace analysis. Another aspect of the utility of the glow discharge is that it is in essence a surface analysis technique. It was mentioned that the ions bombarding the

surface penetrate only a few atomic layers before their energy is dissipated. Glow discharge sputters material in a layer-by-layer fashion, allowing the composition of thin films to be determined.

Photons

As the sputtered atoms diffuse from the cathode and into the inert gas atmosphere, they will immediately begin to collide with energetic species within the plasma. The atoms of the analyte are excited by collisions with electrons, inert gas atoms, ions, and metastable species. As these excited atoms relax, they emit photons with wavelengths corresponding to their elemental composition. The light emitted by the excited atoms of argon, as well as the analyte species, is what gives the glow discharge its characteristic glow. The light emitted from the glow discharge is the basis of its widespread use as an atomic emission source. Moreover, the generally non-selective sputtering technique removes a number of atoms from the entire surface of the cathode, making the glow discharge a true multi-elemental technique. If an optical spectrometer is scanned over the UV-VIS range, the analyst can determine the elemental composition of the sample. The efficiency of this process is improved greatly if a multi-channel detection device, such as a photodiode array or CCD is used. The composition of thin or multiple layers can be identified and with proper calibration, the depth of these layers can be determined as well.

Ions

The atoms liberated from the surface of the analyte can be excited, allowing the composition of the sample to be determined optically. These atoms can also undergo collisions with sufficient energy to ionize them. The predominant mechanism for the ionization of analyte species in the glow discharge is Penning ionization involving collision with a metastable argon atom. Electrons and argon ions have also been suggested as collision partners capable of ionizing sputtered material. Regardless of the mechanism, glow discharges form primarily singly charged ions and the ionization efficiency is typically about 1%. While excited ions are capable of emitting radiation that can be detected by optical spectroscopy, the ions find their greatest utility when sampled into a mass analyzer. Glow discharge mass spectrometry (GDMS) has been commercially successful and is a widely used technique. The popularity of GDMS is due to its low detection limits, spectral simplicity, isotope ratio measurements and uniform elemental sensitivities. However, this improved performance does come at a cost. While optical methods such as emission are noninvasive, GDMS relies on the physical extraction and focusing of the ion beam generated within the GD plasma. GDMS is therefore more difficult and requires the use of intricate hardware. However the benefits of mass spectrometry compensate for this added complexity.

As a spectroscopic source, the three primary uses for the glow discharge are as an atom, photon or ion source. The discharge is a stable, effective means of producing these species. The glow discharge has been used as a source for most traditional forms of spectroscopy. Figure 3-1 highlights the applications of the glow discharge. As a

generator of atoms, the stable atomic populations have been probed with atomic absorption (AA), and atomic fluorescence methods (AF). Winefordner, et al. have attempted single atom detection using laser excitation to probe the atoms generated by a glow discharge.²⁸ As an atomic emission source, the plasma processes generate photons that are an effective means of rapidly and simply determining the bulk and trace composition of a sample. The glow discharge has also been used to analyze thin layers on the surface of materials as well.²⁹ Another form of glow discharge, the hollow cathode lamp, has been the industry standard for the generation of photons of specific wavelengths for use in atomic absorption measurements. The mass analysis of ions generated by the glow discharge is a very successful means of sample analysis. Conversely, GD ion sources have been used to evaluate and explore some of the fundamental aspects of mass spectrometric devices as well. A GD ion source coupled to a Fourier transform ion cyclotron resonance (FTICR) mass analyzer has achieved the greatest mass resolution of a mass spectrometer to date.³⁰ To reiterate, the glow discharge plasma produces atoms, photons and ions. The widespread acceptance and use of the glow discharge as a spectroscopic source is a testament to its effectiveness.

Methods of Powering the Glow Discharge

The performance of the glow discharge is largely determined by its electrical characteristics. Given the diverse applications of the glow discharge, many different means of powering the glow discharge have been used. While a comprehensive discussion of these different techniques is beyond the scope of this work, a brief discussion of each will put the research presented into perspective. The glow

discharge has been powered by direct current, radio frequency and pulsed power modes.

Direct Current (dc) Glow Discharge

Powering the glow discharge with continuous, direct current is unquestionably the most familiar and most used means of driving the GD plasma. The reasons for its continued use is that these rugged, dependable supplies are inexpensive, simple to operate and very stable. All of the advantages and applications of the glow discharge thus far have been realized using the dc mode. As the industry standard, the other modes of powering the discharge are measured against the dependable, effective performance of the dc glow discharge.

The discharge is a self-cleaning plasma owing to the sputtering mechanism. When the dc discharge is engaged, often a pre-burn period is included before analysis is undertaken. Most samples have some surface contamination due to their contact with air. These include oxide layers, water vapor and other such contaminants. This pre-burn step cleans the surface of the cathode and stabilizes the discharge. The pre-burn step can range from a few seconds to minutes depending on the sample and experimental conditions used.

After this stabilization period, the dc discharge provides a very stable plasma and therefore a steady atom population. Effectively, the sputtering mechanism serves to “dissolve” atoms of the analyte into an argon “solvent.” The continuous operation of the dc mode sets up a concentration gradient of atomic species. While this gradient is steady state, the number densities of the different plasma species can be quite

different. Much work has been performed on quantifying the plasma species in the dc mode. In fact, this knowledge has been put to use in mathematically predicting the performance of the dc discharge. While Bogaerts and Gijbels have led this work, the comparison of their models with experimental work performed in conjunction with Winefordner and Harrison serves as an excellent review of research in this area.³¹

The glow discharge establishes a stable concentration gradient. Therefore, if the analyst consistently samples the same region of the discharge, results are very reproducible. While any region of the discharge may be sampled, emission experiments are normally positioned to probe the negative glow region due to its higher emission intensity. Likewise, absorption measurements are taken either in the dark space or further into the negative glow region so that the highest population of atoms, with a relatively low emission background is obtained. Because mass spectrometry requires the physical transfer of the ions into the mass analyzer, MS source configurations are limited by the necessity of including a means of ion sampling. Results from mass spectrometry studies have shown that the ion signal from the dc discharge is best sampled in the negative glow region at about 6 to 7 mm from the cathode.

The dc mode has two predominant limitations. The first is that the dc discharge is low power. The spectroscopic peers of the discharge, the inductively coupled plasma (ICP), electrothermal vaporization (ETV) and laser induced plasma (LIP) sources all use powers in the realm of kilowatts or greater to generate an analytical signal. The dc discharge is typically operated at 1 kV and milliamps of current with powers generally ranging from fractions to tens of watts. The low

energy, cool plasma formed by the glow discharge is the source of some of its analytical advantages, but some samples necessitate the use of higher powers.

The second limitation of the dc discharge is that it requires a conductive, or at least semi-conductive matrix in order to establish a plasma. While this is not a problem for the metallurgical or the semiconductor industries, many samples of analytical interest such as glasses, soils and ceramics are non-conductive. The dc plasma is incapable of sampling these materials directly, excluding the wide and increasingly important realm of non-conductive materials from analysis. Two methods of analyzing non-conductive materials have been proposed. Powdered samples may be mixed with a conductive matrix to allow a stable plasma to be established.³² This adds a sample preparation step and also opens the opportunity for sample contamination, limiting two of the advantages of the technique. The second method for the analysis of non-conductors is by the use of a secondary cathode.³³ In this technique, a conductive ring is connected to the dc power and placed just above the surface of a non-conducting sample. Some bombarding ions and fast atoms will strike the non-conductor and sputter-remove some of the sample. Thus, the dc discharge is able to perform the analysis of a broader range of sample types.

Radio Frequency (rf) Glow Discharge

Increasing interest in the analysis of non-conductive samples has led to a different mode of operating the glow discharge. Due to the inability of the dc discharge to analyze non-conductive samples directly, Wehner and co-workers³⁴ proposed the use of a rapidly oscillating power supply to power the discharge. The

application of high voltage to the surface of a dielectric material induces a capacitor like response, where the surfaces of the two electrodes take on an applied potential. This potential is dissipated by electrons or ions. This does not result in a plasma and no net flow of current is observed. However, if the voltage is oscillated rapidly, on the order of frequencies of 1 MHz or greater, the re-application of the potential on the surface will be faster than the inherent charge decay. By this method, the smaller of the two electrodes, normally the cathode, obtains a negative bias voltage. When this bias voltage is sufficient to cause the breakdown of the gas, a sustained discharge may be established. Thus, non-conductive materials may be sputtered and excited much in the same way as in the dc source.

Typical rf sources operate at a frequency of 13.56 MHz and deliver anywhere from 15 to 100 W of power. Under these conditions a plasma can be established using conductive materials and even non-conductors as the cathode of the discharge. Therefore both are able to be analyzed. An additional advantage is that the rf mode is less affected by surface oxides and contaminants so that rf discharges tend to ignite immediately and have shown long term stability without the need for a pre-burn sequence.

The ability to analyze non-conductive materials is the greatest advantage of powering the GD in the rf mode. Radio frequency discharges are therefore most popular when the analysis of non-conductors is emphasized. Radio frequency discharges also have no problems analyzing conductive materials as well. Therefore, the rf glow discharge could be considered the most versatile GD source.

Despite its versatility, use of the rf discharge is complicated by a number of factors which diminish its popularity. In terms of equipment, rf power supplies are often considerably more expensive than those for dc. Also, a matching network is necessary to couple the rf power to the sample properly. Lastly, of no small concern is the possibility that an improperly shielded rf supply will act as a radio transmitter, causing considerable problems with other equipment being interfered with or damaged by the electronic pickup.

Another factor that inhibits many from using the rf discharge is that rf powered discharges, while robust, do not show the same intensity as dc discharges. A reduced sputtering rate is often observed in an rf discharge. Therefore, the emission from rf discharges is considerably lower than when powered in the dc mode. In addition to this, the mechanisms responsible for excitation and ionization within the rf discharge are not fully understood. This may also cause investigators and industrial manufacturers to be hesitant to use the rf discharge. Despite these shortcomings, the rf discharge is still an accepted and viable analytical technique. As research on the rf mode continues, perhaps more wide-spread use will develop.

Pulsed Glow Discharge

The two methods discussed to this point have one thing in common. Both are operated in a continuous mode. That is, the power generators run continually, sustaining the discharge and setting up a steady, sputtered atom population. While both are successful analytical techniques, both suffer from being considerably lower power than competitive techniques. In addition, even though a relatively cool plasma

is generated, sustained operation of either the dc or rf glow discharge will eventually heat the sample leading to thermal effects, inconsistent performance and even melting of the sample. The idea of pulsing the glow discharge was initially studied with the hope of combating these two problems. Pulsed methods have exhibited certain well known advantages. First, much higher powers can be obtained if the high power levels do not need to be maintained for very long. Second, an intermittent source allows relaxation effects, such as cooling to take place. The pulsing of a source is standard practice in many fields such as laser spectroscopy and pulsed NMR in which short-lived pulses produce extremely high signal intensities which in turn result in improved performance. Promising results for the field of glow discharge spectroscopies were experienced in the mid 70's when Piepmeier et al. reported intense emission from a pulsed hollow cathode discharge.³⁵ Therefore, it was expected that by pulsing the glow discharge more atoms, ion and photons would be generated.

While higher powers can be applied to the discharge cell, there are some experimental concerns that may be raised. Continuous operation provides a steady signal over a 100% duty cycle. A pulsed mode could be unstable due to the intermittent application of power. Will the pulsed discharge initiate consistently and generate a reproducible signal for analytical work? In addition there are a number of additional experimental factors that could adversely affect analysis, or at least complicate optimization such as the duty cycle and frequency of the pulses. Pulsed generators are more complex and expensive than dc sources. Likewise, additional equipment must be used to gate and collect the transient signal generated by the pulsed mode. Considerable challenges must be overcome when analyzing pulsed discharges

with a scanning systems, whether they are optical or mass analyzers. The best, or at least most efficient, results will be obtained when a pulsed source is coupled to an instrument capable of compensating for its low duty cycle. When dealing with emission, direct readers or monochromators with gated, intensified CCD's are optimal. For mass spectrometry, the coupling of a transient source with a time-of-flight mass spectrometer seems ideal. We have found that the pulsed glow discharge does produce higher signals than the continuous GD. Moreover, complementary effects of high power and low duty cycle have offered advantages beyond those anticipated. Pulsing the discharge offers a number of opportunities for increased performance and study of the glow discharge phenomenon.

Advantages of the Microsecond Pulsed Glow Discharge

Enhanced Sputter Rates

When operated in the dc mode, voltages in the 600 to 1200 V range are applied to the cathode, with 1000 V being typical for analytical emission work. The dc mode has operating currents ranging in the single digit milliamps, but sometimes as high as tens of milliamps in the Grimm-type source at high pressure. The pulse generators used in this work were capable of delivering up to 3 kV to the sample with 2 kV being typical. The current flowing through the pulsed discharge is in the tens to hundreds of milliamps with currents as high as a few amps being seen for some applications. The greater number of electrons should lead to more ions. The greater potential across the cell will accelerate the incoming ions responsible for sputtering. Due to the higher

number and average energy of the impinging ions, the sputter yield is expected to increase.

Weight loss measurements were made using a thin copper foil sampled by a Grimm-type discharge.³⁶ A dc discharge was operated at 1200 V in a 5 torr argon atmosphere, resulting in a 37 W continuous discharge. The sputtering rate was measured to be around 26 mg/minute. A pulsed discharge with a pulse width of 10 microseconds and peak voltage of 2 kV was run in a 3 torr argon atmosphere. At this pressure, the peak power of the discharge was 422 W equaling an average power of 0.42 W. The net sputtering rate of the pulsed discharge was 3.5×10^{13} atoms per pulse. If the sputtering rate of the dc discharge is compared on the same 10 microsecond time scale, only 2.5×10^{12} atoms are removed. Therefore, the pulsed discharge shows a 14-fold enhancement over the dc discharge when compared on the same time scale. While the pulsed discharge removes material from the surface more efficiently, its drastically reduced duty cycle results in a lower average sputtering rate than in the dc mode.

In addition to the increased sputtered population during the pulse-on time, the pulsed discharge offers a variety of factors that can be used to control the sputtering rate. Layer analysis will be greatly affected by this ability as the duty cycle and frequency may be reduced to facilitate the analysis of very thin layers or increased to remove thicker layers more quickly.

Enhanced Atomic Emission

While the over-all average sputtering rate for the pulsed discharge is lower than for the dc mode, the pulsed discharge creates a transient population of atoms that is much higher than in the dc. The higher atom populations coupled with the more energetic plasma species formed in the high power discharge result in much greater emission intensity. Emission signals from glow discharges and hollow cathode lamps using the pulsed mode have displayed from 1 to 3 orders of magnitude greater emission than when operated continuously. In addition, the various operating conditions within the pulsed discharge may favor the population of certain atomic energy levels resulting in increased emission of specific lines.

Enhanced Ionization

It is no surprise that the higher energy pulsed plasma will not only result in greater emission, but greater ionization rates as well. Enhancements in analytical signals from ions have been seen in both optical and mass spectrometry. In optical spectroscopy, the difference between the pulsed mode and dc mode can be quite dramatic, with weak ionic emission lines suddenly emerging from the background. Likewise, mass spectral signals have shown enhancements of 3 fold or higher in the pulsed mode.

Temporal Resolution

During the lifetime of the pulsed plasma the discharge is initiated, sustained and then terminated followed by relaxation effects. Each pulse is a distinct, separate

event. Several mechanisms within the discharge have shown different temporal profiles that are only able to be distinguished due to the rapid initiation and decay of the plasma. By delaying the detection gate some analytical advantage may ensue. An example of such an advantage would be to delay atomic absorption or fluorescence measurements until the GD emission disappears so that measurements may be taken upon a spectrally dark background. Several other results will be discussed in the next several chapters. The pulsed discharge also allows a more clearly defined picture of such fundamental processes, such as diffusion, within the discharge chamber.

Chemistry

The glow discharge is, in essence, an atomic reaction cell. For normal analytical purposes the composition of the analyte is of the highest interest. However, the stability and reproducibility of the discharge make it an effective atom reservoir. This repetitious production of atoms and energetic species allow a number of studies to be performed. Gas phase kinetics can be studied as well as the formation of unusual species such as metal argides. The plasma chemistry can be drastically affected by the introduction of oxidizing or reducing agents into the vacuum chamber. Water vapor has been introduced to study its effects on rare earth-oxide equilibria.³⁷ Introduction of gettering agents have also been reported to remove undesired gas contaminants.³⁸ The composition of the gas can be altered, such as mixing argon in helium, to establish a desired effect. The pulsed mode can aid these studies by allowing the kinetics within the initiation or decay of the plasma to be probed.

Concluding Remarks

The primary use of the glow discharge is as a simple, rapid, multi-element spectroscopic source for direct solids analysis. The GD plasma generates atoms, ions, and photons which allows the composition of the sample to be determined. By pulsing the glow discharge, a more powerful and versatile plasma is obtained. Increased power has led to greater sputter yields, atomic emission, and ion populations. The increase in signal has been accompanied by only a slight increase in background noise. Therefore the signal-to-noise ratios and resulting detection limits of the glow discharge have been improved. In addition to enhanced analytical performance, pulsed discharges have also allowed the study of several fundamental aspects of the glow discharge. Therefore, the minor additional expense and complexity added by pulsing the discharge are outweighed by the opportunity for improved performance.

CHAPTER 4 EMISSION OF THE PULSED GLOW DISCHARGE

Theory of Pulsing the Glow Discharge

Pulsed glow discharges have been researched for at least thirty years. Early work was principally concerned with pulsing of the hollow cathode glow discharge. These studies included measurement of the excitation, ionization and temporal profiles of the emission from the hollow cathode lamps in order to improve their utility as a light source for AAS or AFS. The principal effect of pulsing the power to the hollow cathode was to achieve greater irradiance by the application of higher peak powers. The resulting sensitivity and detection limits of the pulsed method have shown considerable improvements when compared to continuous dc operation. Our research has taken the previous work a step further by lowering the pulse width by two or more orders of magnitude. Pulses of 10 microseconds, rather than milliseconds or larger, have the advantage of being closer to the rate of formation of analytical species. Thus, the shorter pulse widths may offer a keener insight into the kinetics of the discharge.

By reducing the duty cycle of the glow discharge, much higher peak power may be applied while maintaining an acceptable, low average power. The pulse powers used ranged from 10 W to 2 kW. This results in an intensified, transient signal, while negative effects from continuous operation, such as heating of the sample, are greatly reduced. A predominance of the work to date has concentrated on pulsing the hollow cathode with a high frequency pulse with widths in the millisecond

time regime. It is hypothesized that by reducing the duty cycle further, the glow discharge can be driven to even greater peak powers without degrading to an arc discharge. In 1996, Hang *et al.* reported the coupling of a microsecond regime pulsed glow discharge to a time-of-flight mass spectrometer.³⁹ Results from this new instrument have shown distinct advantages, both in generating a high intensity-low noise signal and in allowing temporal resolution between analyte and gas species. The microsecond pulsed glow discharge as an atomic emission source has also been the subject of investigation as a low cost, simple, almost maintenance-free alternative to mass spectrometry.

The characterization and application of this novel source for spectroscopy have been the goals of this laboratory for the last half of this decade. Of primary interest is the development of a prototype microsecond pulsed time-of-flight mass spectrometer system as a powerful tool for solids analysis. This desire has led to renewed interest in atomic emission spectroscopy due to its unique insights into the fundamental properties of the discharge. This chapter will cover the emission characteristics of the pulsed source. Emission plasma diagnostic techniques are used to investigate the fundamental operation of the pulsed GD. The next chapter covers the application of the microsecond pulsed mode to a GD-TOFMS spectrometer.

Experimental

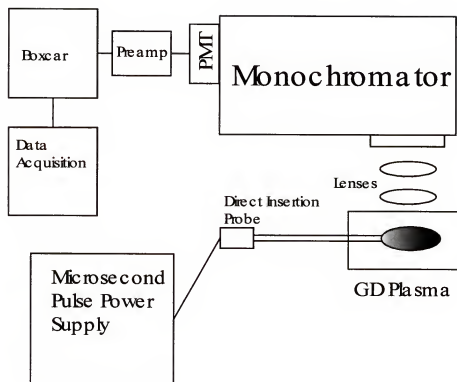
A schematic diagram of a microsecond pulsed glow discharge atomic emission setup is shown in Figure 4-1a where the emission from a diode glow discharge source is monitored via a scanning monochromator. A 4mm diameter disc was mounted onto

a direct insertion probe pictured in Figure 4-1b. A Macor shield was placed on the tip of the probe to prevent arcing. The metal cap was only used in work with the radio frequency glow discharge. Once in place, the probe was inserted into the vacuum chamber, a six-way cross with quartz windows. The emission from the glow discharge was measured from two positions, both head on and perpendicular to the surface of the cathode. The orthogonal setup is shown in Figure 4-1. In both configurations two quartz lenses, matching the f-number of the monochromator, were used to image the emission of the glow discharge onto the monochromator slit.

A scanning monochromator was employed (Spectrapro-500i, Acton Research, Acton, MA, USA) to collect the emission of the glow discharge. A 3600 grove/mm holographic grating was used to filter the light to a photomultiplier tube (Model R955, Hamamatsu, Bridgewater, NJ, USA). The current output from the PMT was amplified by either a small transimpedance amplifier (Model A-1, Thorn EMI, Rockaway, NJ, USA) or a low noise current preamplifier (Model SR570, Stanford Research Systems, Sunnyvale, CA, USA). Both were used interchangeably and will only be discussed further where their use affected experimental results. The signal from the preamplifier was collected by a gated boxcar (Model 250, Stanford Research Systems, Sunnyvale, CA, USA). The signal was then digitized and sent to a computer employing an analog-to-digital converter (Model 245, Stanford Research Systems, Sunnyvale, CA, USA).

To couple power to the cathode, the direct insertion probe had a high voltage vacuum feed-through. A high voltage dc power supply (Model OPS-3500, Kepco,

a)



b)

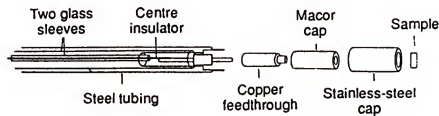


Figure 4-1. Instrumental configuration for emission studies.
a) Emission setup (axial); b) Direct insertion probe.

Flushing, NY, USA) powered the discharge in the continuous mode. The output of this high voltage source was modulated by an in-house pulsing circuit for any work involving pulse widths in the millisecond range. Two pulsed power generators were used throughout the microsecond pulsed experiments. The high power pulse generator from Velonex (Model 350, Velonex, Santa Clara, CA, USA) had similar performance to the IRC model (Model M-3k, Instrument Research Company, Columbus, MD, USA) and their use need not be distinguished from one another unless specified. The pulse power supply was capable of driving the glow discharge at up to 3.5 kV, but experiments were performed between 1 and 2.5 kV. The pulse width of the discharge varied between 2 and 300 microseconds, while the repetition rate was held between 1 and 5000 Hz. Little constraint was placed on the combination of these parameters as long as the duty cycle remained below 1%.

The temporal profiles of most transient signals, when not integrated by a boxcar, were displayed and recorded on a fast-sampling (2GSa/s), digitizing oscilloscope (Model 54542C, Hewlett-Packard Company, Palo Alto, CA, USA). The voltage of the high voltage power supply was measured via a 1000:1 high voltage probe. The current of the discharge was measured as the voltage drop across a 5.6 Ω high precision carbon resistor.

Ultra-high purity argon (99.995% pure, Airco, BOC group Inc., Murray Hill, NJ, USA) was used as the fill gas with no further filtering or gettering. Most analytical work was performed using NIST 490 series copper (various trace levels of materials), or discs cut from pure copper (>99.5% purity) sheet.

Temporal Considerations

The application of a 10 microsecond, 2 kV pulse to a copper cathode in a 1 torr argon atmosphere sets in motion a cascade of events. A highly energetic plasma is formed, generating atoms, ions and photons. The loss of the potential between the electrodes, at the termination of the voltage pulse, means the electrons are no longer accelerated and the plasma becomes non-self-sustaining, and quickly decays.

Using a scanning monochromator with a PMT only capable of measuring a very narrow bandwidth of the UV-Vis spectrum is not the most efficient means of monitoring pulsed discharge emission. A more suitable means of detection would be a direct reading spectrometer or a gated diode array. Only with such devices will the true, multi-element nature of the glow discharge be realized. However, a boxcar in conjunction with a PMT served adequately for these exploratory emission measurements.

The transient nature of the pulsed discharge and the method of signal collection are represented in Figure 4-2. The applied voltage starts at 0 Volts and rapidly drops to its peak value of negative 2 kV. The negative potential is maintained for a pulse width of 10 microseconds and is then removed. The slow falling edge is due to the RC constant of the glow discharge circuit. The next line represents the emission signal generated by the plasma. The temporal profile of the peak will vary depending on a number of experimental conditions such as pulse width and pressure. Therefore the delay time (t_d) and the width (t_w) of the data gate must be adjusted to match the emission signal. The third line represents the boxcar gate and determines what part of the signal is collected, integrated and recorded. Figure 4-3 shows the

temporal profile of the Cu I, 217.89 nm line in conjunction with the 2 kV pulse sustaining the discharge and the data gate. Atomic emission peaks just as the voltage pulse terminates.

The only reason one would want to deal with the added complexity of pulsing the discharge is if some analytical advantage were to be obtained. The microsecond pulsed discharge does have several potential benefits that have generated considerable interest. The primary trait of the pulsed glow discharge is the greatly enhanced emission from excited atoms and ions. Figure 4-4 depicts the emission of the Cu 324.7 nm spectral line in both pulsed and continuous dc modes. The pulsed discharge exhibits emission intensity 20 times greater than its dc counterpart. The pulse discharge also generates little other noise, so considerable enhancement in signal-to-noise and signal to background have been reported. Application of the pulsed mode to a Ti hollow cathode lamp (HCL) led to signal-to-noise improvements of 1000 times or greater for several emission lines.⁴⁰

The two main factors responsible for the increase in emission are shown in Figure 4-5. The dc discharge is powered using voltages between 800 and 1200 V. The pulsed glow discharge is can be operated at 1 to 3.5 kV. The current, shown to be 35 mA in this case, is close to an order of magnitude greater than during dc operation at the same experimental conditions. The unique plasma generated has the advantage of running at hundreds and even kilowatt levels of peak power generating intense emission, while the low duty cycle maintains lower average power levels than the dc mode. Essentially, the GD plasma is off for over 99% of the time. This leads to a

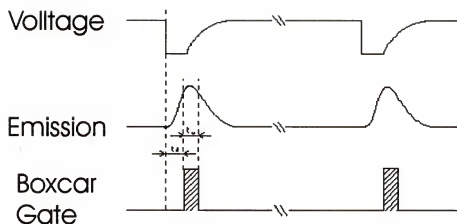


Figure 4-2. Pulsed signal collection.

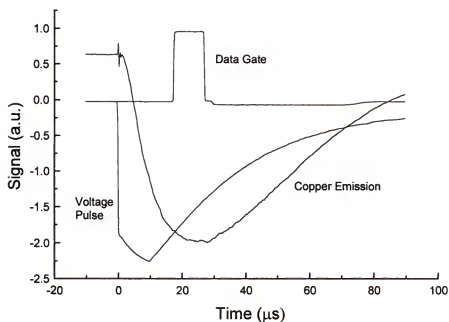


Figure 4-3. Temporal profiles of applied voltage, emission signal and data gate. Conditions: 2 kV pulse, 1 torr Ar, Cu I, 217.89 nm.

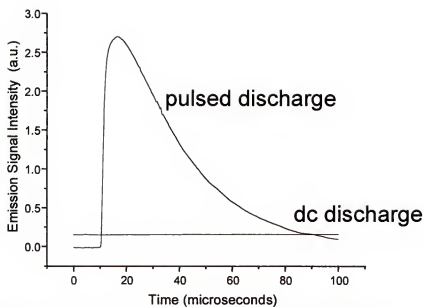


Figure 4-4. Comparison of pulsed and dc glow discharge emission. Conditions: Pulse: 2.5 kV, 3.5 torr Ar, dc: 1.2 kV, 5 torr Ar, Cu I, 324.7 nm.³⁶

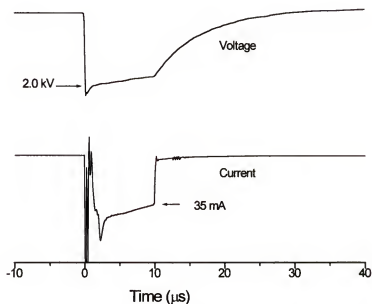


Figure 4-5. Voltage and current profiles for microsecond pulsed glow discharge. Conditions: 2.4 torr, 500 Hz, 10 μ s pulse width.

secondary advantage that the cathode does not heat up. This has improved analysis of certain elements prone to the thermal variation and should enhance the stability of the plasma during long periods of operation.⁴¹

Electrical Characteristics of the Pulsed Discharge

The glow discharge is essentially an electrical cell consisting of two electrodes immersed in an inert argon atmosphere. Like any electrical circuit, the glow discharge conforms to Ohm's Law. The relationship between the current and voltage is a useful means of classifying a gas discharge. Figure 4-6a shows three different discharges and their corresponding current-voltage relationships. When a sufficient potential is applied across a gas discharge cell the gas breaks down, forming ion-electron pairs. The voltage at which this breakdown occurs is marked V_b . The voltage needed to sustain the discharge is less than the breakdown voltage and is marked V_n .

After a short transition period, a luminous discharge is seen between the cathode and anode. This luminous plasma is referred to as the glow discharge. In the normal glow discharge regime, the plasma does not cover the entire surface of the cathode. As the current is increased, neither the voltage nor current density increases as the plasma spreads to cover the surface of the cathode. Once the cathode is covered, any increase in the current will result in an increase in the current density and voltage. A cartoon of this phenomenon is pictured in Figure 4-6b. When this happens, the discharge is said to be an "abnormal" glow discharge. Most analytical discharges, including those studied in this work, operate in the abnormal regime.

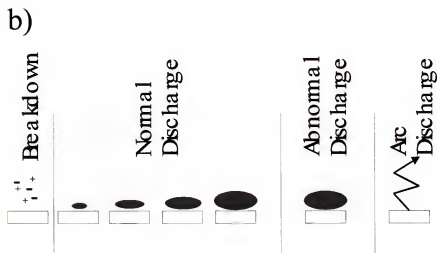
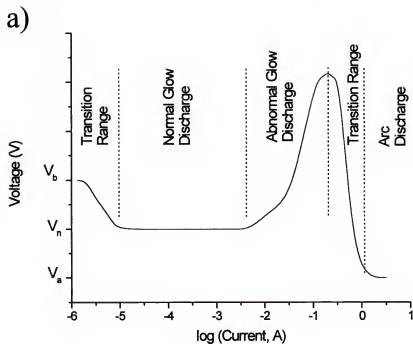


Figure 4-6. Characteristics of abnormal glow discharges.

a) Voltage-current relationship for gas discharges;⁴³ b) transition between normal and abnormal glow discharge operation.¹³

As the current is increased further, the cathode begins to heat up due to the increasing number of surface collisions with bombarding ion species. The heating of the cathode can be sufficient to cause thermal vaporization of the cathode. The increased number density of charge carriers and the high potential fields alter the i - V relationship of the discharge and the current is increased while requiring a lower voltage to operate (marked V_a). Shortly, the surface of the cathode is heated to the point that thermo-ionic electron emission from the cathode becomes prevalent. An arc discharge is formed, marked by a bright plasma and the vaporization of large amounts of the cathode material.

Arc discharges have been used effectively for trace elemental analysis of solids and have seen considerable of commercial success, peaking in the 1970s.⁴³ However, arc discharges have only modest precision and accuracy, producing quantitative results within 20-30%. The spectroscopy of the arc discharge is also complicated due to the thermal effects generated in the formation of its plasma. The primary advantage of the pulsed glow discharge is its ability to generate very high signals while maintaining the benefits of a glow discharge plasma.

The pulsed discharge is operated at up to amps of current and correspondingly high peak powers. In the initial stages of our research, it was necessary to determine that the plasma generated was a glow discharge and not an arc discharge. The current-voltage relationship was monitored in a 1.5 torr argon atmosphere. Figure 4-7 shows the response of the discharge current to changes in the voltage. The figure shows that an increase in voltage results in a linear increase in the current. This i - V relationship is indicative of the abnormal glow discharge as shown in Figure 4-6a. The pulsed

method allows much higher voltage and current to be applied to the discharge without forming an arc discharge. Therefore, we should expect the same performance from the pulse discharge as continuous discharges, only with the added benefits of greater emission and ion signals due to the more energetic plasma formed.

Two other observations suggest that the pulsed discharge, although obtaining currents similar to arc discharges, is a glow discharge. The diffuse, luminous plasma formed by the pulsed mode is typical of the glow discharge than the bright emission generated by arc discharges. Also, the pulsed discharge, with its low duty cycle, has shown evidence that it operates at a lower temperature than the dc discharge.⁴⁴ The process of the arc discharge vaporizes the cathode and is therefore subject to experimental deviations due to thermal effects. The pulse discharge does not show evidence that this is the case. Thermal sputtering effects, affecting the elemental analysis of such elements as zinc, are reduced in the pulsed discharge.⁴¹

Continuing the study of the current-voltage relationship within the pulsed discharge, the current was measured while the applied voltage remained constant and the pressure within the chamber was altered. A linear response, shown in Figure 4-8, was obtained. Since the strength of the emission of a plasma is often directly related to the current of the discharge, increases in voltage and pressure should result in greater emission.

Applying Ohm's Law, one can obtain a measure of the resistance of the glow discharge cell. Before the voltage is applied, the low pressure argon atmosphere acts as a poor conductor, with a resistivity (resistance \times area/separation) on the order of 10^{14} ohms-m.¹³ When the voltage applied to the cathode results in a dielectric

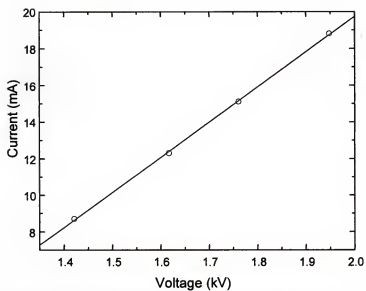


Figure 4-7. Relation between current and voltage at 1.5 torr Ar.

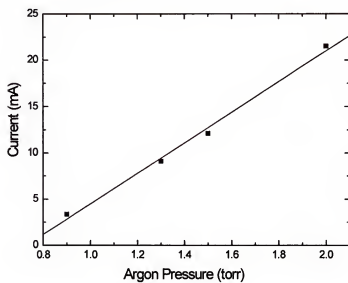


Figure 4-8. Relation between current and pressure at 1.6 kV.

breakdown of the gas, the plasma becomes a good conductor (approximately 10^3 ohms-m). The resistance of the discharge, based on the current and voltage experiments described, is plotted in Figure 4-9 for both constant pressure and voltage.

Parameter Studies of the Emission Signal

The performance of the any glow discharge is linked to its electrical characteristics and therefore, the effect of current, voltage and pressure should be measured. As expected, when the pressure of the cell is held at one value and the voltage applied to the discharge is increased, the emission increases. Figure 4-10 shows the effect of increased voltage on the temporal profile of a copper atom emission line observed axially. Increasing the voltage between 1 and 2.5 kV causes an exponential increase in the emission of the copper line. Because so little is known about the pulsed glow discharge, it was also important to understand what changes in experimental parameters would effect a change in the temporal profile of the emission and therefore hinder collection of the signal. The temporal profiles of the emission lines shown in Figure 4-10 all peak at the same point, indicating that once adequate gate conditions are set, alterations in the voltage should not affect signal collection.

Pressure has a similar effect on the pulsed emission. Increasing the pressure by a factor of two increases the emission signal intensity by up to a factor of ten. Figure 4-11 shows the emission intensity over a pressure range from 0.5 torr argon to 1.0 torr. An additional note about the temporal behavior of the discharge may be added. When the emission is observed axially (as in Figure 4-11), the emission signal is integrated

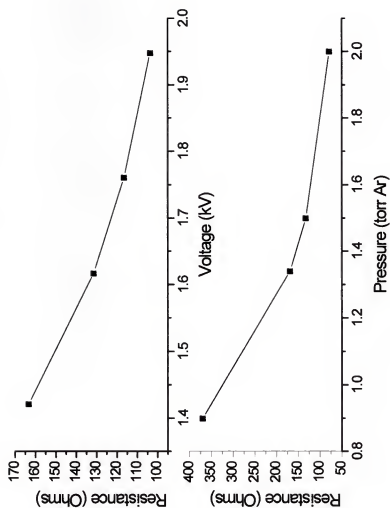


Figure 4-9. Calculated resistance based on i-V measurements.
a) Constant pressure, 1.6 torr Ar; b) Constant voltage, 1.6 kV.

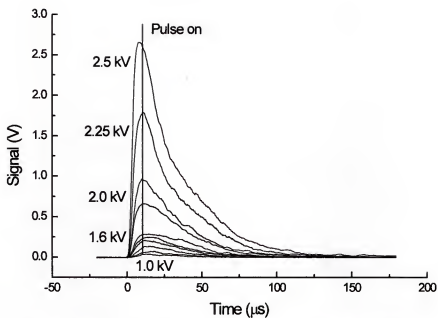


Figure 4-10. Effect of applied voltage on pulsed emission intensity.
Conditions: 0.8 torr Ar, Cu I, 218.17 nm.

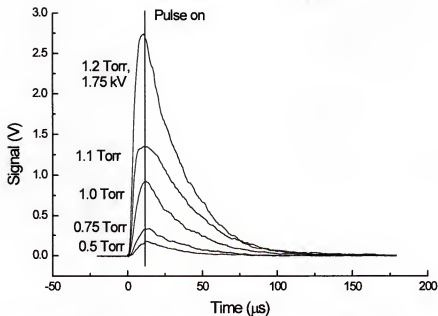


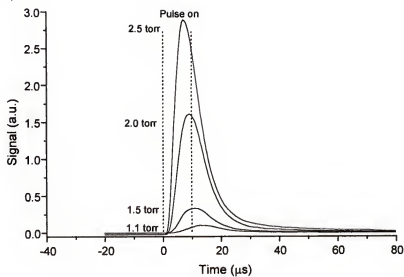
Figure 4-11. Effect of pressure on pulsed GD emission intensity.
Conditions: 2.0kV Cu I, 218.17 nm.

over the entire volume of the GD chamber and therefore shows little change in its temporal characteristics. However, increasing the pressure of the glow discharge visibly compresses the cathode dark space and negative glow regions the regions of the plasma.

The spatial compression of regions within the discharge could complicate the collection of the analytical signal when emission is measured orthogonal to the cathode surface. Figures 4-12a and 4-12b show the effect of increasing pressure on the orthogonal emission of copper atom and ion lines. Clearly, the mechanism responsible for generating the Cu II, 224.7 nm line is more sensitive to pressure changes. Monitoring the temporal profile of certain emission lines with regards to experimental parameters such as current and pressure could lead to a better understanding of the fundamental mechanisms responsible for excitation and ionization within the glow discharge. The ability of the pulsed discharge to alternate produce a transient population provides a means by which to study kinetic processes within the plasma.

The effect of pressure and voltage on a series of copper atom, copper ion, and argon ion lines were studied. The temporal profiles of these emission lines contain a very rich, but also complex, mix of data and will be discussed in the results section. Due to the change in the temporal emission profile when the pressure is changed, signals were collected while monitoring emission lines generated from the dc discharge. The dc emission results show the same trends, but lack the kinetic information that the pulsed emission provides.

a)



b)

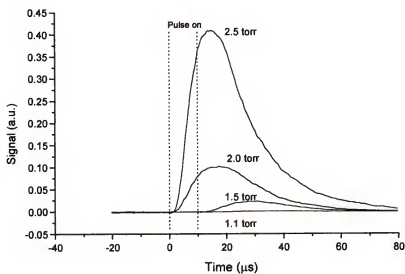


Figure 4-12. Effect of pressure on copper atom and ion temporal emission profiles. Conditions: 2 kV, 50 Hz.

a) Cu I, 324.7 nm line (1.0 n.d. filter); b) Cu II, 224.7 nm line.⁴⁵

Figure 4-13 is a plot of the emission signal of several different plasma species *versus* pressure. Each line in Figure 4-13 shows the relative increase in signal with respect to the emission intensity measured at 0.5 torr. The emission intensity of the copper species, both the atom and ion lines, shows a 90 fold or greater increase. When the pressure changes from 0.5 to 1 torr, the number density of argon increases by a smaller amount, thus the argon signal only increases by a factor of 16. Measurement of sputtering rates showed a slight increase in the sputtering rate when the pressure was increased. However, it was not commensurate with the increase in emission. A reasonable suggestion that accounts for the selectively enhanced emission of analyte over the gas species is that there is a finite volume, starting from the cathode and stretching out into the negative glow region, in which energetic collisions take place. 100 % of the sputtered species originate and diffuse throughout this region. As increases in pressure compact this region, the number density of analyte ions in this small region could play an important factor in the enhanced emission.

By increasing the applied voltage with the pressure kept constant, a similar trend in the emission of the different plasma species is seen. Figure 4-14 is a plot of the relative increase in emission, due to an increase in voltage. The increase in voltage produced an approximate doubling in argon ion emission intensity. On the other hand, the emission from the analyte species shows over an order of magnitude enhancement. As evidenced in the pressure studies, there seems to be a selective enhancement of the analyte emission intensity compared to the fill gas emission intensity.

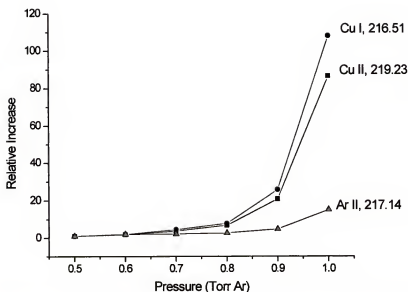


Figure 4-13. Relative increase in emission intensity from selected lines.
Conditions: dc: 800 V, Cu cathode.

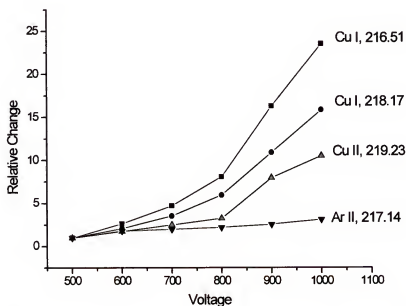


Figure 4-14. Relative increase in emission intensity from selected lines.
Conditions: dc: 0.9 torr Ar, Cu cathode.

The results show that high pressure and high power seem to selectively favor the atom and ion emission of analyte species while the argon emission increases by a less significant amount. Using dc power, an increase in voltage from 500 V to 1000V resulted in a greater than 20 fold increase in emission intensity. The pulsed glow discharge operates at voltages between 1 and 2.5 kV. The emission that is obtained in the pulsed GD mode shows a similar increase. In fact, the trend in the pulsed GD is the same as for the dc mode with the exception that due to the much higher power of the pulsed GD, the greatest enhancement in emission is from high energy species and ion lines.

Additional Characteristics of the Pulsed Discharge

The dc plasma is relatively easy to control because it only has two plasma parameters that can be altered, the pressure and power. The power is normally controlled by the applied voltage, since most power supplies operate in the constant voltage mode. However, constant current and constant power supplies are available. When the dc power is pulsed, the transient nature adds the pulse width and frequency as parameters, which must be characterized.

Frequency

The effect of frequency was measured by setting the monochromator to 216.51 nm and capturing the temporal profile on the digitizing oscilloscope. Figure 4-15 shows the emission generated by a 1.5 kV, 50 microsecond pulse as a function of

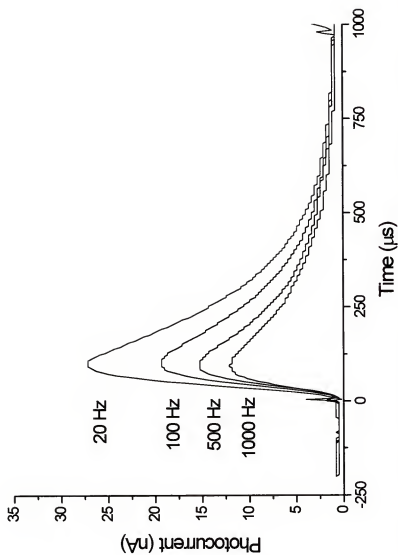


Figure 4-15. Frequency effect on atomic emission with Velonix power generator. Conditions: 50 μ s pulse, 1.5 kV, 1.0 torr Ar, Cu I, 216.51 nm.

repetition rate (20 and 1000 Hz). Over this range of frequencies, there is a trend for the emission to decrease with increasing frequency.

To test if the gas flow or pressure fluctuations were responsible for the decrease in emission when the frequency was increased, an experiment was designed using a hollow cathode lamp. The sealed environment of the hollow cathode lamp would eliminate any effects from gas flow or fluctuations in fill gas pressure. Figures 4-16a and 4-16b show the effect of frequency on an atom and ion line, generated by applying a microsecond pulse to a hollow cathode lamp. In both cases, the emission intensity between 20 and 1000 Hz showed a similar trend as the diode glow discharge. Even though a steady decline in emission signal is observed, the emission intensities between 20 and 1000 Hz only vary by a factor of two. If one considers the order of magnitude increase in intensity between the continuous and pulsed mode, the shift due to frequency is minor. Moreover, most experiments are performed at only one frequency, so this effect would not influence spectral results unless the frequency needed to be shifted during an analysis.

The cause of this loss in emission has not been determined with certainty. However, our experience seems to indicate that this is not a function of the plasma as much as it is a function of the power supply used to drive the glow discharge. Supporting this supposition is the data shown in Figure 4-17, which shows the peak emission intensity of the Cu I, 324.7 nm atom line and Cu II, 224.7 nm ion line as a function of frequency. While there is some difference in emission across the frequency range, the deviation is only 2-10% rather than a factor of 2 to 3.

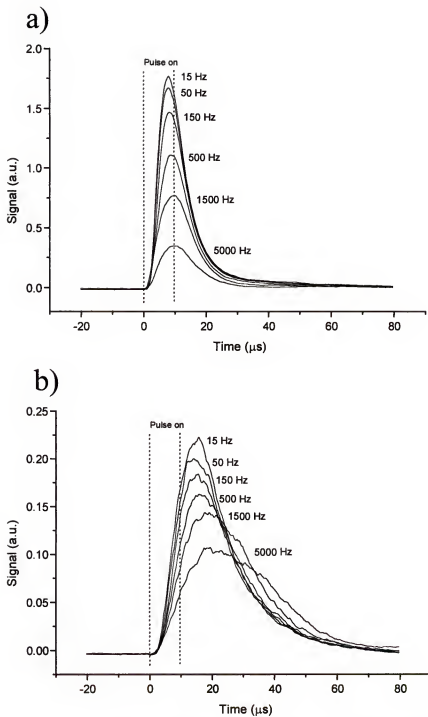


Figure 4-16. Frequency effect on copper atom and ion emission lines of a hollow cathode lamp. a) Conditions: 2.1 kV, 2.4 torr, Cu I, 324.7 nm; b) Conditions: 2.0 kV, 2.4 torr, Cu II, 224.7 nm.⁴⁵

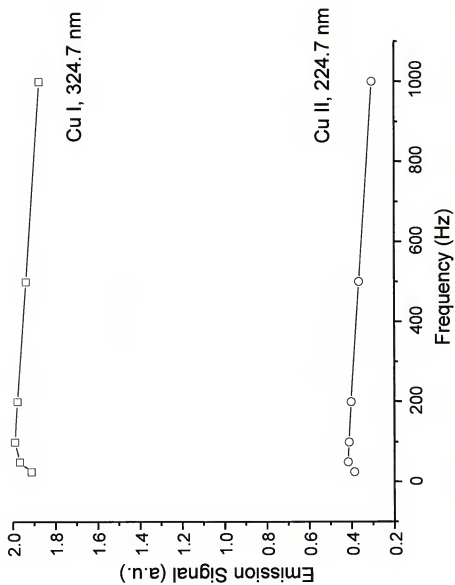
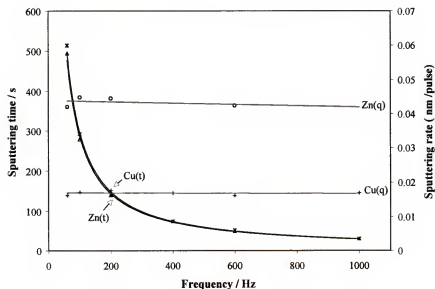


Figure 4-17. Frequency effect on atomic emission with IRCO power generator.⁴⁷

The difference between Figures 4-15, 16 and 17 is that the earlier data were taken using the Velonix power supply, whereas the latter used the IRCO power supply. The IRCO generator, which is based on solid state technology, has a more stable output than the Velonix generator which is predominantly based on vacuum tube technology. In most experiments, the frequency is held constant, and therefore, the frequency response does not affect analysis. Regardless of which power supply is used, the deviation over the frequency range is small and is reproducible enough to be corrected for if needed. Thus it can be reasonably argued that altering the frequency would have only a small effect on analysis.

Control of the frequency is most important where thin layer analysis is concerned. A high frequency will remove a large amount of material in a small time, whereas, a low frequency results in low sputter removal. The analysis of layers varying in thickness could demand a change in the frequency of operation used over the course of an analysis. Using the IRCO power supply, the change in signal is so slight that it could probably be ignored altogether. With the Velonix supply, the change in emission due to a change in frequency is reproducible enough that a small correction factor could be used to adjust the data. We have recently reported the use of frequency to control the time needed to sputter through a deposited layer.⁴⁷ Using the IRCO power supply in conjunction with a Grimm-Type source, the time to sputter-remove layers of copper and zinc on steel were measured. Figure 4-18a shows the sputtering time vs the frequency as well as the sputtering rate. When a layer is sputtered away, the emission signals of the top and bottom layers intersect at the

a)



b)

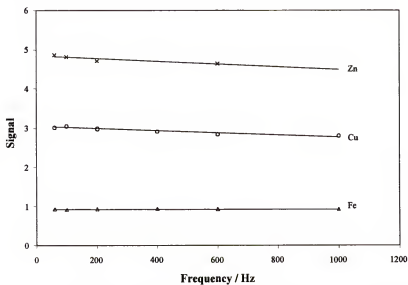


Figure 4-18. Effect of frequency on pulsed Grimm-glow discharge processes. a) Frequency effect on sputtering rate; b) Frequency effect on emission intensity.⁴⁷

midpoint of the layer. The sputtering time was defined as the time, in seconds, that it took to reach the crossing point. If frequency has little effect on the plasma, as we suggest, then doubling the frequency should result in a 50% decrease in the sputtering time. The data shows that operating the discharge at 200 Hz results in a sputtering time of 141 seconds. Doubling the frequency to 400 Hz results in a sputtering time of 74 seconds. As long as the other conditions of the glow discharge are held constant, the sputtering time and emission intensities (Figure 4-18b) remain relatively unchanged regardless of frequency between 60 and 1000 Hz.

Pulse Width

Unlike the frequency, the width of the voltage pulse applied to the GD has a large effect on the glow discharge plasma. Figure 4-19 shows the effect of increasing the pulse width between 2 and 200 microseconds on a copper atom line. Increasing the pulse width of the discharge has several different effects on the emission signal. Of course, the temporal profile broadens as the pulse width increases, but the emission intensity is shown to increase as well. The copper line shows a distinct post peak region that appears and grows more prominent at the longer pulse widths. This phenomenon is similar in appearance to ion profiles observed in mass spectrometry in studies of GD pulses in the millisecond regime. A considerable increase in the ion signal of the analyte just at the point of termination of the voltage was reported.⁵⁸

The change in pulse width has a very different effect on the Cu II 224.7 nm line (Figure 4-20). The emission of the copper ion line increases until just after the

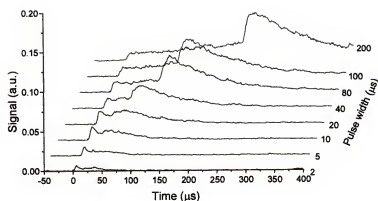


Figure 4-19. Pulse width effect on Cu I 521.8 nm line. Conditions: 2kV, 50 Hz, 2.4 torr.⁴⁸

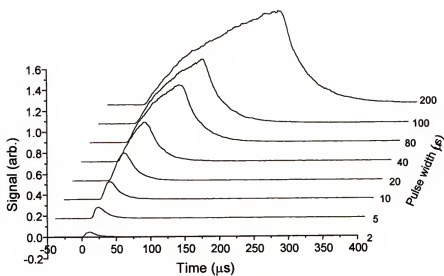


Figure 4-20. Pulse width effect on Cu II, 224.7 nm line. Conditions: 2kv, 50 Hz, 2.4 torr.⁴⁸

termination of the electrical pulse. There is a distinct difference compared to the copper atom line behavior seen in Figure 4-19. Unlike the effect of increasing frequency, which decreased emission intensity in the same manner for both atoms and ions, increasing pulse width affects atom and ion emission differently. This could be the result of the recharging of the capacitor of the pulse generator or could be the result of a fundamental process within the discharge. However, no conclusive evidence to indicate which factor is more plausible has been obtained. When the pulse width is increased, the voltage output is the same. Likewise, the pressure and current should not change either. Therefore, it is likely that the differences in the temporal profiles of the two lines display a fundamental effect and could be an indication of how the energy levels involved are populated.

Figures 4-21a and 4-21b show the effect of pulse width on two argon lines. The atom and ion line of argon show two distinct temporal profiles that differ from one another and from the copper lines. Kinetic data can be obtained from studying the effect of the pulse width. However, due to the complexity of the pulse width influence on the emission characteristics, it was decided that in-depth pulse width studies were beyond the scope of the present work. Alterations in the width of the pulse showed a complex, non-linear effect. The ten microsecond pulse width was chosen as a standard because it displayed stronger emission than the 2 and 5 μs pulses,⁵⁰ but did not show effects that mimicked the millisecond pulse, such as the 200 μs pulse. By keeping one pulse width, the temporal profile of many lines could be monitored and compared on the same basis. The temporal differences between gas, analyte atom, and analyte ion signals are also most easily observed with shorter pulse widths.

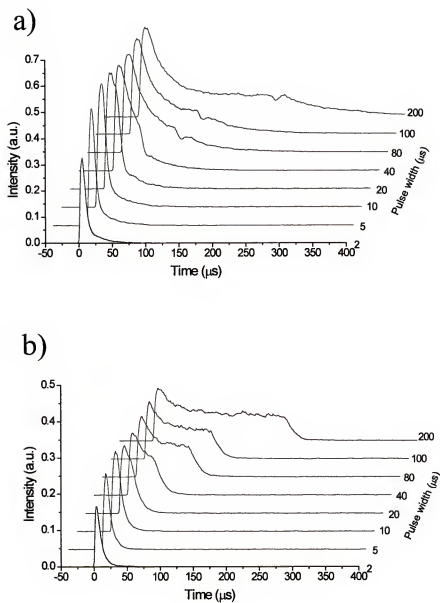


Figure 4-21. Pulse width effect on an argon atom and ion emission line.
a) 2kV, 2.4 torr Ar I, 696.5 nm; b) 2kV, 2.4 torr, Ar II, 294.2 nm.⁴⁹

In general, the pulsed glow discharge was operated with a 10 μ s pulse width and with frequencies between 200 and 600 Hz. The higher frequency sacrificed only a very small amount of emission intensity while allowing many pulses to be collected and averaged per second therefore improving S/N. The shorter pulse width showed the most distinction in the temporal profiles of the plasma species. In addition, shorter pulse widths may approach the same time scale as certain kinetic rates, allowing them to be studied in greater detail.

Results of Emission Studies

The application of a short duration, high voltage pulse creates a highly energetic, transient plasma. This energetic plasma has displayed two primary benefits for emission spectroscopy. The first benefit is the greatly enhanced emission possible in the pulsed mode. The second advantage is the temporal effects that are generated by the intermittent application of power to the discharge.

Enhancements in Emission Intensity

Figure 4-22 displays the emission from a copper hollow cathode lamp filled with neon. The lamp was first powered in the dc mode, generating the top spectrum and then the pulsed mode, which is shown on the bottom. The scales on the left of both spectra are equal. However the emission from the pulsed mode was first passed through a neutral density filter, which reduced the emission intensity by a factor of 100. The Cu I, 309.4 nm line, which shows an intensity of one volt during dc operation, showed an intensity of approximately 2 volts during the pulsed mode. Taking into consideration the filter, the peak pulsed emission intensity is 200 times

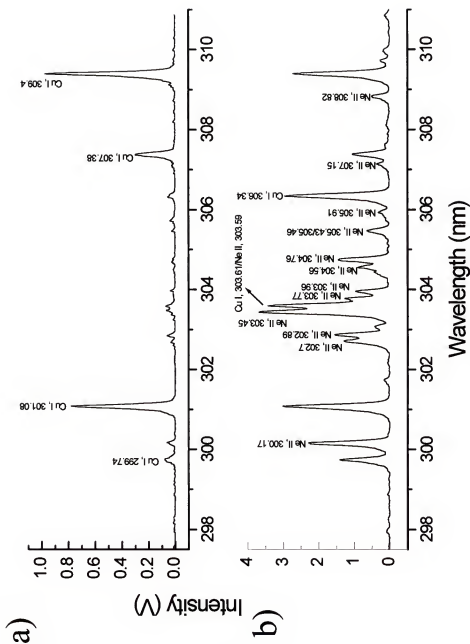


Figure 4-22. Comparison of emission spectra between dc and ms pulsed GD modes.

a) dc mode; b) Pulsed mode (1.0 n.d. filter).

greater than the continuous mode. The emission of all the lines within the pulsed discharge shows a similar increase in intensity.

Another feature of the pulsed spectrum is the prominence of lines that appear in the pulsed spectrum that are either minute or not even able to be seen within the dc spectrum. The higher energy plasma in the pulsed mode not only generates more emission in terms of intensity, but there are a number of additional lines that can be seen as well. Figure 4-23 shows the spectrum of a copper cathode in an argon atmosphere illustrating this effect. While the major emission lines are saturated in the pulsed spectrum, two copper atom lines (320.8 nm and 330.8 nm) that were undetectable in the dc mode appear. A number of argon lines appear in the pulsed spectrum. During our probing of the pulsed plasma, it was noticed that nearly every referenced emission line for copper can be seen in addition to several lines that were not positively identified. However, lines originating from fill gas species show increased emission as well, although not to the same extent. The abundant emission of these weak emission lines and lines originating from gas species could serve a useful diagnostic purpose, by allowing the study of many transitions within the glow discharge which are not able to be detected in the dc mode. Likewise the emission from the gas species may offer insight into the function of GD phenomenon. However, the number of emission lines within the discharge originating from both the sputtered matrix and fill gas could overlap with lines from other elements of interest within the sample. Trace analysis could be assisted by the increased emission only to be hampered by spectral overlap. One would consider the alternative of mass

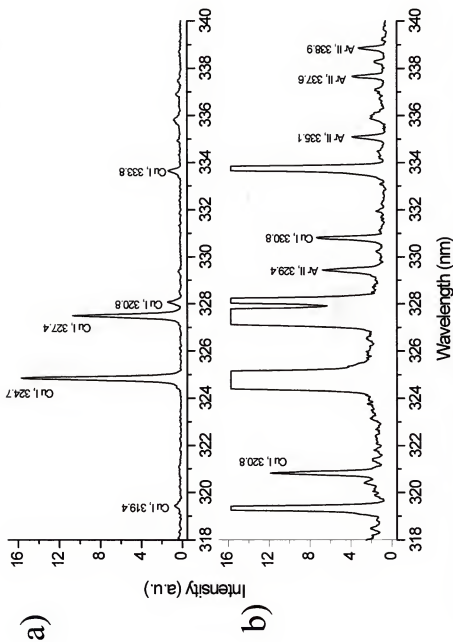


Figure 4-23. Comparison between dc and pulsed emission spectra in argon atmosphere.
a) dc mode; b) pulsed mode.

spectrometry, with its low spectral overlap and simple spectra to be a natural direction for this research. It is generally possible to find spectral lines that do not have spectral overlap. High resolution spectrometers capable of resolving the spectral lines are another option. Finally, the pulsed discharge may assist in offering temporal resolution of lines originating from sputtered and gas species.

Another feature of the pulsed discharge emission is that the background does not increase to the same extent as the emission enhancement. This results in a considerable increase in signal to background. Depending on the line used, signal-to-noise increases from several hundred to several thousand have been obtained.³⁹ To illustrate this effect, the continuous and pulsed modes are compared in the region between 500 and 600 nm (Figure 4-24). The standard deviation of the background noise measured between 540 and 545 can be compared between the dc and pulsed modes. The dc mode shows a 27% rsd, whereas the rsd of the pulsed glow discharge is only 13 %. Moreover, the emission from the pulsed discharge is nearly an order of magnitude greater as evidenced by Cu I, 521.8 nm line. Finally, several lines that cannot be seen in the dc mode appear in the pulsed spectrum; Cu I 529.3, Ar 565.1, Cu I 570.0, and Cu I 578.2. The pulsed mode offers increases in signal, greater signal to noise, and populates many weak lines that are not able to be seen in the continuous mode.

Temporal Effects

The transient nature of the glow discharge has shown several characteristics, which could either improve its performance for emission spectroscopy, or allow

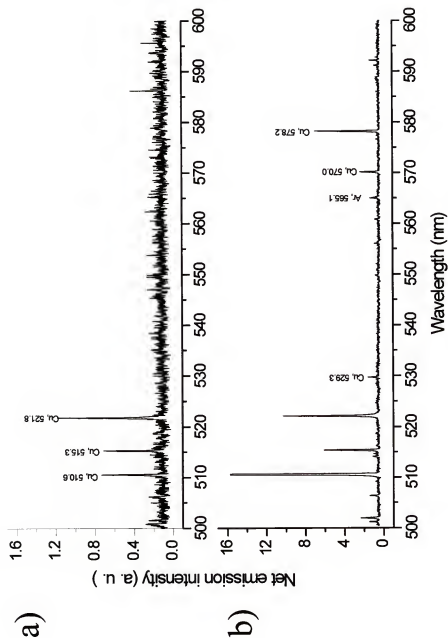


Figure 4-24. Spectral comparison between dc and pulsed GD at 2.4 torr.
a) dc: 720 V, 3.9 mA; b) Pulsed: 2.2 kV, 500 Hz.⁴⁵

certain fundamental effects to be studied. By disturbing the chemical equilibrium of the system with a high voltage pulse and then allowing the system to relax, information concerning the initiation and decay of the plasma can be monitored. This leads to a better understanding of what role certain mechanisms play within the plasma. Taking full advantage of the temporal nature of the pulsed plasma will result in optimized operating conditions. Figure 4-25 shows the temporal profiles of several argon and copper atom lines in a 1 torr, 1.5 kV glow discharge. Both argon lines peak at the same time. All three copper atom lines peak together, but at a time 5.5 microseconds later than the argon species. This indicates that the mechanism for the excitation of these lines is different. A general pattern emerges when a number of sputtered atom, sputtered ion and gas species lines are observed.

Figure 4-26 shows the temporal profile of the 4 major discharge species indicating the general behavior of these lines. The graph shows that Ar II lines peak first. The primary mode of excitation of argon ions would be electron impact ionization. This would take place immediately in the plasma as electrons are accelerated toward the anode. Once the power is turned off, the electrons that remain no longer have the driving force of the potential field and they lack the energy to ionize argon. Like the argon ions, the argon atoms form almost immediately. Excited argon atoms can be formed by a number of different mechanisms, mainly electron and fast atom impact. Some electron impact excitation is evidenced by the very rapid rise time of the argon atom emission peak, although the fact that argon atom lines peak at a later time indicate other mechanisms are at work.

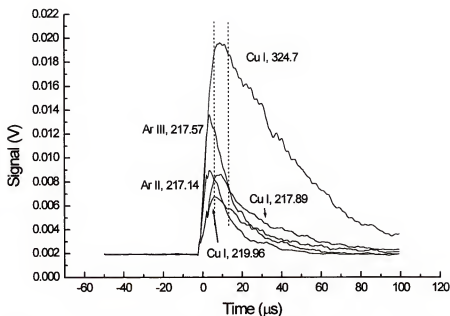


Figure 4-25. Temporal profiles of copper and argon lines.
Conditions: 2kV, 1 torr.

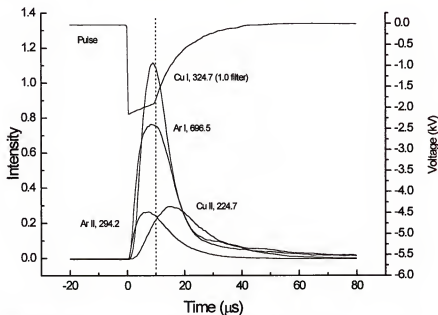


Figure 4-26. Examples of temporal trend of Ar I, Ar II, Cu I and Cu II lines. Conditions: 500 Hz, 10 microsecond pulse width.

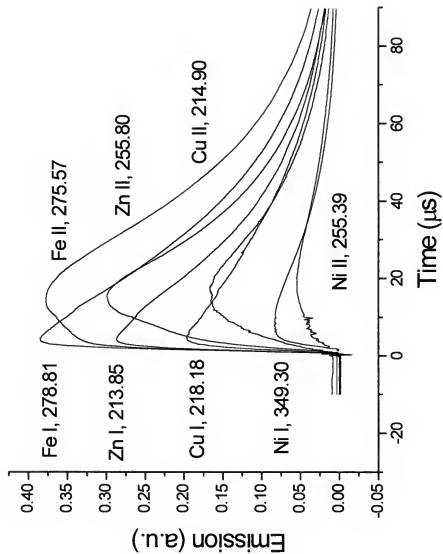


Figure 4-27. Temporal trends of atomic and ionic emission lines for several elements.

Atoms of the analyte must first be sputter-removed from the surface before being excited. Therefore, the rising edge of the copper atom emission has a slight delay. Some copper atoms are excited by electron impact, but the primary means of excitation is thought to be collisions with other energetic species within the discharge. The temporal profile for atomic emission reaches its peak just as the discharge is turning off. In longer pulses, such as in Figure 4-19, there is a distinct peak at the termination of the voltage pulse. The final plasma species displayed are copper ions. The primary mechanism thought responsible for sputtered ion formation is Penning ionization. Penning ionization consists of collisions with long-lived metastable atoms of argon. The temporal profile of the copper ion line seems to support this theory. The ion signal peaks several microseconds after the pulse is turned off. Since the metastable atoms are long lived, perhaps a millisecond or so, they will be available to ionize sputtered species long after pulse termination. It has been proposed that the metastable population is greatest at pulse termination since the processes such as electron impact, which depopulate the metastable state do not operate once the power is terminated.⁵¹

This phenomenon, regarding the temporal profiles of different species, is not limited to copper. Figure 4-27 shows the temporal profiles of 5 atom and 5 ion lines originating from several different bulk samples. All of the atomic lines peak during the application of the pulse voltage; yet, all of the ion emission signals peak several microseconds after the pulse termination. This distinction in the temporal profiles could potentially enhance the sensitivity of certain lines. By choosing an appropriate delay and width for the data gate, gas species could be discriminated against. This led

to further investigation with the time-of-flight mass spectrometer, as discussed in the next chapter. In addition to the discriminatory temporal effects, the potential to study the kinetics of different mechanisms of the discharge still remains.

CHAPTER 5 PLASMA DIAGNOSTICS

Emission spectroscopy, while sometimes less sensitive and spectrally more complex than mass spectrometry, offers certain opportunities which mass spectrometry does not. Emission spectra of atomic and ionic species provide a wide range of diagnostic information about plasma behavior.

Absorption, Diffusion and Sputtering

Some insight into the function of the plasma may be gained by understanding how material is removed from the cathode and is transported throughout the chamber. Emission spectroscopy provides temporal profiles of the population of certain excited states, while absorption spectroscopy allows the population of the ground state to be monitored.

A copper hollow cathode lamp was positioned perpendicular to the surface of the cathode. A lens was used to focus the beam to a 2 mm spot directly in front of the GD cathode. On the opposite side of the vacuum chamber, a second lens was used to collect and focus the beam from the hollow cathode onto a monochromator slit. The signal from the PMT of the monochromator went to a preamplifier before being displayed and recorded on the digital oscilloscope. The absorption measurements were made by measuring the transmittance of the hollow cathode through the pulsed

discharge. The spectrometer was set to the 324.7 nm copper line. As copper atoms are generated by the pulsed discharge, they will be sputtered from the surface and diffuse into the sampling region. Atoms within the beam of the HCL will absorb the HCL radiation. The attenuation is related to the population by Beer's Law.

Figure 5-1 shows the signals generated by the hollow cathode lamp and glow discharge. When the slit is blocked, no light enters the monochromator and the 0% transmittance position is marked. The hollow cathode lamp is then turned on, with the slit uncovered. The signal response marks the 100% transmittance mark. When the pulsed discharge is activated, there will be a short emission peak from plasma species, followed by a decrease in the HCL signal. The decrease is the absorption signal. Finally, with the hollow cathode off, the glow discharge is run, generating an emission signal at 324.7 nm.

To measure absorption, the emission signal (GD only) is subtracted from the signal generated from the HCL and the glow discharge (GD + HCL) to correct for the emission peak. The HCL signal marked the 100% transmittance and the blocked slit marked the 0% transmittance level, with the modified GD + HCL signal acting as the measurement of absorption. These numbers are then converted to % transmittance. The transmittance is converted to absorbance units by the equation: $A = -\log(T)$.

Figure 5-2 shows the temporal profile of the Cu I 324.7 nm emission line intensity compared to the temporal profile of the absorbance signal. The emission signal, while strong, reflects only a small part of the total atomic population generated. Choosing experimental conditions that maximize the use of the sputtered material is critical in achieving the best analytical performance. Understanding the transport and

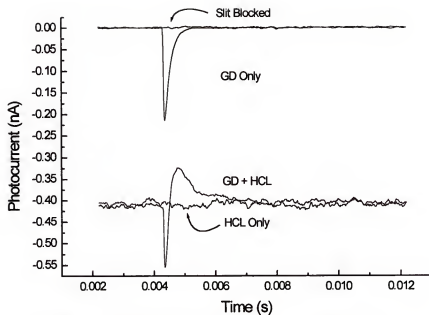


Figure 5-1. Emission signals used to calculate absorption measurements.

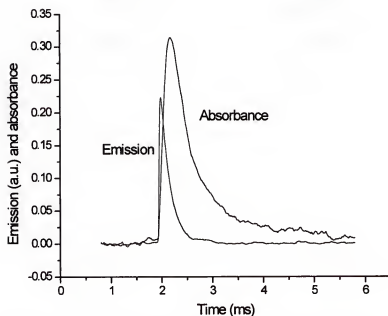


Figure 5-2. Temporal profile of atomic emission and atomic absorption. Conditions: 2.25 kV, 1 torr Ar, Cu I, 324.7 nm.

behavior of the sputtered material is useful in optimizing the utility of the glow discharge.

In previous chapters, we have mentioned that the voltage of the discharge plays an important role in the strength of the emission signal. The increase in the potential field accelerates electrons, which achieve higher energies and form a more energetic plasma, resulting in more ions. The potential field has a similar, though lesser, effect on ions in the discharge. Not only are more ions formed, but due to the stronger electric field, these ions strike the cathode surface with more energy. Figure 5-3 shows the effect of increasing the discharge voltage on the absorbance signal. The growth of the absorbance signal in addition to the increases in emission intensity indicate that increasing the discharge voltage enhances both the amount of sputtered material removed and the efficiency with which the material is excited.

Absorbance measurements may also assist in understanding how material is transferred throughout the chamber. As indicated earlier, the hollow cathode was focused right in front of the discharge cathode. The beam diameter was about 2 mm at the focal point, indicating the region between the surface and 2mm into the discharge was measured. To achieve spatial measurements, the direct insertion probe was moved back and forth to sample different regions within the discharge. With 0 mm marking the original position of the GD cathode, where the HCL beam samples the area from the surface of the cathode to a point 2 mm into the plasma, the direct insertion probe was then backed away in increments of 1 mm. Figure 5-4 shows the absorbance vs the distance the cathode was moved. The temporal profiles indicate the diffusion of the material through the chamber.

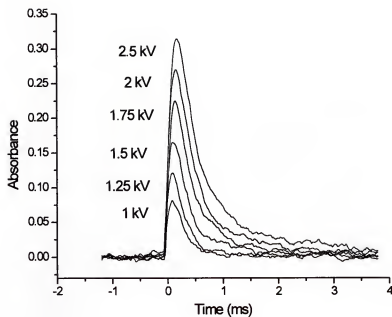


Figure 5-3. Absorbance of the pulsed GD with respect to voltage.
Conditions: 1 torr Ar, 10 μ s pulse.

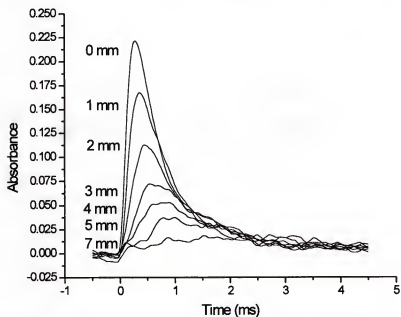


Figure 5-4. Absorbance measurements with respect to distance from the cathode. Conditions: 1.5 kV, 1 torr Ar.

To understand the effect of pressure, the same diffusion study was repeated at 3 different pressures, resulting in the data shown in Figure 5-5. Lowering the pressure lowered the absorbance signal. This indicates a smaller number density within the HCL probe volume, which in turn suggests a lower sputtering rate. By examining the absorbance profiles with respect to time and distance, the diffusion of the sputtered material can be studied. At 0.5 torr, the absorbance traces at each distance peak very near the same time. At 1 torr, an increasing delay in the time needed to reach the peak absorbance is observed as volumes further from the cathode are probed. Thus, the effect of pressure on the diffusion of material may be investigated.

The temporal profiles of the absorbance may also be compared to the emission profiles for atoms and ions. As mentioned earlier, the pulse width displayed a very complex effect upon the emission intensity of both copper atom and ion lines. Absorbance measurements were taken to test if the pulse width influenced the amount of material that is removed. Figure 5-6a shows the emission intensity from a copper atom line at 20 Hz while varying the pulse width. Recall, at lower frequencies, the pulse width had a much greater effect on the emission intensity while powering the GD with the Velonix pulse generator. Figure 5-6b shows the absorbance measurement of the ground state line of copper with respect to pulse width. Figure 5-6 shows how the ground state population relates to the excited state of the copper emission line.

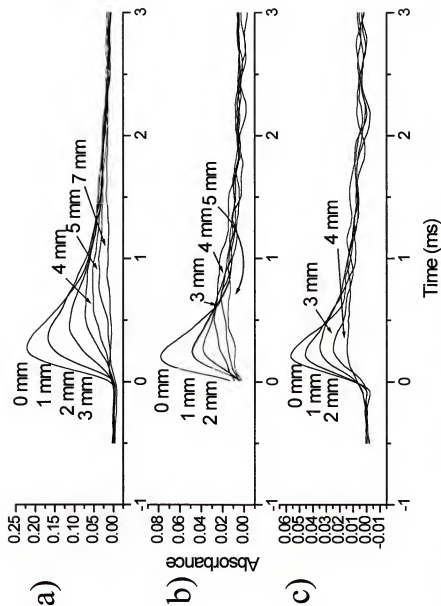


Figure 5-5. Absorbance measurements of the pulsed discharge with respect to distance and pressure. a) 1 torr; b) 0.7 torr; c) 0.5 torr.

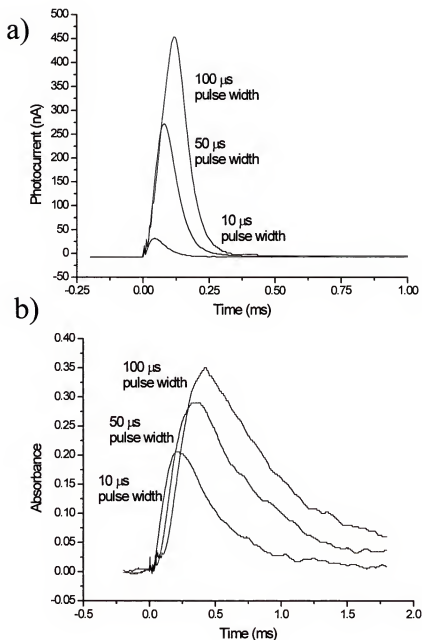


Figure 5-6. Temporal profiles of atomic emission and absorbance with respect to pulse width. Conditions: 1.5 kV, 1 torr Ar, 20 Hz..
 a) Emission Cu I, 216.51 nm line; b) Absorbance of ground state atom line.

To contrast the temporal profile of the atom emission line intensity *versus* the ground state population, the data in Figure 5-7 were collected. These data displays the copper ion emission from the 219.23 nm line. Figure 5-7a displays the ion emission intensity at three different pulse widths compared to the absorption of the ground state atom line generated while measuring the emission.

When the copper atom emission, ion emission, and absorbance signal of the ground state atom are plotted together, a pattern develops. Figure 5-8 shows traces of these three signals. The copper emission signals have been normalized. The pattern of the two emission signals has been seen before, where the peak of the ion line is delayed from the atom line peak. It is suspected that this is due to Penning ionization of the copper atoms by argon metastable atoms in the "after peak" region. An interesting observation can be made regarding the temporal profile of the ion emission. Both the ion emission and the absorbance signal seem to have the same shape. However, the emission signal has a shorter temporal profile and different shape. One would expect that the ion profile would mimic the atomic concentration, since the primary ionization mechanisms involve collisions, the frequency of which would be influenced by number density. With more atoms in the discharge, more ionization collisions can take place. Since the atomic emission profile does not seem to mimic the absorbance profile as closely, could the mechanism for atomic emission of the atom line involve processes which are not as concentration dependent? The higher electron density in the pulsed discharge may suggest that electron impact excitation may play a larger part in the excitation of certain lines than previously thought.¹⁷

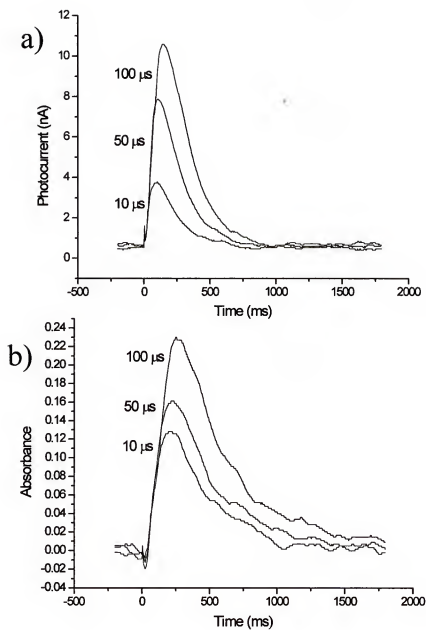


Figure 5-7. Temporal profiles of ionic emission and absorbance with respect to pulse width. Conditions: 1 torr Ar, 100 Hz.
a) Emission 1.75kV, Cu II, 219.23; b) Absorbance of ground state atom line.

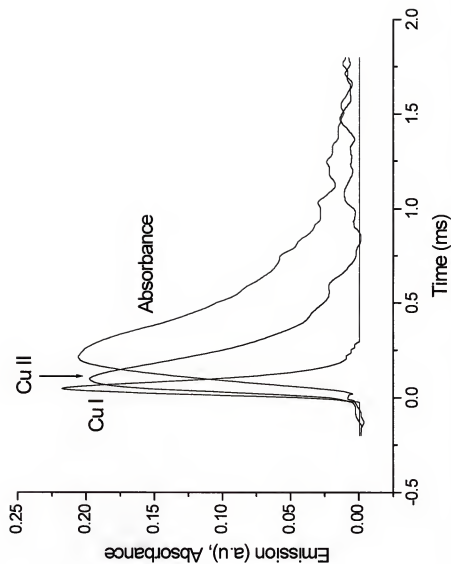


Figure 5-8. Temporal profiles of atomic and ionic emission compared to the absorbance signal of ground state atoms. Conditions: 1.6 kV, 1 torr Ar, 20 Hz, Cu I, 324.7 nm, Cu II, 219.23 nm.

Supporting this hypothesis, just as the electrons disappear at the termination of the pulse, the atomic emission reaches a maximum. Another curiosity is that the ion emission lags behind the atom emission, indicating that ions are formed later in the discharge process. For instance at the 250 microsecond mark in Figure 5-9, strong ion emission is seen, while the atom emission has almost completely died away. If ions, which require a great deal more energy to form than excited atoms, are being formed, why is there not strong emission from copper atoms at 250 microseconds? The only explanation is that the collision partner responsible for the excitation of atoms is missing. While the process responsible for excitation is absent, the collision partner responsible for ionization selectively ionizes rather than excites analyte atoms.

Earlier, it was mentioned that increasing the frequency resulted in a slight decrease in emission intensity. This effect is either a fundamental property or an instrumental effect. Using a series of brass samples (70/30 Cu-Zn brass, Alfa Aesar 13504), the sputtering rate was measured over a range of frequencies. Weight loss measurements were taken after 40 minutes of sputtering. Figure 5-9 shows the results of this study.⁵² A sharp decrease in the sputtering rate was observed when the discharge was operated at 1000 Hz. To study this phenomenon further, absorbance measurements were taken (Figure 5-10). Absorbance measurements were taken using a copper cathode. When the pulsed discharge was operated between 20 and 500 Hz, the pulsed glow discharge generated a discrete, stable, reproducible packet of atoms with each pulse, regardless of frequency. However, as the frequency approaches 1 kHz, the generation of atoms declines. The trace of absorbance at 1 kHz shows a distinct decrease in the amount of atoms formed. This effect is likely a function of the

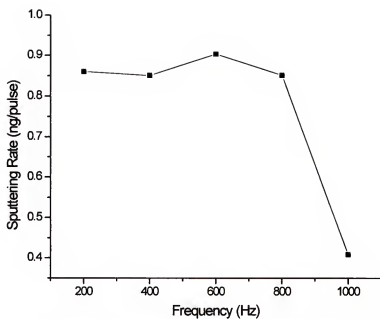


Figure 5-9. Sputtering rate of the pulsed glow discharge for a range of operating frequencies. Conditions: 10 μ s, 3 torr, 1400 V, 20 minute of sputtering.

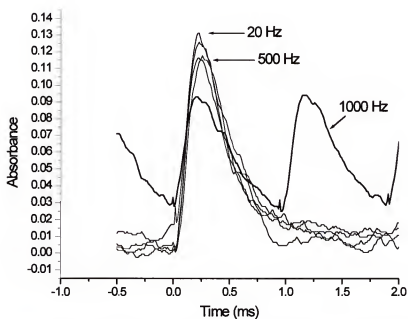


Figure 5-10. Absorbance signal of ground state copper atoms for a range of operating frequencies. Conditions: 1.5 kV, 1 torr Ar.

capacitor charging time of the high power pulse generator. At 1000 Hz the absorbance signal from each pulse overlaps. At this time it is not known what effect the overlap of atoms will have on the performance of the GD.

Measurement of Rotational and Excitational Temperatures Within the Plasma

Temperature is a direct measurement of energy, therefore there has been quite an interest in determining the temperature of plasmas. There are several means of measuring the temperature of a plasma using optical spectroscopy. However, measurement of temperature depends on the plasma volume being tested to be in local thermodynamic equilibrium (LTE). For a plasma to be in LTE, the rate of collisional deactivation must be much greater than the radiative deactivation. If this condition is met, the excitation temperature should equal the vibrational, rotational, kinetic and thermal temperature of the plasma. Unfortunately, for analytical glow discharges, a major mechanism for deactivation is radiative decay, resulting in the characteristic glow of the discharge.

The temperature, as determined optically, is based upon measuring the relative intensities of selected emission lines and then correlating them to their energy levels and transition probabilities. Optical measurements are based on a Boltzmann distribution, which assumes LTE. Because the GD plasma is not in LTE, optical measurement of the temperature will yield different results based on the species being investigated. Therefore, monitoring atoms, ions, electrons, or molecules will result in different excitational, vibrational, and electronic temperatures. As long as the limitations of these measurements are understood, the temperatures obtained can have

a certain diagnostic value by reflecting the distribution of atomic or ionic populations, as well as indicating the energetics of the plasma. Thus, such temperature measurements are often used to compare different atomic emission sources.

The rotational temperature of a molecule is often assumed to be a close reflection of the gas kinetic temperature. The low energies of the rotational transition and the rapid exchange between the rotational and kinetic energy of a molecule have led to the use of several molecules as monitors of gas temperature. Molecular bands of OH, O₂, N₂⁺, and CN are the most common molecules used because the force constants and equilibrium bond lengths for different excited levels of these molecules are well known. Likewise, the emission lines of iron in the 372-377 nm region are often used to measure excitation temperatures. The temperatures measured were obtained from the slope of a Boltzmann plot. The method for obtaining such measurements is covered in several reviews,^{4,13} and the specific experimental details of this study have been published.⁴⁴

Using the R branch transitions of the N₂⁺ band emission at a pressure of 1.5 torr argon and 0.3 torr nitrogen, rotational temperatures for the continuous dc (2.5 W) and rf (60 W) plasma were determined to be 550-650 K and 550 K, respectively. Temperatures between 400 and 450 K were measured for the microsecond pulse mode. Altering the pressure between 0.6 to 3.0 torr for all modes and altering the frequency (10 to 500 Hz) of the pulsed mode did not change the measured temperatures. This study showed that there was a clear difference between the microsecond pulsed mode and the dc which was independent of pressure and frequency.

The continuous dc mode has a duty cycle of 100%, whereas the pulsed mode has a greatly reduced duty cycle. One means of increasing the duty cycle and therefore bridging the gap between the pulsed and dc modes would be to increase the frequency. However, increasing the frequency did not alter temperature measurements. The only other means of increasing the duty cycle is to increase the pulse width of the discharge. Figure 5-11a shows the results of increasing the pulse width while firing the microsecond and millisecond discharge at 30 Hz. A sharp rise in temperature is noticed when the pulse width is increased, up to 1 millisecond. Pulses of 1 ms or greater show little increase and have a similar temperature to the dc mode. This data would seem to indicate that some form of equilibrium is reached within 1-2 ms of the discharge initiation. In contrast to the rotational temperature, the excitation temperature calculated from the Boltzmann plot of FeI emission showed no change in temperature with an increase in pulse width. Figure 5-11b shows the results of this experiment. A constant temperature between 3600 and 3900 K was found for the dc, millisecond pulsed, and microsecond pulsed glow discharges.

The change in the rotational temperature indicates that it takes 1-2 milliseconds to reach equilibrium. The lack of a change in the excitation temperature suggests that the particular interactions that dominate excitation processes maintain their relative roles in the microsecond, millisecond and continuous dc operation. This may seem contrary to results, which have already been discussed, such as the huge relative increase in certain ion and atom ratios observed in the pulsed emission spectra. However, due to the lack of LTE, the excitational temperatures are only true for the lines that are measured.

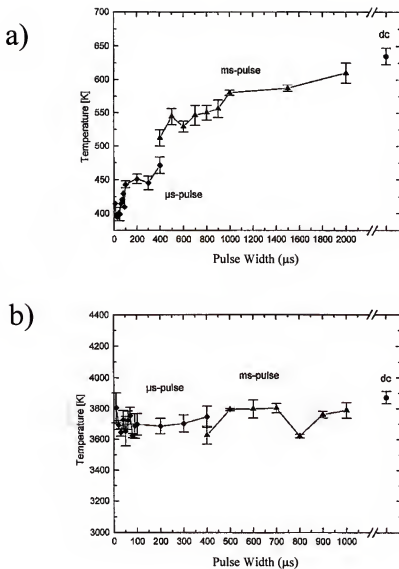


Figure 5-11. Glow discharge plasma temperature measurements as a function of duty cycle. Conditions: Microsecond pulsed 100 W/peak, 30 Hz; ms-pulsed 0.25 W, 30 Hz; dc 2.5 W.
 a) N_2 rotational temperature of μs , ms, and dc discharge; b) Fe excitation temperature of μs , ms, and dc discharge.⁴⁴

Electrostatic Probe Measurements of the Glow Discharge Plasma

In the glow discharge, the primary region of interest for the analytical chemist is the negative glow region. It is here that most optical measurements are made, as well as sampling into a mass spectrometer. The species present in this region consist of neutral gas species and sputtered atoms, ions of both, and electrons. From a diagnostic standpoint, both MS and AES have the limitation of reporting results that are the average values of relatively large plasma volumes. Electrostatic probes allow measurement of local regions within the discharge and were used for a series of diagnostic measurements.

The probe consisted of a 0.245 mm diameter tungsten wire. This wire was fed through an insulated vacuum probe. A 4.5 mm length was exposed to the plasma, resulting in a surface area of 0.212 mm^2 . Two power supplies were used to apply a potential to the probe. A function generator was used to apply a $10 V_{pp}$, saw-toothed wave to the probe, while a second power supply was used to create a dc offset for this wave. The GD chamber was a stainless steel six-way cross and was filled with 1 torr argon. The GD cathode was a copper disc, 4.5 mm in diameter. Figure 5-12 shows a cartoon of the experimental set up.

A dc power supply (HP 6131) and function generator (HP 3325A) were used to apply a potential to the electrostatic probe. A variable resistor was used to match the impedance of the probe. A digitizing oscilloscope (HP 54542C) was used to monitor the voltage between the GD chamber and ground, and to measure the current as the voltage drop across a 50 ohm carbon resistor. The probe was inserted into the vacuum chamber and was placed horizontal and centered to the cathode. The glow discharge,

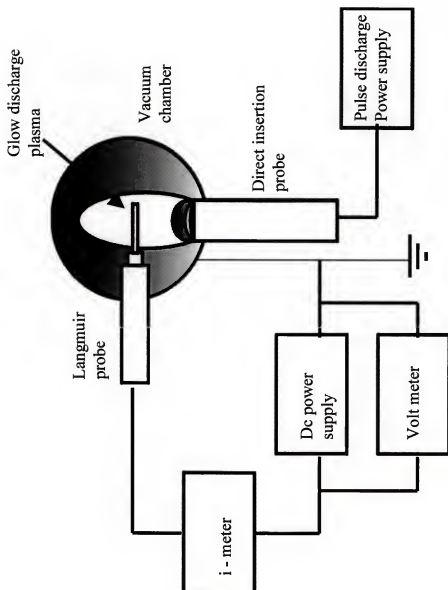


Figure 5-12. Experimental sketch for plasma diagnostics using an electrostatic probe.

whether the continuous dc mode or the microsecond pulsed mode, was operated as described earlier, with the exception that the chamber was floated with respect to common ground by insulating it from the table.

The theory of the use of an electrostatic probe is reasonably simple. However, some assumptions must be made. The work we have done assumes local thermal equilibrium within the plasma, even though experimental evidence has indicated otherwise. Likewise, interferences due to the cylindrical shape of the probe and shielding were not known and therefore not included in calculations. What remains is a simple comparison between the pulsed and dc discharge plasmas. With the above understanding, a contrast is made between the dc and pulsed plasmas in terms of their electron density and electron temperature. Despite the above limitations, reasonable data were obtained.

When an isolated probe is inserted into a plasma, species within the plasma will impinge upon its surface based on their flux. Since electrons have a much smaller mass than ions, the potential field across the cell accelerates them to a much higher degree. Due to their mobility, many more electrons will strike the surface of the probe, causing the probe to become negative with respect to the plasma. This effect creates a local electric field that will repel further electrons from the probe. If a voltage is applied to the probe and swept from negative to positive, ions and electrons can be selectively sampled. If the current to the probe is plotted against the applied voltage, data concerning the temperature and number density of the plasma is obtained. Moreover, since the electric field of the probe is quite small, only the local region of the plasma is disturbed while sampling. Thus electrostatic probes are

capable of giving spatially resolved information on the number density and temperature of the charge particles within the glow discharge while not disturbing the plasma.

Figure 5-13 shows a current-voltage diagram obtained for a dc discharge. The line segment AB corresponds to the ion saturation current. In other words, the negative voltage applied to the probe attracts ions to the surface until the flux of ions reaches a maximum. Along BC, the voltage of the probe allows electrons to begin to leak across the potential barrier based on their kinetic energy. CD is the region of the electron current saturation, where increasing the potential of the probe no longer results in the desired flux of electrons. The point marked V_f is the voltage that a floating probe will achieve. Note that the negative voltage corresponds to the potential at which the influx of electrons is matched by the potential barrier generated by these electrons striking the surface. The point marked V_p is considered the actual voltage of the plasma.

When the natural log of the current is plotted against the potential applied to the probe, the straight portion of the curve is related to the temperature. Figure 5-14 displays such a semi-log plot. The temperature is calculated by using the equation:

$$\text{Slope} = e/kT_e$$

Where e is the elemental charge of an electron (1.60×10^{-19} coulombs), k is Boltzmann's constant (1.38×10^{-23} J/K), and T_e is the electron temperature. The temperature calculated for a 750 V dc plasma using the above data is around 2700 K, which is about 0.23 eV. This corresponds well with values reported in the literature.^{4,13}

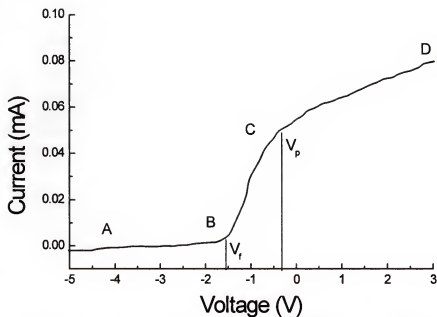


Figure 5-13. Current-voltage measurements with an electrostatic probe.

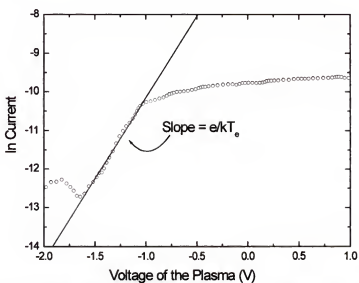


Figure 5-14. Method of electron temperature measurement based on Langmuir probe measurements.

Electrostatic probe measurements were first applied to the dc plasma to form a base for comparison with the pulsed glow discharge. Figure 5-15 shows a graph containing traces of the current to voltage relationship over a range of pressures. These traces were used to estimate the electron temperature with respect to pressure, shown in Figure 5-16. Similar traces measured over a range of voltages were added to estimate the electron density based on the current flow to the probe over the range of voltage and pressure. The results are shown in Figure 5-17. Results from these data indicated that the electron temperatures within the dc plasma ranged from 2000 to 3500 K for the parameters studied. These figures also show that an increase in applied power or pressure will result in an increase in both excitation temperature and electron density. As the distance from the cathode is increased, the electron density declines, while the temperature remains relatively unchanged.

Measurements in the pulsed discharge were not as readily obtained. The high voltages generated and the transient nature of the pulsed discharge complicated the gathering of data. The complexity of running the stepping function through a cycle while capturing data regarding the transient pulsed signal was deemed too difficult. Therefore, the probe voltage was held constant while measurements were taken and then manually switched to another voltage before continuing. Figure 5-18 shows the voltage and current on the probe, respectively. The constantly changing voltage and current never reach a steady state and result in the very complex data shown in Figure 5-18. The pulsed measurements are complicated by the added parameter of time, and so cannot be processed in the same manner in which the dc data were handled.

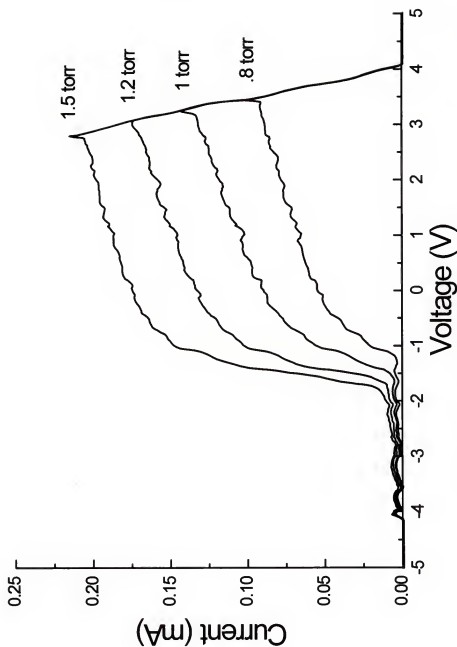


Figure 5-15. Current-voltage probe measurements of a dc glow discharge. Conditions: 750 V.

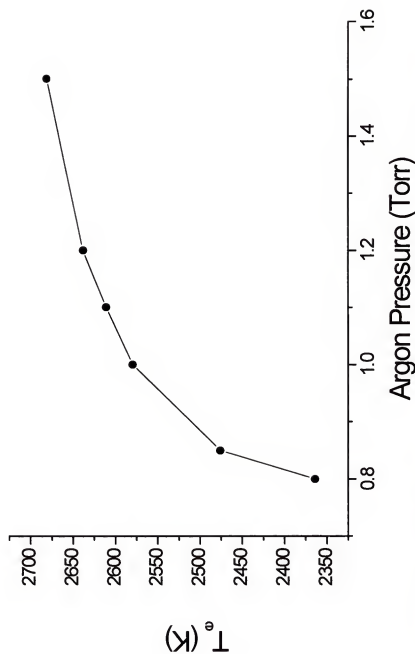


Figure 5-16. Electron temperature of dc discharge vs pressure as calculated from probe measurements.

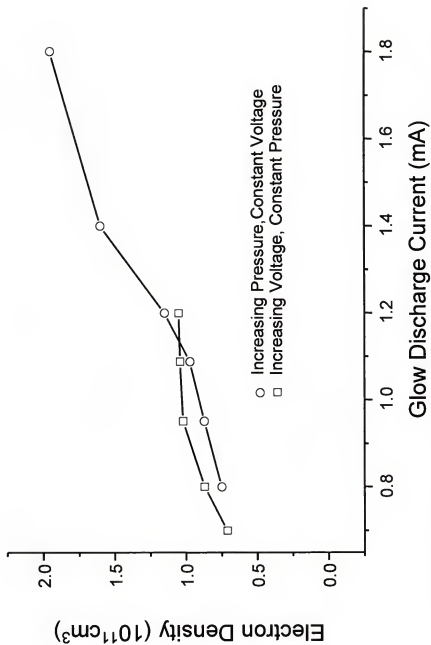


Figure 5-17. Electron density with respect to voltage and pressure for a dc discharge.

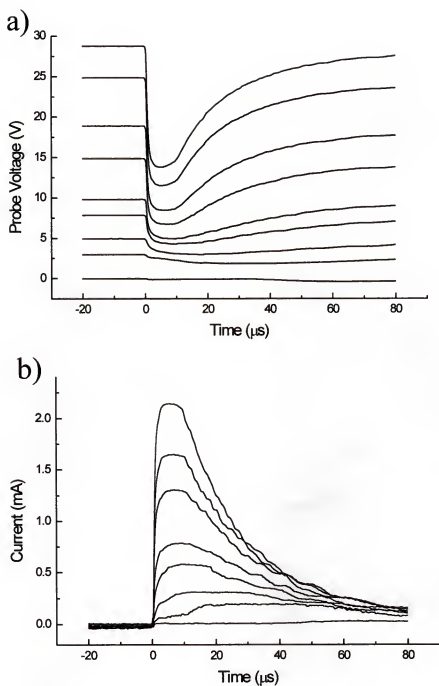


Figure 5-18. Current and voltage measurements from an electrostatic probe in a pulsed glow discharge. a) Voltage on the probe; b) Current measurement.

A re-creation of the current-voltage diagram, similar to the dc work, was attempted by replottting the probe current and voltage as a function of time. Therefore, current-voltage plots for the values at 5, 10, and 15 microseconds after the initiation of the pulse are obtained. Figure 5-19 shows the current voltage plots obtained for the pulsed discharge at a given set of times. With these recreated plots, the temperature and electron density can be measured.

The electron temperature of the pulsed discharge during pulse is almost an order of magnitude greater than the dc mode. This supports the hypothesis that the greater power possible during the pulsed discharge forms a more energetic plasma. This energetic plasma is formed because of greater energy gained by electrons in the increased potential field of the pulsed GD. Figure 5-20 shows the greater peak temperature of the pulsed plasma and its rapid decay after the termination of the power. This plots shows the electron temperature at 2 pressures and 3 different operating voltages. The data indicates that changes in pressure and voltage have only a small effect on the electron temperature.

Figure 5-21a shows the calculated electron density as a function of applied voltage. Figure 5-21b shows the calculated electron density as a function of pressure. The observed values indicate that there is an increased electron population during the pulse on-time, which quickly decays after power termination. The peak number densities are nearly an order of magnitude greater than the continuous dc mode. The results indicate that a 1000 volt dc discharge and a 1000 volt pulsed discharge would have nearly the same electron number density.

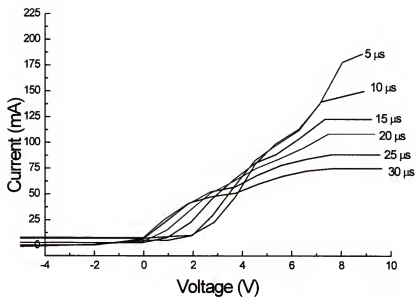


Figure 5-19. Current-voltage plot for a 10 μ s pulsed glow discharge.

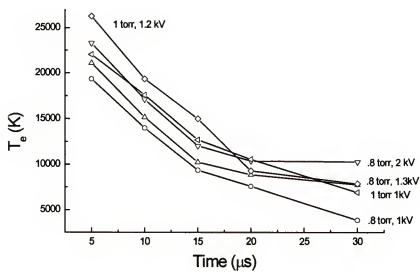


Figure 5-20. Electron temperature measurements for the pulsed discharge.

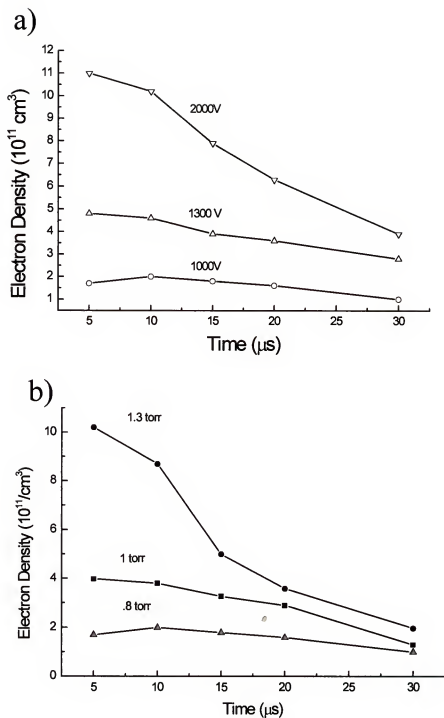


Figure 5-21. Electron density measurement of the pulsed glow discharge. a) Constant pressure of 0.8 torr; b) Constant voltage of 1000 V.

The Langmuir probe measurements, while crude, did support the data obtained using other plasma techniques. The probe allowed the excitation temperature and electron density for the continuous and pulsed mode to be measured. The pulsed discharge formed a more energetic plasma with an order of magnitude increase in electron temperature and electron number density. This increase is linked to the larger applied currents and voltages made possible by pulsing the glow discharge. The increased energy and number of electrons in the plasma offer some insight into the enhancements seen with optical emission and mass spectrometry.

CHAPTER 6 MICROSECOND PULSED GLOW DISCHARGE TIME-OF-FLIGHT MASS SPECTROMETRY

Introduction

Background

Work in our laboratory has centered on the development of the glow discharge as an ionization source for bulk and trace elemental analysis of solids using mass spectrometry. Due to its ability to perform diagnostics on the pulsed plasma, a renewed interest in emission spectroscopy was developed. The relevant results are discussed in the previous chapter.¹⁶ The application of a high potential to the sample, which acts as the cathode in a simple, low pressure argon cell, causes an electrical breakdown which forms an ion population representative of the sample composition. A mass spectrometer may then sample this population, recording its composition. Sputter rates of the different elements rarely differ more than a factor of ten, as opposed to the rates of evaporation, which may differ by several orders of magnitude.¹⁷ Due to the lack of fractionation, the atom population generated by the glow discharge is regarded as an accurate reflection of surface composition.

Modern glow discharge mass spectrometry began when a dc glow discharge was coupled to a quadrupole mass spectrometer.⁵³ Consequently, the GD ion source has been interfaced with most types of mass spectrometers. Today, glow discharge mass spectrometry is accepted as an effective technique for the trace elemental

analysis of solid materials. The most common application of the GD plasma has been to use a continuous plasma to atomize and ionize the sample. Our laboratory has been instrumental in the development of the GDMS technique. Our most recent interest has been the application of the microsecond pulsed discharge to the field of mass spectrometry.

In a plenary lecture entitled "The Future of Plasma Spectrochemical Instrumentation," Hieftje reviewed the limitations of current analytical instrumental methods in order to predict future advancements.⁵⁴ He concluded that the detection limits of mass spectrometry are constrained by the efficiency of sample utilization. Sample utilization is dictated by the transmission of the mass analyzer and the efficiency of the interface that separates it from the plasma source. In terms of desirable characteristics of the plasma source, "What is needed is better control of sample introduction, atom formation and the plasma environment that fosters atomic excitation and ionization." Moreover, the next generation of analytical sources must derive more information from each spectroscopic measurement.

Compared to the existing types of glow discharges, the microsecond pulsed discharge meets many of the above criteria and offers unique analytical opportunities. In terms of a plasma source, the pulsed discharge offers the advantages of high signal intensity and greater signal-to-noise due to the greater powers achieved during the short pulse. Moreover, both the pulse width and frequency are additional means of controlling the removal of the sample. In terms of deriving more information from each spectral event, the short pulse lends itself to the study of plasma interactions.

Diffusion, kinetics and other information (that is not obtainable using the dc mode) can be derived from the pulsed source.

An adequate means of probing the plasma is necessary to take advantage of the abilities of the microsecond pulsed glow discharge. Unfortunately, most mass analyzers are scanning instruments. Although the signal from these instruments may be gated, the effective duty cycle is incredibly low and the utilization of sample is equally inefficient. However, there is a mass spectrometer that is uniquely suited to the collection and recording of pulsed packets of ions – the time-of-flight mass spectrometer. Due to the TOF mass analyzer's unique ability to record pulses, we have coupled the microsecond pulsed GD ion source to a reflectron time-of-flight mass spectrometer.

Time-of-flight mass spectrometers have the fastest speed and highest transmission of all mass spectrometers. Moreover, their operation necessitates the sampling of a pulsed packet of ions. Therefore, the union of the microsecond pulsed glow discharge ion source with a time-of-flight mass spectrometer seems ideal.

Experimental

Due to time and length restrictions, many of the details of the instrument will not be covered and the reader is referred to a review of our prototype instrument.⁵⁵ Instead, an overview of the relevant instrumentation and operation of the source shall be discussed. The flight tube and other components of the mass analyzer were purchased from Comstock (Model RTOF/210, Oak Ridge, TN, USA). However, the ion source was completely designed and built in-house at the University of Florida.

The TOF instrument was designed for an orthogonal sampling structure. Figure 6-1 shows a schematic of the mass spectrometer.

To obtain a mass spectrum of an analyte, the sample was mounted on a direct insertion probe precisely as in the emission work. This probe was inserted into a probe port, past a ball valve, and through an adjustable bellows to rest several millimeters from the sampling orifice of the mass spectrometer. The pressure in the first stage was varied between 0.5 and 2 torr argon, with 1 torr being considered standard. Due the differential pumping scheme, the second stage had a nominal pressure of 2×10^{-4} torr during operation and the third stage, which housed the flight tube and detector had a pressure in the 10^{-6} torr range during operation.

Figure 6-2 is a cartoon of the sampling interface, which allows a closer view of the sampling of ions into the mass analyzer. The cathode was able to be placed at a variable distance from the sampling plate, which contained the orifice to the mass spectrometer. Ions formed in the glow discharge chamber are sampled through the 1 mm orifice, forming a supersonic jet due to the pressure differential. Some ions are deflected at the skimmer, however, a tight packet of ions is transferred into the next stage of the mass spectrometer. This packet is then focused by ion optics including a series of 3 einzel lenses, steering plates, and another slit that further focuses the ion beam. The focused ion beam streams past a repeller plate that is biased slightly negative to deter any stray ions from entering the flight tube. At a preset delay from the pulse initiation, the repeller is quickly pulsed to a positive 100 Volts for 2 microseconds. This repels a small portion of the ion beam into the flight tube.

Top View of GD-TOFMS

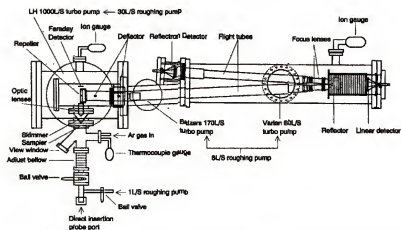


Figure 6-1. Sketch of pulsed glow discharge time-of-flight mass spectrometer.

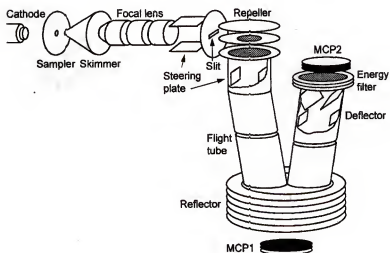


Figure 6-2. Expanded view of TOFMS instrument.

The ions are then accelerated by the potential between two plates and are separated according to their mass while traveling down the flight tube. After passing through the reflectron region, the atoms arrive at the two microchannel plates (Galileo Electrooptics, Sturbridge, MA, USA) that serve as the detector.

Two means of signal collection were employed. The first method involved taking the signal from the detector and passing it through a 50 Ohm pull-down resistor and a fast preamplifier (SR 445, SRS). This signal was then displayed on a 500 MHz digital oscilloscope (TDS 502A, Tektronix, Beaverton, OR, USA). This signal was also recorded by a computer connected to the scope via a GPIB interface. This mode is both quick and dynamic. Therefore it is used for all routine bulk and minor elemental analysis as well as monitoring parameters.

The second method of detection involved the use of a picosecond time analyzer (PTA) (9308, EG&G Ortec) and a picosecond time discriminator (9307, EG&G). This very high-speed time analyzer was able to collect, process and store a mass spectrum every 80 microseconds. Thus this novel device could accumulate the mass spectra and act as a counting mode, greatly increasing sensitivity. The enhanced sensitivity of this mode required that the signal be accumulated over a set time period. Therefore, the PTA could not be used in monitoring the focusing of the signal, nor monitor real-time changes of the different parameters.

Overview of Microsecond Pulsed GD TOFMS

A time-of-flight mass spectrometer separates ions on the basis of their mass by the use of an electric field. Sample ions are all given the same accelerating

force by the electric field as they enter the flight tube. Smaller ions move more quickly down the tube and larger ions arrive at the detector later. The mass spectrum is then a recording of the arrival times of these species. It is due to this difference in flight time that the technique derives its name. In order for the TOFMS to work properly, the ions to be analyzed must all enter the acceleration region at the same time. In other words, the TOFMS requires pulsed injection of ions. Therefore, the coupling of the powerful microsecond pulsed glow discharge with a time-of-flight mass spectrometer seems like an ideal mating.

In addition to handling pulsed ion sources, time-of-flight mass analyzers have the most simple instrumental operation, fastest speed and greatest throughput of the available mass analyzers. Therefore, a pulsed GD time-of-flight mass spectrometer is a powerful analytical tool capable of gathering a great amount of data very quickly. The informing power of the mass spectrometer is magnified by its resolution, low number of spectral interferences, and its high sensitivity. Figure 6-3 shows a mass spectrum of a NIST 495 copper sample, showing some of its trace constituents, which illustrates the utility of the mass spectrometer. In terms of informing power, the pulsed discharge TOFMS is able to acquire an entire mass spectrum of the sample with each pulse of the plasma. In just a very short mass range we discover trace amounts of Ti, Cr, Fe, Mn, Ni and Co within the matrix. In terms of spectral simplicity, even the more complex elements have only half a dozen isotope ratios, compared to emission spectroscopy in which each element has hundreds of emission lines. The spectral simplicity greatly reduces the chances for spectral overlap. Only the ^{56}Fe and the ^{58}Fe seem to have any spectral overlap with other plasma species

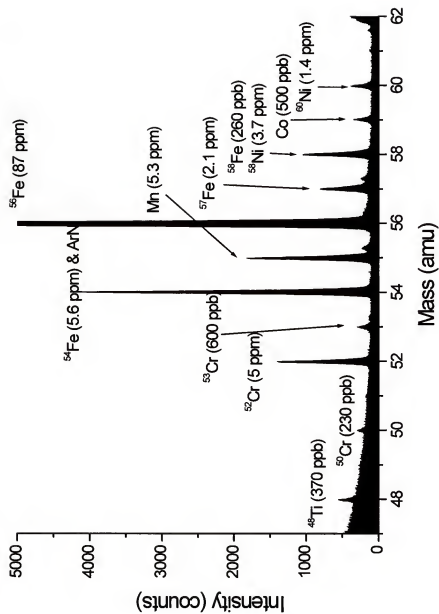


Figure 6-3. Mass spectrum of NIST 495 copper. Conditions: 2kV, 1 torr argon.

(ArN^+ and ^{58}Ni respectively) in Figure 6-3. Finally, the informing power of the mass spectrometer is marked by its sensitivity. For instance, the cobalt concentration is only 500 ppb, yet is easily distinguished from the background. Therefore, the pulsed GD-TOFMS system allows the complete elemental analysis down to the trace (<500 ppb) level on a pulse-to-pulse basis. Due to the speed of the mass spectrometer, the pGD may be operated at high frequencies, therefore allowing a great number of mass spectra to be collected and averaged in a short period of time.

An additional ability due to the transient nature of the source and pulse-injection mode of the spectrometer is that temporal resolution of the signal is made possible. Due to the different mechanisms responsible for the ionization of fill gas and the analyte species, both have different temporal profiles. Figure 6-4 shows a mass spectrum of a copper cathode in an argon atmosphere displaying the temporal distribution of the two species. This plot is made possible by altering the delay between the high voltage pulse, which powers the pulsed GD, and the repeller pulse, which samples ions into the mass spectrometer. The profiles are similar to the temporal differences evident in emission spectroscopy, although they are more pronounced due to the fact that only the ionic species are seen. It is important to note that this effect was first discovered while performing emission spectroscopy, which highlights the effective use of emission as a diagnostic tool. Determination of the fundamental causes and parametric influences, which are able to be studied quickly and easily via emission, have led to the improved performance of the mass spectrometer. One of the improvements in performance of the pulsed TOFMS system is the use of the temporal nature of the signal to bias against spectral interferences.

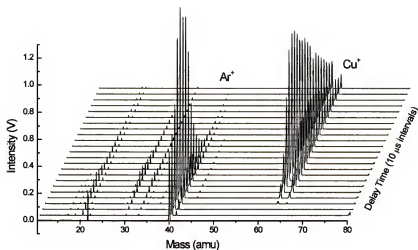


Figure 6-4. Waterfall plot showing temporal separation between argon and copper ions.

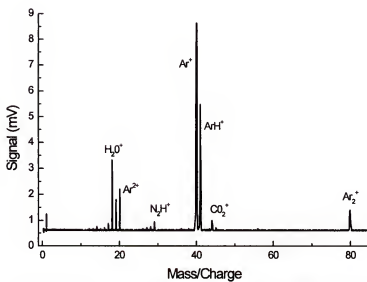


Figure 6-5. Gaseous interferences in mass spectrometry. Conditions: 1 torr, 2kV, 10 μ s delay.

Spectral Interferences

Despite its low spectral complexity and relatively few spectral overlaps, there are several species which complicate elemental analysis. Most of these interferences arise from the fill gas, molecular impurities within the fill gas, or contaminants on the surface of the cathode. Figure 6-5 is a mass spectrum of the various species that can complicate the elemental analysis of a sample. Several species originate from the fill gas itself, such as Ar^+ , Ar^{2+} , ArH^+ , and Ar_2^+ . While other species arise from leaks within the vacuum system such as H_2O^+ , N_2H^+ , and CO_2^+ . The presence of all these species occlude the mass spectral analysis of elements below 30 amu. Therefore, the analysis of such important elements as Si, Al, Mg, Na, and F could potentially be hampered. In addition to this, calcium isotopes, with primary mass peaks at 40, 41 and 44, are completely covered by species of argon and carbon dioxide.

Temporal Resolution

The pulsed glow discharge offers a unique method of reducing, minimizing and in some cases eliminating the spectral contribution of these elements. Figure 6-6 re-plots the argon and copper ion intensity from Figure 6-3 as a function of the delay time. If a mass spectrum is taken at a delay of 90 microseconds, near the peak of the argon signal, there will be only a very weak signal from the copper species. If, however, one delays the taking of the mass spectrum till 200 microseconds, near the peak of the copper signal, a spectrum rich in copper but consisting of an argon signal only 20% of its peak value will result. Alternatively, if the spectrum is taken at a

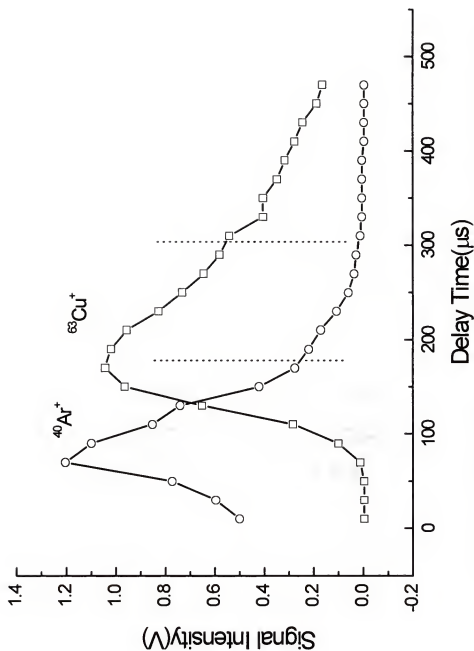


Figure 6-6. Argon and copper ion signal intensity as a function of delay time.

delay of 300 microseconds, only 50% of the analyte signal is sacrificed to achieve a 90% reduction in the gas species. This phenomenon, in itself, could be quite useful analytically. However, by controlling the parameters of the glow discharge, we are able to effect an even greater separation of the two signals. Our research efforts have thus been occupied with both characterizing the instrument performance and in using the parameter studies to maximize the separation between the analyte and gas interferents.

Factors Affecting Temporal Resolution

A brief discussion of how the temporal resolution is achieved will be a useful framework for the pages to follow. Figure 6-7 is a cartoon of the generation and sampling of the ions in the GD-TOFMS instrument. The top of the figure titled "sputtering" represents the pulse on-time. The plasma lasts only 10 microseconds, but sets in motion a chain of events which results in the mass spectral signal. During the pulse on time, argon ions are formed, primarily by electron impact ionization, and some impact the cathode surface causing sputtering. Other argon ions close to the MS orifice are immediately sampled. Any copper ions generated at this time are formed close to the cathode and are immediately attracted to the negatively charged cathode. Only atoms are allowed to diffuse into the GD chamber.

The second step occurs after the termination of the high voltage pulse. Once the source of the energetic electrons is removed, no more argon ions are formed. On the other hand, the copper atoms, which are beginning to diffuse through the chamber, can undergo collisions with argon metastable atoms, which are both long lived and

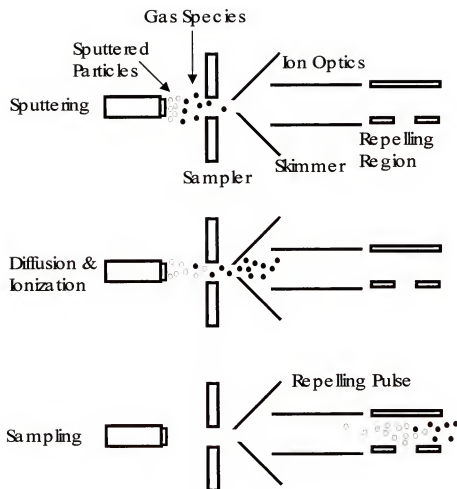


Figure 6-7. Sampling of pulsed ions into TOF mass analyzer.

have enough energy to ionize copper. As the ion packets continue to diffuse, they enter the region of the skimmer and ion optic lenses. Here, another form of discrimination is possible. By focusing and maximizing the analyte species signal, an energy bias may be formed against the gas species.

When the ion packet reaches the repeller region, the ions formed in the 10 microsecond discharge, are now spread into a diffusing band that is 250 microseconds wide. This packet contains many of the argon and gas species in the forefront. Because the analyte species needed to be both sputtered and ionized by metastable argon, analyte ions comprise the tail of this ion cloud. The repeller then samples a 2 microsecond slice of this passing packet of ions. By delaying the repeller an appropriate amount, a slice comprised of mostly analyte, with few interferent species can be achieved.

While the GDMS is a well-accepted means of determining the elemental composition of solids, the pulsed mode offers several considerable advantages. First, the higher power of the pulsed discharge creates an ion signal that is an order of magnitude greater than the dc mode. Additionally, there is little increase in the background or noise, resulting in greater sensitivity and greater detection limits. Secondly, the temporal separation between the gas species within the discharge and the analyte signal results in a cleaner spectrum with greatly reduced interferences. Figure 6-8 shows a mass spectrum of copper when operated in the dc and pulsed modes. The pulsed mode produces a copper signal that is an order of magnitude greater than the dc spectrum, while greatly reducing the spectral contribution of species from argon, water and nitrogen.

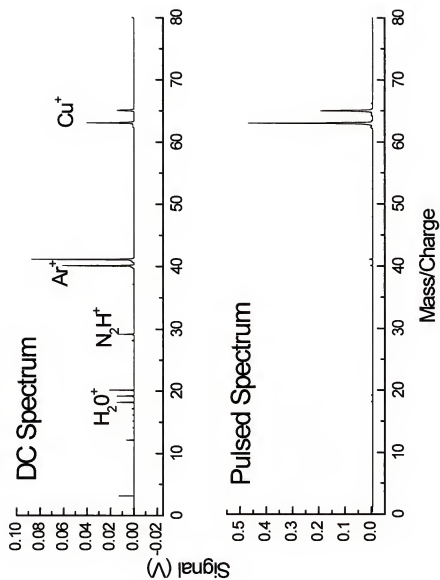


Figure 6-8. Comparison of dc and pulsed glow discharge mass spectra.

Parameters Studied

Studying the effects of the different parameters will result in a better understanding of the plasma and the instrument. These studies should lead to better performance either from better control over sampling, focusing, and detection, or improved methods and instrumentation. Like the results from emission spectroscopy discussed previously, several of the most important experimental parameters are the voltage, pressure, pulse width, and frequency. Due to the fact that mass spectrometry depends on the transportation of material from the plasma, unlike the un-invasive emission technique, there are two other experimental parameters that play an important role in the operation of the pulsed GD ion source. The first of these is the distance that the cathode is positioned from the sample orifice of the mass spectrometer. As this is increased or decreased, the mass spectrometer will sample different locations within the GD plasma. This can have a dramatic effect on both the analyte and gas species sampled. Figure 6-9 shows the effect of increasing the cathode-to-orifice distance (C-O distance). The second parameter is the delay time at which the repeller samples ions into the flight tube.

The next section will deal in detail with the effect of voltage, pressure, and cathode-to-orifice distance, which have the greatest effect both on signal intensity and the degree of separation from the gaseous species. However, an overview of some of their effects should prove useful before delving into more detail. The mass spectrometer is a wonderfully informative, sensitive technique, but one must always keep in mind that it is also a complex device – a mass and energy separator. A mass spectrometer only reports what ions hit the detector. There are a series of steps before

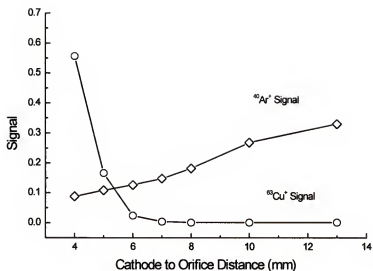


Figure 6-9. Effect of cathode-to-orifice distance on argon and copper ion signals.

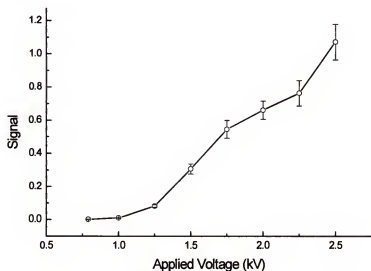


Figure 6-10. Effect of voltage on ion signal from m/z 56 in steel sample.

the analyte ions are detected. These steps include, ionization and recombination in the source, the sampling of the local region within the discharge, the complex effect of focusing the ions via ion optic lenses, and the repeller delay at which ions are sampled. If one is not rigorously careful, one can make dangerous assumptions. In other words, "mass spectrometers will lie to you if you let them." For this reason it is very important to understand the operation of the device so that parametric effects in the plasma and parametric effects on the instrument are not confused.

The voltage and pressure have much the same effect as in emission spectrometry in that their increase will result in a higher signal intensity. Figure 6-10 shows the peak of the ion signal over a range of applied voltage. An increase in voltage results in a dramatic increase in ion signal. Pressure behaves likewise, although there is an upper limit to the amount of pressure that the source may operate at, due to the necessity of keeping very low pressures within the mass spectrometer to which it is coupled.

Because mass spectrometers rely upon the sampling of ions, parametric studies are complicated because many of the parameters have an interactive effect. Unlike emission, where an increase in voltage will result in more photon emission, increasing the voltage of an ion source may also decrease the signal of certain species or perhaps change the temporal profile of the ion signal altogether. Figure 6-11 shows an advantageous effect on the signal of the gas species produced by increasing the applied voltage. Figure 6-11a shows the mass spectral signal from a 2kV discharge at a 20 microsecond delay. The gas species mentioned before are all present. Figure 6-11b. displays the effect of lowering the voltage applied to the glow discharge to 1kV.

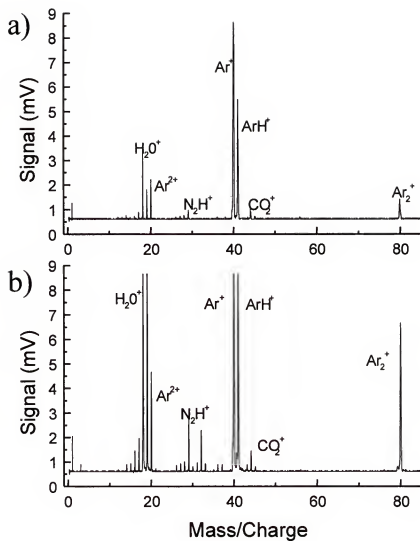


Figure 6-11. Effect of increased voltage on gas species ion signal.

Conditions: 0.9 torr, 200 Hz, 20 μs delay, SRM 1262a.

a) 2 kV discharge; b) 1 kV discharge.

The signals from many of the species such as water, oxygen, argon, and argon hydride increase dramatically. Also increased is the ion signal of the Ar_2^+ dimer. An explanation for this effect is based upon the energy of the discharge, and effects caused by the ion lenses. The plasma formed by a higher voltage would form higher energy species. However, the sputtered atoms are primarily ionized by Penning ionization at the later stages and post pulse period of the pulsed glow discharge plasma. Therefore, it is expected that these species will have the same energy. At lower voltage, when the signal is focused, a greater portion of the gas species has a similar (low) energy as the analyte. At higher applied voltage, the gas species would have a higher energy, whereas the analyte would still be primarily formed by Penning ionization. Therefore, when the analyte signal is focused, a distinction between the energy of the two species is made and the resulting spectra show a decrease in gas species. Investigation of these sorts of phenomena has resulted in a better understanding of the underlying principles of both the spectrometer and the plasma, and should lead to improved analytical performance.

Parameter Studies of the Pulsed GD TOFMS

Reporting the results of our parametric studies may be a more difficult endeavor than obtaining the experimental data. The major parameters, voltage, pressure, and cathode-to-orifice (C-O) distance all affect the temporal profile and focus of the ion signal and therefore change the delay time chosen to optimize the analytical signal. To be represented properly, the data should be plotted in four dimensions! However, not only is it difficult to plot such complex data, it is equally

difficult to extract information from such figures. Instead, the data is presented in a series of graphs meant to demonstrate not only the complexity, but also the utility of such studies.

Having mentioned the difficulties involved in displaying the parametric study data, let us review what parameters are to be covered. Like the emission data, voltage and pressure play an important part in the intensity of the signal. However, in the emission work, the temporal profiles of the plasma species were unchanged by a change in voltage or pressure. Unlike the emission studies, where photons are effectively extracted at the speed of light, the mass spectral signal is affected by changes in the diffusion of the ions within the vacuum chamber. Both the voltage and pressure have differing effects upon the ion signals of the analyte and gas species. Likewise, the cathode-to-orifice distance plays a significant role in obtaining an analytical signal. In order to display the effects of these parameters, a series of graphs will show the effect of high, medium and low voltage on the mass spectral signal when the cathode-to-orifice distance is altered between 4 and 8 mm. Next, the voltage will be held constant while the effect of high, medium, and low pressure is presented. The C-O distance will be changed as well. Finally, the temporal profiles of some specific plasma species will be reviewed in more detail and the effect of distance, pressure and voltage will be summarized.

Data concerning the pulse width and frequency will not be included. Frequency did not affect the mass spectral signal significantly. Results were similar to those in emission, with signal intensity varying by no more than 15%. On the other hand, the pulse width had a significant effect on the temporal profile of the ion signals

involved. However, increasing the pulse width did not seem to have any clear advantage, and perhaps showed some disadvantage. Greater pulse width results in a wider ion packet. Wider ion distributions lengthened the time to perform analysis, showed lower peak ion signal intensity, and caused the gaseous and analyte signals to overlap. Since one of the specific goals of this work was to determine the optimal conditions for their separation, a 10-microsecond pulse was applied to a copper cathode in an atmosphere of argon for all the data presented.

Voltage Studies

As indicated by Figures 6-9 and 6-10, both low voltage and large C-O distances tend to reduce the analyte signal and emphasize the gas species present. Figure 6-12 shows the ion signal with respect to the delay time at a 6 mm and 4mm C-O distance. The voltage was set to 1200V, one of the lower settings used during the parametric studies. At 6 mm, the mass spectrometer only samples a region deep into the negative glow of the discharge. This region shows relatively strong signal from gas species, but the analytical signal is so weak, it is barely able to be seen. Due to diffusion within the chamber, the analyte ions have spread out into a thin cloud. Therefore, the analyte signal is shallow, long and weak. The copper ion signal seems to peak between 200 and 300 microseconds and is very weak compared to all other species within the plasma. At distances further than 6 mm studies showed that the analyte signal at low applied voltages was difficult to detect.

When the data at the same experimental conditions is taken at 4mm, there are some significant changes (Figure 6-12b). The analyte signal peaks at 130

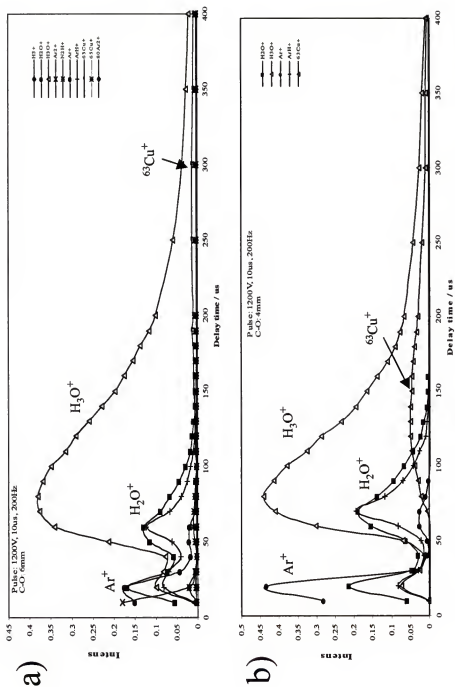


Figure 6-12. Temporal profiles of ion signals low voltage.⁴⁶
a) 1200 V, 6 mm; b) 1200 V, 4 mm.

microseconds and is considerably stronger than the 6mm data. Another phenomenon is that the gas species display 2 distinct peaks. One peak is centered around 10 microseconds and another at approximately sixty microseconds. A pattern within the data forms, in which the gas species peak very early in the plasma and then show a second peak immediately preceding the analyte peak. What is known is that voltage, pressure, C-O distance, and lens settings have a great effect on this phenomenon.

The voltage of the discharge was next changed to a moderate level. 1600 volts was applied to the source and the temporal profiles of the ionic species were recorded over a number of cathode-to-orifice distances (Figure 6-13). Similar to the previous data, at medium voltage very little ion signal was obtained further than 6 mm. Figure 6-13a shows the temporal profiles of the ions at 6mm. The higher voltage has resulted in a larger signal than the lower voltage and a definite peak for the two isotopes of copper can be seen at a delay of 200 microseconds. The double peak of the gas species can also be clearly seen. A 4 mm C-O distance is a more effective position to sample plasma for analysis as it consistently shows stronger analyte signals.

Some plasma chemistry is evident in Figure 6-13 as well. In the first peak of the gas species the argon signal is much higher than the argon hydride ion. Likewise, the ion signal from water is greater than the H_3O^+ signal in the pre-peak region. However, in the second peak, which appears just at the inception of the analyte signal, the signal from these species has reversed intensity, with ArH^+ and H_3O^+ being greater than their value in the pre-peak region and their non-protonated counterpart. It is apparent that a large amount of protonation transpires within the GD chamber, where water molecules and argon atoms act as a Lewis base to combine with a proton.

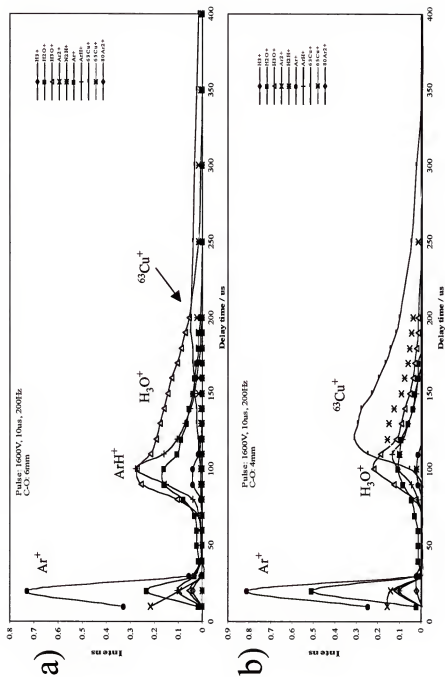


Figure 6-13. Temporal profile of ion signals moderate voltage.⁴⁶ a) 6 mm; b) 4 mm.

The source of the H^+ is mostly likely water, as hydrocarbons from backsreaming of pump oil would result in a significant carbon ion peak which is not observed. No significant CuH^+ peaks are observed either. Most likely, the H^+ ions are formed by electron impact and quickly react with the gas species such as argon and water molecules. This explanation accounts for temporal delay of the hydride ion species peak and for the lack of sputtered atom-hydride species.

The GD is a stable generator of atomic and ionic species. This makes it very valuable in the study of gas phase chemistry. The protonation reactions evidenced are but one example of the many possibilities of the use discharge as a chemical reaction cell. However, at this time this potential remains untapped. The pulsed discharge will play a very important role in studying the chemistry of the glow discharge. The continuous sources, which will present an averaged, steady-state stream of ions to the mass spectrometer. For instance, the protonation of argon and water with respect to time noted above, would not be observed in a continuous source. Only by presenting an intermittent packet of ions can such effects be studied.

Figure 6-13b shows the results for the medium voltage study at 4mm. The gas species have the same intensity as at 6mm and seem to have a slightly more uniform shape. However, at 4mm the copper ion signal is finally becoming stronger than the gas species. At four millimeters into the discharge, a region just inside the negative glow is sampled. Since the cathode dark space is necessary order for the plasma to be self-sustaining, measurements at 2 and 3mm have shown strong analyte intensity, but are also much less stable. Thus, a 4 mm C-O distance was good compromise. As the voltage increases, not only is a more energetic plasma formed, but more sputtering

results as well. Sampling the region close to the negative glow without interfering with its operation results in the highest signal, and coincidentally a better separation between the gas and analyte ions.

As expected, the highest voltage produced the greatest ions signals for each C-O distance. At an applied voltage of 2kV, a signal from copper can be seen even at 8 mm from the cathode. Figure 6-14a displays the ion signals obtained at a C-O distance of 8 mm. Due to diffusion, the copper signal is weak and spread over a long time period. While analytical measurements would most likely be performed at a shorter C-O distance, changing the cathode-to-orifice distance allows the diffusion of ions to be studied. Figure 6-14b shows the dramatic rise in the analyte signal when the C-O distance is reduced to 6 mm. Since less diffusion has taken place, the signals of all the species are more compact. Figure 6-15 shows a 2200V GD signal at 4 mm. Several distinct differences are seen in the temporal profiles. First, the pre-peak of gas species is nearly completely eliminated. Second, the secondary peak of the gas species is reduced by a factor of three. Finally, the copper (analyte) signal is the most dominant feature of the plot. The best results are achieved with a short sampling distance in conjunction with high voltage. In addition to having the strongest signal, by setting the repeller pulse delay after the peak of the copper ion signal, a spectrum relatively free of gas interferences would result.

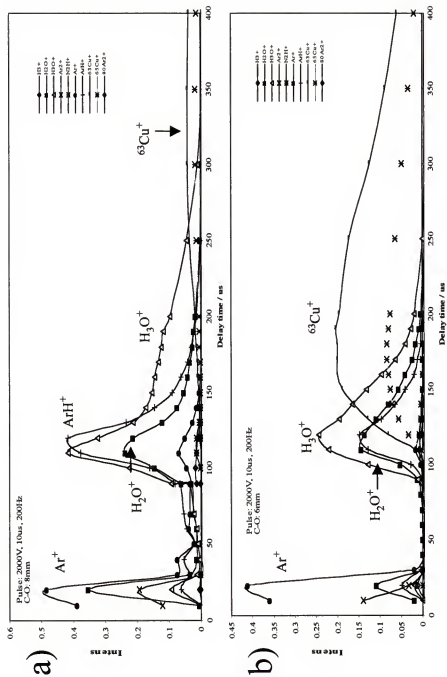


Figure 6-14. Temporal profile of ion signals, high voltage.⁴⁶ a) 8 mm; b) 6 mm.

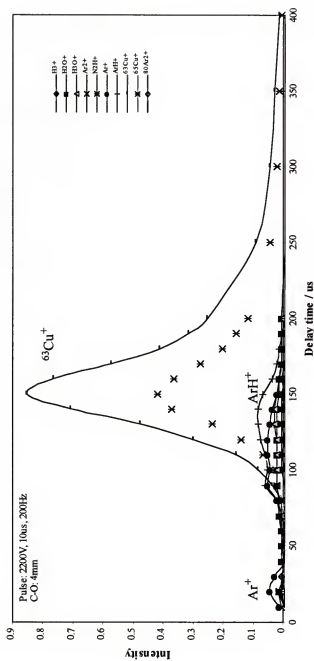


Figure 6-15. Temporal profile of ion signals. Conditions: high voltage, 4 mm C-O. ⁴⁶

Effect of Pressure

Recalling the effect of pressure in the emission work, an increase in pressure resulted in an increase in the cathode signal and also resulted in a greater level of ionization. Pressure has a similar effect on the ion signal measured by the mass spectrometer. Unlike emission measurements, mass spectrometry depends upon the diffusion of ions into the sampling region before being extracted and detected. Because the pressure is the most influential parameter on diffusion in the glow discharge source, it exhibits a strong effect on the ion signal.

Starting from low pressure and ending at high pressure, the temporal profiles of the ion signals were recorded as a function of pressure at a C-O distance of 8, 6, and 4 mm respectively. Figure 6-16 summarizes the results taken at 0.5 torr argon. As expected, a low pressure and long C-O distance result in a low analyte ion signal. The analytical signal from $^{65}\text{Cu}^+$ is just barely able to be seen at 8 mm, with increasing strength at shorter distances. In addition to low analyte signals at 0.5 torr, there is no separation of the analyte and gas species at any distance. The Ar^+ ion signal seems to be the dominant species within the first 40 microseconds, followed by H_3O^+ at later delay times.

A pressure of 1 torr argon is considered typical operating conditions for most GDMS work. As the pressure is increased to 1 torr, the signal originating from the cathode species increases significantly. Figure 6-17a shows the temporal profile of the major plasma ions at a distance of 6 mm. The copper signal can be seen, but is stretched over a long time period. One difference between the mass spectrum of the pulsed discharge and the dc discharge should be mentioned at this time.

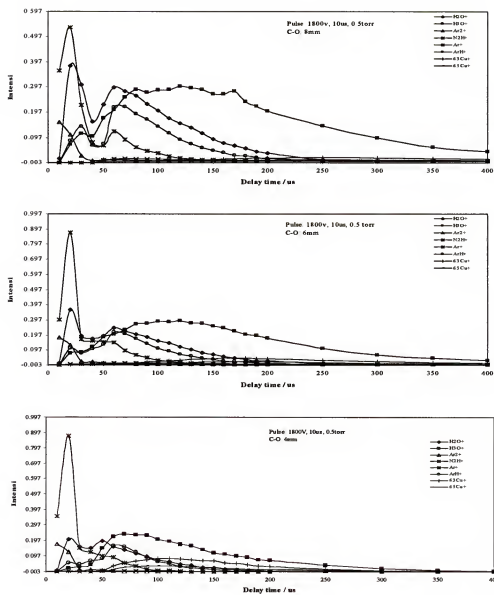


Figure 6-16. Temporal profile of ions signals. Conditions: low pressure.⁴⁶

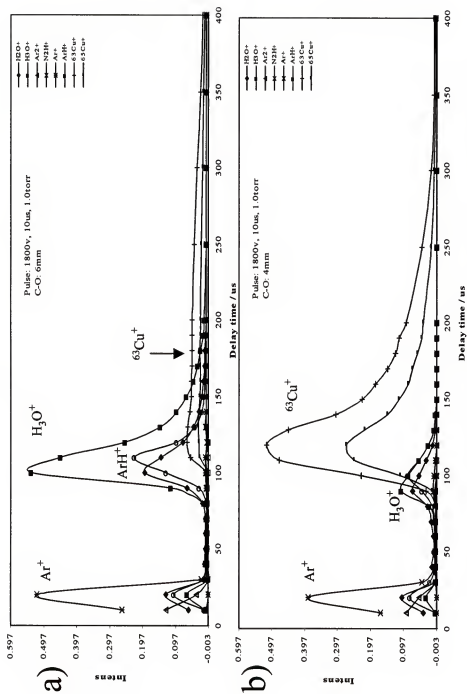


Figure 6-17. Temporal profile of ion signals. Conditions: moderate pressure.⁴⁶
a) 6mm; b) 4mm.

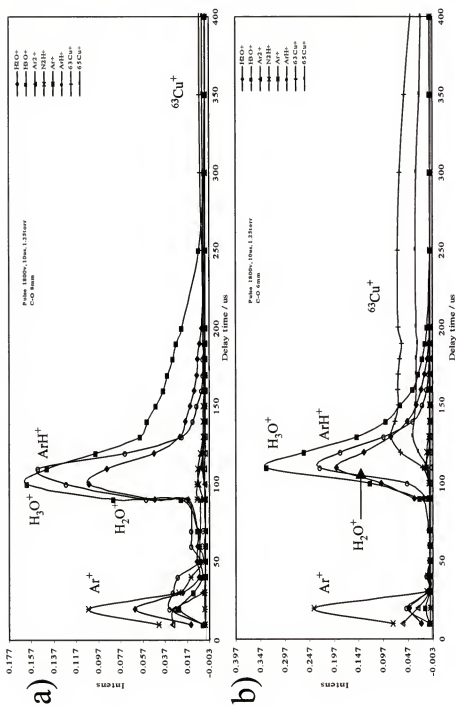


Figure 6-18. Temporal profile of ion signals. Conditions: high pressure.
a) 8mm; b) 6mm.

Our work with the dc ion source both with quadrupole and TOF mass spectrometers have shown that six to seven millimeters is the best sampling distance. Comparing the signals in Figure 6-17a and 6-17b nearly an order of magnitude in signal intensity is gained when the pulsed discharge is sampled at 4 mm. Examining Figure 6-17b more closely reveals that not only is the copper signal increased, but the gas species are reduced as well.

A pressure of 1.25 torr argon was used to compare to the previous pressure studies. Figure 6-18a and 6-18b show the ion profiles at 8 and 6 millimeters, respectively. At 8 mm, the gas species signal dominates with a very diffuse copper signal being seen out above 300 microseconds. The data taken at 6 mm show the two peaks of the gas ions. The second peak displays a fairly compact temporal profile with 90% of its area lying between 100 and 150 microsecond delay. The copper ion signal, on the other hand, stretches from 120 microseconds to past 400 microseconds, indicating that interference free spectra can be achieved at the later delays.

Figure 6-19 shows the temporal profiles at 4 mm and at 1.25 torr argon. Similar to the profiles obtained at the highest voltage, the highest pressure, when measured at a cathode-to-orifice distance of 4mm, showed the greatest analyte signal intensity and the greatest separation between analyte and gas species. The phenomenon in which the first peak of the gas signal disappears is repeated. Likewise, the second gas peak is reduced when compared to the data taken at 6 mm.

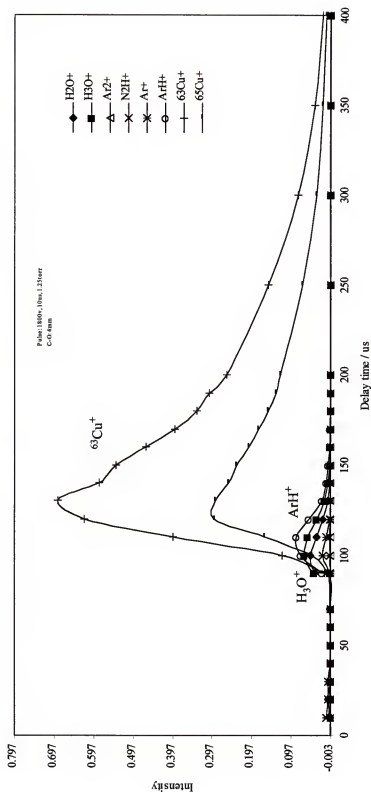


Figure 6-19. Temporal profile of ion signals. Conditions: high pressure, 4 mm C-O.⁴⁶

Summary of Parametric Study Results

The results of the parameter study indicate that the optimal experimental conditions call for high applied voltage and high pressure. There is a limit as to how high these parameters are able to go. Higher voltages are more prone to arc, which disrupts analytical measurements. High pressures may also cause arcing and can only be increased to the point at which the later vacuum stages can tolerate. Typical operating parameters were set at 2 kilovolts applied voltage and a pressure of 1 torr argon. The cathode was positioned at 3 or 4 mm from the sampling orifice. These conditions resulted in a strong analyte signal with significant, and sometimes complete, reduction of the interfering gas species signal. If a particular analysis necessitated greater signal, such as in trace analysis, the pressure and voltage were increased accordingly.

Alterations of plasma conditions such as the pressure, voltage and C-O distance allow a unique insight into both the chemistry and the physics of the pulsed glow discharge. Determining the processes within the pulsed discharge will benefit the practice of continuous sources as well. Several conditions of the pulsed discharge can be altered in order to study a variety of effects from diffusion, excitation, oxide formation, and others. For example, the effect of changing the pressure on the presence of H_3O^+ within the discharge may be studied. Figure 6-20 was produced while keeping the voltage at 1.8 kV and C-O distance at 6 mm. The pressure compacts the H_3O^+ signal significantly. The double peak of the molecular ion can also be seen at higher pressures. Pressure adjustments can be used to study the production of ions and diffusion of plasma species.

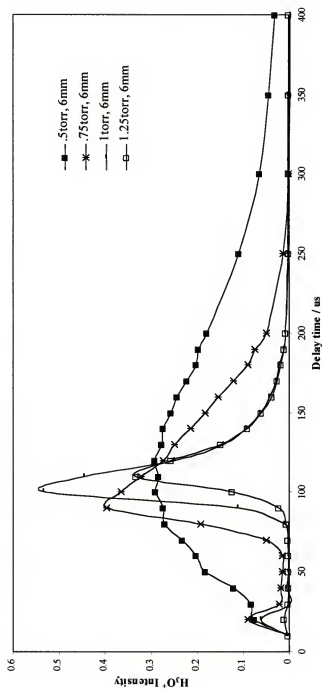


Figure 6-20. Temporal profile of H_3O^+ signal as a function of pressure at 6 mm.⁴⁶

Increasing the voltage produces a decrease in certain gaseous species such as H_3O^+ and produces a very different effect in the ArH^+ as seen in Figure 6-21a and 6-21b. This is advantageous from the standpoint of analytical analysis as high voltage produces a strong analyte peak, while reducing the contribution of the gaseous spectral interferences.

Not only have the parametric studies been used to examine the gas phase reactions in the plasma, but have also been used to optimize the ion signal of the analyte. Figure 6-22 summarizes the effect of increasing the voltage upon the $^{65}\text{Cu}^+$ signal derived from a copper cathode. The pulsed glow discharge shows a great number of analytical areas of interest. These include improved performance, elucidation of plasma fundamentals, and a better knowledge concerning the interplay between the mass spectrometer and the ion source.

Mass Spectral Results

The coupling of a pulsed glow discharge to a time-of-flight mass spectrometer has been discussed in terms of its instrumentation and operation. By careful control of the experimental parameters, a distinct separation between signals from the sputtered species and gaseous interferences can be achieved. Figure 6-23 illustrates the temporal separation possible with a copper (NIST 495) cathode in an argon atmosphere. The signals from such gas species as Ar^+ , ArH^+ and H_2O^+ are short lived and disappear before the signal from the analyte species peaks. The result is a spectrum rich in analyte species and relatively free of spectral interferences from

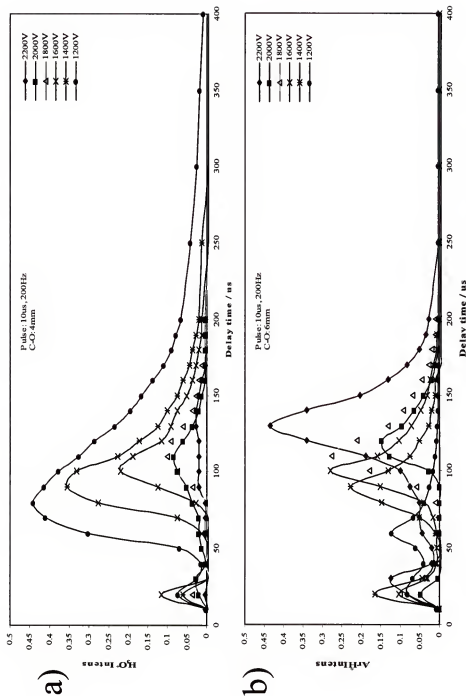


Figure 6-21. Temporal profile of ion signals from protonated species with varied voltages.⁴⁶ a) H_3O^+ , 4 mm; b) ArH^+ , 6 mm.

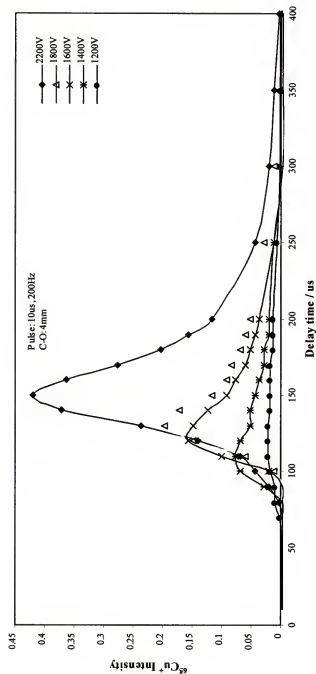


Figure 6-22. Effect of voltage on the temporal ion signal of copper. ⁴⁶

unwanted gas species. This is particularly useful when dealing with certain low mass elements and in trace analysis.

While the separation between gas and sputtered species is easily achieved for bulk analysis, effective separation of these species for trace analysis is more difficult. Figure 6-24 shows a high sensitivity spectrum of the same sample as in Figure 6-23, only at slightly less than optimal conditions. If the system is not optimized, an incomplete separation will occur and even slight amounts of the gas species will completely occlude the mass analysis of elements in which spectral overlap occurs, especially when trace analysis is desired. Comparing the signals of the gas species to the ion signal at mass to charge 56, the major iron peak resulting from 96 ppm iron in the copper, should illustrate how serious a problem this could be. While mass spectrometry is well valued for its few spectral interferences, gas species do complicate the analysis of important low weight elements and methods for their reduction are needed.

Careful control of the experimental parameters will improve both bulk and trace analysis, but also afford the opportunity to study the fundamental operation of both the plasma and the mass spectrometer. Voltage and pressure are two parameters that can perturb the chemistry of the discharge. By altering these conditions, important studies concerning the diffusion of ionic species can be made. Figure 6-25 shows the temporal profiles of several ionic species at two different pressures. The effects of pressure are the compacting of the temporal profile, the degree of separation between sputtered and gaseous species, and the intensity of the various species. Optimization of these effects will lead to better analytical performance.

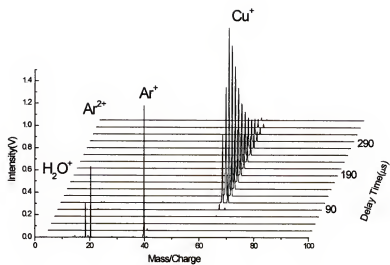


Figure 6-23. Temporal profile showing complete separation of Cu and Ar signals.

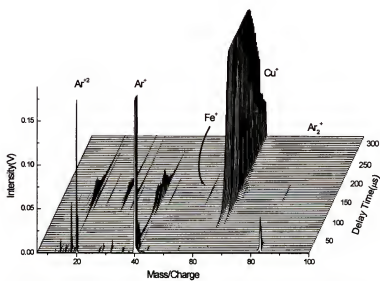


Figure 6-24. High sensitivity mass spectra of Cu sample.

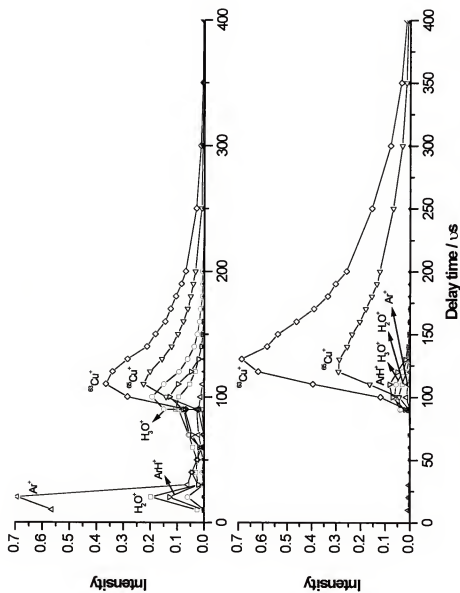


Figure 6-25. Effect of pressure on temporal profile of ion signals.

Figure 6-26 is a plot of the $^{65}\text{Cu}^+$ ion signal with respect to the delay time at several C-O distances. Not only have these studies optimized conditions for analysis, but also allow measurements of the diffusion of ionic species within the plasma. Knowledge of the formation of the different species and the transportation of material within the plasma has been gathered.

Figures 6-27, 6-28, and 6-29 are plots of the mass spectra with respect to delay time at 5, 6 and 7 mm respectively. The variations in both the gas and sputtered ion signals are evident at the different cathode-to-orifice distances. Plotting the ions signals with respect to mass, intensity, temporal profile and cathode-to-orifice distance records the population of the ionic species with respect to space and time. Therefore the TOF mass spectrometer is a powerful method of investigating the pulsed source. Not only can the elemental composition of the sample be determined with every pulse, but the fact that changing the C-O distance by as little as 1 mm causes measurable alterations in the temporal profiles indicates that spatial measurements with a fair amount of resolution can be obtained. The parametric study of the plasma conditions now serves as a map to guide further research. The glow discharge is a dependable atomic reaction cell, which is made even more flexible by pulsed operation. The pulsing of the discharge makes possible kinetic studies of this gas phase chemical reactor. Reactions such as the heavy protonation of several of the gas species have already been mentioned. However, many more experiments can be designed. The injection of various species into the fill gas could be achieved by a minor modification of the ion source. The effect of reductive or reactive gases is of interest as well.

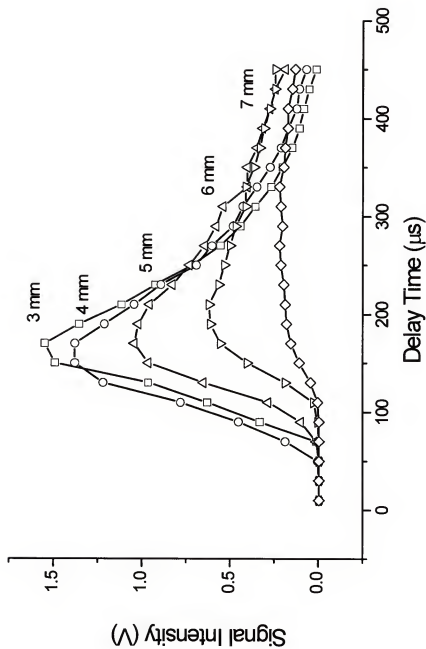


Figure 6-26. Effect of cathode-to-orifice distance on ion signal of copper.

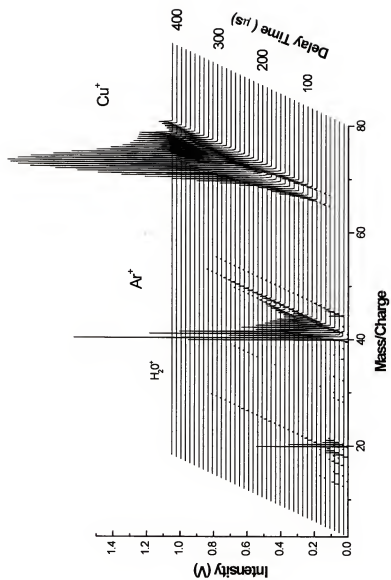


Figure 6-27. Mass spectrum of copper in argon at a C-O of 5 mm.

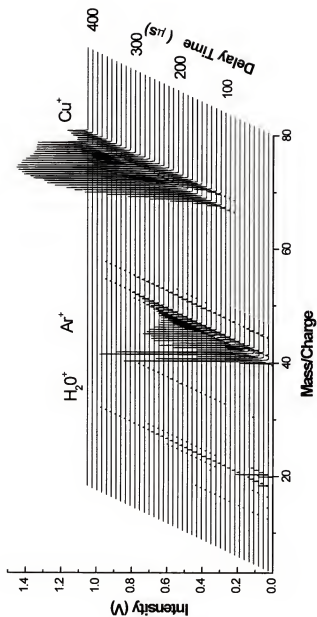


Figure 6-28. Mass spectrum of copper in argon at a C-O of 6 mm.

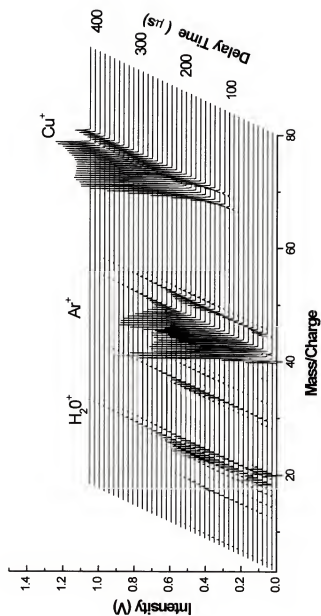


Figure 6-29. Mass spectrum of copper in argon at a C-O of 7 mm.

Also, adding small amounts of helium or neon, which have metastable atoms of much higher energy than argon, could be of potential analytical use.

The greatest ability of the pulsed GD TOFMS lies in the rapid, effective analysis of solid samples. All glow discharges have shown great utility in the area of solids analysis. The microsecond pulsed discharge is a step in taking the performance of GD plasmas to the next level. The high power and efficient sample utilization of the pulsed discharge, in addition to the temporal nature of the discharge, have offered several unique opportunities to study the plasma mechanisms and to improve performance. The performance of the pulsed GD TOFMS system is characterized below.

Relative Sensitivity Factors

When an ion source is coupled to a mass spectrometer, the mass spectrum obtained is a semi-quantitative measurement of the sample composition. Many factors influence the signal intensity of the plasma species. These include: sample composition, matrix type, cathode geometry, cooling effects, discharge power, discharge gas, source pressure, sample geometry, gas flow rate, the type of mass spectrometer and the detection system.⁵⁷ Therefore, for quantitative analysis, mass spectrometry practitioners rely on the use of relative sensitivity factors (RSF's). Regardless of the source, RSF's must be obtained for each element under the parameters used for analysis.

There are two definitions of relative sensitivity factors.^{57,58} We prefer to use the definition found in reference (59). The definition of a relative sensitivity factor of

an element, X, is the ratio of its sensitivity to the sensitivity of a reference element, R. Sensitivity is defined as the amount of signal intensity (I) per unit of concentration (C). Therefore, an RSF can be written as:

$$RSF_{X/R} = (I_X/C_X)/(I_R/C_R)$$

In this regard, all of the above factors regarding source atomization, ionization, sampling and detection can be summed in one term. Calculated RSF's for the pulsed glow discharge vary by little more than a factor of two to three. Ion sources based on thermal effects are matrix dependent and can vary by orders of magnitude based on the composition of the matrix.

Part of the beneficial performance of the glow discharge is that many of its fundamental processes are relatively non-selective. Unlike thermal methods, which suffer from fractionation, the method of atomization within the GD plasma is non-specific. When an ion bombards the surface of a GD cathode, the energy imparted may be enough to sputter an atom. The atom in question may be of any type as long as the energy imparted is enough to overcome the energy binding it to the surface. Sputtering rates for a number of elements often vary less than a factor of 6 for pure elements. Likewise the method proposed as being the primary process for ionization of the sample within the glow discharge, Penning ionization, is relatively non-selective as well. Argon metastable atoms have enough energy to ionize all but a few elements. The general nature of both the sputtering and ionization processes within the glow discharge result in the low RSF's for the technique.

To determine the RSF's of the pulsed discharge, compacted discs were prepared using a powdered spectrochemical standard (SPEX, Spex-Mix 1000) and

copper powder (AESAR/Johnson Matthey, <74 micron, 99.9% purity). Copper comprised 90% of the sample to insure good performance and a stable plasma. Forty nine elements are present in the SPEX-Mix 1000 powder. Most are in their oxide form, but several were in other forms such as: boron (H_3BO_3), calcium (CaF_2), cesium (CsNO_3), lithium (Li_2CO_3), phosphorous ($\text{NH}_4\text{H}_2\text{PO}_4$), potassium (KCl), rubidium (RbCl), sodium (Na_2CO_3) and strontium (SrCO_3). Each element comprised 0.127% of the pressed pellet. Four discs were baked in a vacuum oven for an hour to remove water, allowed to cool and then analyzed. The glow discharge was then run with a 10 microsecond pulse at 2000V, 200Hz, and 1 torr argon. The cathode-to-orifice distance was 4 mm. The signal was then maximized for the copper species, allowed to average 500 times and then recorded. Figure 6-30 summarizes the results of the four discs, normalizing the elements shown to the Fe signal. Most elements show a relatively uniform signal response, which tends to weaken as the atomic mass increases. Few species deviate by a very large amount. Exceptions to this trend are Hg, Cl, and I. Mercury's unusually high signal is an expected result of its very low melting point, whereas, chlorine and iodine have some of the highest ionization potentials of the elements measured and are very close to the energy of the meta stable atom of argon. Tantalum and thallium are known to have low sputtering rates, about half that of Fe. Therefore, Cl, I, Ta and Tl would be expected to have relatively low sensitivity factors. Despite the low sensitivity for these elements, the pulsed glow discharge produces a relatively flat signal across the entire periodic table.

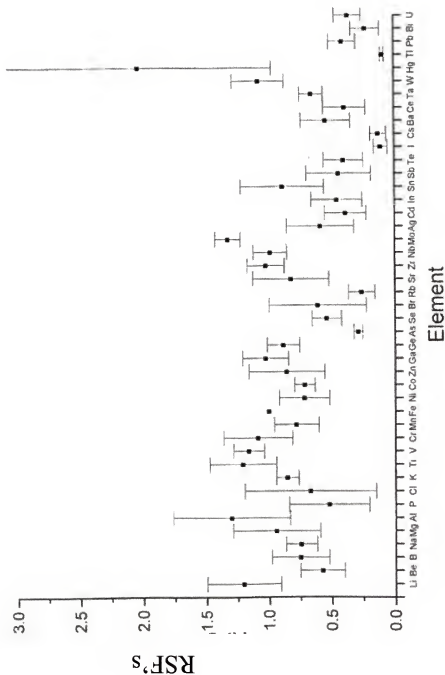


Figure 6-30. Relative sensitivity factors as obtained from Spexmix (normalized to iron signal).

Isotope Ratios

The pulsed GD TOFMS system produces isotope ratios for the elements ionized in the plasma. The accuracy of these measurements is particularly important in geological and nuclear research. Figure 6-31 shows trace amounts of tin and antimony in NIST brass. The numbers above each peak indicate the natural abundance values. The ion signals only vary by 5-7% from reference levels. This number is not ideal for the accuracy desired in high-end nuclear and geological applications, but is sufficient for many other analyses. Figure 6-32 shows the effect of the repeller pulse delay time on the ratio of the two copper isotopes. From the peak to the tail, the isotope ratio is fairly accurate, varying within 10% of the expected natural abundance. This indicates that isotope ratios remain accurate over a number of different delay times. This is important if longer delay times are used in order to remove a spectral interferent when performing trace analysis.

Trace Analysis and Detection Limits

The speed and transmission of the time-of-flight mass analyzer are important factors in its role as a trace element detector. Another advantage of mass spectrometry is its low background. Comparing mass spectra, both the dc and pulsed mode have the same background signal. Therefore, the greater ion signal generated by the pulsed discharge (routinely up to an order of magnitude) results in a greater signal-to-noise, and thus a greater sensitivity. Greater sensitivity translates into lower limits of detection.

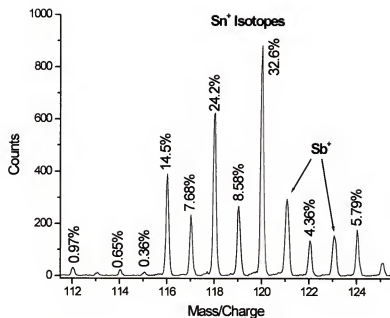


Figure 6-31. Mass spectrum of brass showing tin isotope ratios.

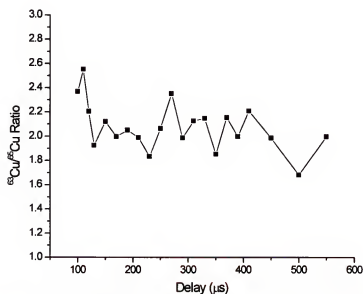


Figure 6-32. Measurement of copper isotope ratios with respect to delay time.

Unfortunately, it is difficult to obtain matrix-matched standards as well as mount the cathode in an analytically reproducible manner. Attempts at making a calibration curve were abandoned. To give an indication of the detection limits a sample with a certified trace elemental composition was examined. Figure 6-33 is a mass spectrum of NIST 495 copper. Trace amounts of iron and antimony can be clearly seen. Above 200 mass-to-charge units, isotopes of lead and bismuth are evident. The exploded view shows a close-up view of the 200 to 210 mass range. The 4 isotopes of lead and the one mass peak of Bi can be seen in closer detail. The small peak from the $^{204}\text{Pb}^+$ isotope is just barely visible above the background. This peak should correspond to 46 ppb of the cathode composition. None of the lead or bismuth peaks were seen in the dc mode of operation. While Figure 6-33 is only a rough indication of the potential of the pulsed glow discharge, at the current time both the understanding of the pulsed plasma and its coupling to the mass spectrometer are still in their early stages of development.

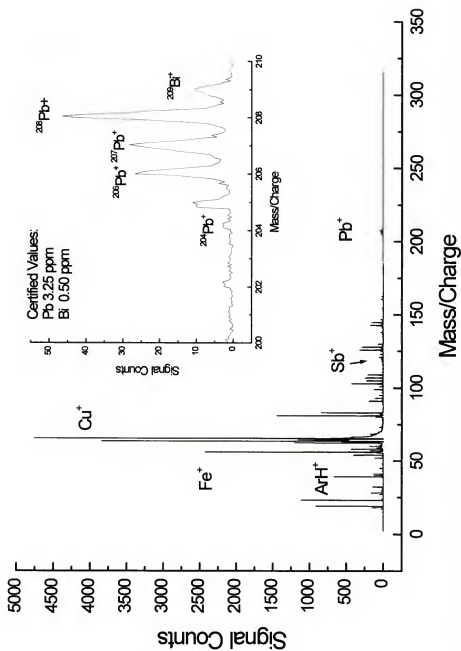


Figure 6-33. Mass spectrum of NIST copper. Insert shows highlights trace levels of lead and bismuth.

CHAPTER 7

INTRODUCTION TO LASER ABLATION SAMPLING INTO A PULSED GLOW DISCHARGE

The pulsed glow discharge is limited to analyzing samples with a conductive or semi-conductive matrix. While there are a vast number of conductive samples that require analysis, many other sample types that require investigation cannot be analyzed. The rf glow discharge is able to analyze non-conductive samples. However, it lacks both the strong signals and transient nature that the microsecond pulsed glow discharge offers.

The pulsed discharge certainly has enough energy to sputter and excite atoms of a non-conductive matrix. It is able to ionize helium, which has a first ionization potential of 24.587 eV. The problem is in the establishment of the plasma. A dc voltage cannot ignite a discharge with a non-conductive cathode, therefore no sampling can take place. One method of analyzing a non-conductor is to grind it, mix it with a conductive matrix, and press a pellet. This method is a proven means of analysis. However, the grinding and mixing processes could lead to contamination. An alternate method would be to atomize the non-conductive matrix and sample the atoms into the atmosphere of the glow discharge. Since helium is ionized (first ionization potential of 24.59 eV), the glow discharge should be able to ionize any materials sampled into the gas phase. One means of achieving this is with the use of

laser sampling. Lasers have the ability to ablate samples regardless of sample geometry or conductivity. Therefore, a combined laser-pulsed glow discharge spectroscopic source was designed. In this and subsequent chapters we will detail the construction and testing of an analytical source involving a laser to ablate material into a pulsed GD. The combined source not only allows the analysis of non-conductive materials, but also allows both the laser and glow discharge processes to be studied.

Lasers have two great advantages for this application. First, with a laser of sufficient power, almost any type of analyte, regardless of physical state or matrix, can be sampled. The laser analysis of solids, liquids, and gases has been reported.⁵⁹ In the case of solids analysis, materials ranging from whole biological viruses⁶⁰ to ceramics and stainless steels have been analyzed spectroscopically using lasers. The second advantage of a laser is that it can be readily coupled with other instrumentation and incorporated into other methodologies. The advantage of such a union allows the properties of both to be studied in a unique light, or perhaps will result in a combined method with greater utility than the two separate techniques.

Due to their utility, lasers have been combined with almost every analytical technique.⁶¹ As a solid sampling device lasers have been combined with arc and spark emission,⁶² dc plasma,⁶³ microwave discharges, ICP emission, ICP-MS and ion cyclotron resonance chambers. Lasers also offer unique opportunities to investigate the glow discharge. The strength of laser techniques is tied to their selectivity. The narrow bandwidth of a laser can selectively ionize certain atomic energy levels. Lasers can also be focused to irradiate a very small area, resulting in good spatial resolution. The bandwidth, focus, and high energy of lasers allow the possibility of

vaporizing or atomizing any sample. Pulsed lasers also enable temporal effects to be studied.

Two limitations of the glow discharge for spectroscopy are that only an estimated 1% of the sputtered population is ionized. Furthermore, the dc discharges most commonly used can only sample conductive materials. Even rf GD sources, which can analyze non-conductive materials, are difficult to use, require the purchase of an rf generator, and also require additional shielding to protect the user and analytical equipment from the dangerous rf frequency. Moreover, the signals generated are weak even compared to the continuous dc mode. The selectivity and power of laser-based methods, with the ability to overcome both of these limitations, offer enticing advantages to the study of the glow discharge.

The selectivity of the laser is based on its narrow bandwidth, short duration, and precise spatial resolution. The power of the laser combines with its spatial resolution to sample and ionize any material, making it a nearly universal sampling technique.

Lasers have been combined with glow discharges to study atomic fluorescence, resonance ionization, optogalvanic spectroscopy and laser ablation.⁶⁴ The two most studied laser-GD interactions have been in laser fluorescence and laser resonance ionization. Laser fluorescent methods have been used to enhance the sensitivity of trace analysis within a bulk sample. The limit of single atom detection has even been approached.²⁸

Resonance ionization increases the sensitivity of mass spectral methods by irradiating the volume of the laser beam with a specific wavelength of light. Atoms

within the discharge absorb laser generated photons with energy corresponding to a specific atomic transition. Glow discharges ionize an estimated 1% of the analyte material. Laser resonance techniques can potentially ionize the remaining 99%. This increases the sensitivity of GDMS by increasing ionization of a desired species, but can also be used to bias against isobaric interferences prevalent in continuous wave sources.

Optogalvanic effects have been studied as well. Pumping a specific electronic transition with a laser can change the current and voltage of a discharge. By monitoring the current and voltage while firing a laser into the GD plasma, several effects can be monitored. For instance, the role of Penning ionization could be monitored by selectively ionizing the argon metastable atoms and determining its effect on the current of the plasma.

Laser Ablation and the Glow Discharge

Hess and Harrison reported the combination of an excimer pumped dye laser with a dc glow discharge.⁶⁴ This combination was used as an ion source for quadrupole mass spectrometry. They reported several findings including the laser sampling of a non-conductive pellet of copper oxide into a tantalum discharge. They also reported some discrimination in the isotope ratios of copper. Due to a combination of the transient signal and the scanning nature of the quadrupole a systematic depression in the heavier isotopes of a given element were observed. In Hess's experiments, the laser was primarily used to vaporize the sample. Due to the increasing availability of more powerful and less expensive pulsed systems, we

decided to couple a Nd-YAG laser with a pulsed glow discharge. The Nd-YAG is about 10-100 times more powerful than the dye laser used in the earlier experiments. The pulsed discharge has enhanced performance when compared to the dc discharge. Finally, the time-of-flight mass spectrometer is uniquely capable of handling pulsed ion signals.

One question that may be asked is, if a laser can vaporize and ionize a wider range of samples than the discharge, why couple the two? Laser ablation, as a source for mass spectrometry, has several difficulties. Due to the power of the laser plasma, the ions formed have very high energy. In addition, laser induced plasmas have a wide energy spread. Laser ablation generates a plasma which has an energy spread ranging from a single eV to an excess of 100 eV. This makes the laser plasma very difficult to focus into a mass spectrometer. The glow discharge on the other hand, is a low energy plasma with a small energy spread. Normally, this is on the order of 1 to 2 eV.

In our initial experiments, we encountered problems when trying to couple the laser to the time-of-flight mass spectrometer. We were unable to detect an ion signal from the laser plasma most likely due to the high energy and wide energy spread of the ions produced. Since we were unable to achieve a mass spectrum, it was decided to study the laser-GD source more extensively using emission spectrometry. By studying its operation and optimizing its experimental parameters *via* emission, a suitable ion source can be developed.

Basics of Laser Induced Plasma Emission

In combining the laser with the pulsed glow discharge it was first necessary to determine the emission characteristics of the plasma generated by the laser striking the material surface. Figure 7-1 is a sketch of the basic instrumental setup. A Nd-YAG laser (YQL, Laser Photonics, Orlando, FL, USA) with a pulse width of 12 ns and maximum energy of 200 mJ was operated at its fundamental wavelength (1064nm) at 20 Hz. The laser beam was focused using a series of quartz prisms and lenses. The beam passed through a pierced mirror at a 45° angle to the laser target. The target was placed on the end of a direct insertion probe and inserted into a stainless steel six-way cross acting as the vacuum chamber. The emission from the laser induced plasma or the glow discharge was reflected by the pierced mirror and focused onto the entrance slit of the monochromator using another series of lenses.

The laser was capable of being externally triggered and it was important to determine the precise temporal character of the firing of the laser and the resultant laser plasma. When a trigger was sent to the laser a finite delay existed between the trigger and the Q-switch signal. The Q-switch triggers simultaneously with the firing of the laser. By scattering some of the laser emission onto a fast photodiode (protected by a 2.0 N.D. filter), the pulse width of the laser was able to be measured. The photodiode signal appeared as a smooth gaussian curve with a 12 ns pulse width. Figure 7-2 shows the temporal profile of several of the Q-switch, data gate and fast photodiode signals. It was necessary to deliver a 5-7 volt pulse with at least a 2 ms pulse width to the flashlamps of the laser. The Q-switch triggered and the laser fired

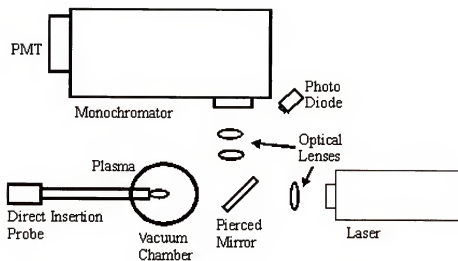


Figure 7-1. Experimental setup for laser ablation sampling into a pulse GD.

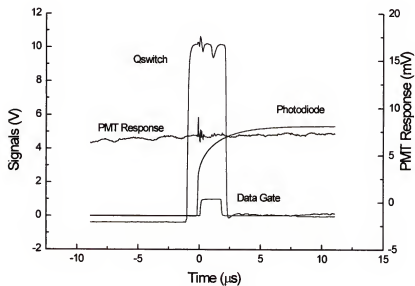


Figure 7-2. Temporal responses of laser emission collection.

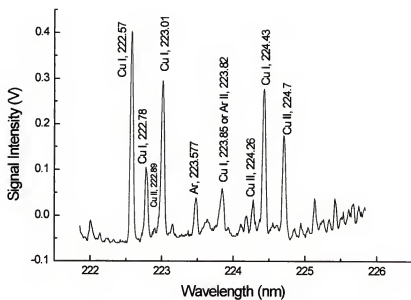
170 microseconds after the rising edge of this pulse. A fast photodiode was used to measure the temporal response of the laser plasma. Although the diode signal quickly saturates, Figure 7-2 shows that a 1 microsecond delay existed between the firing of the laser and the plasma emission. The data gate for signal collection was centered on the peak of the emission signal. Because the laser flashlamps operate at such high voltage it was also important to characterize the noise that the photomultiplier tube (PMT) may pick up during the firing of the laser. The temporal response of the PMT during the firing of the laser with the slit of the monochromator covered is shown in Figure 7-2 as well.

The most prominent characteristic of a laser induced plasma is its high emission intensity. The power of the laser plasma displays itself in the emission spectra by populating several high energy emission lines. For reference, Figure 7-3a shows the dc spectrum between 222 and 226 nm. Several copper atom lines are clearly evident and some argon and Cu II lines are seen as well. When the laser is fired, the emission collected was so strong that it completely saturated the detector. It was necessary to lower the PMT voltage from 740 volts to 400 volts (a reduction of three orders of magnitude) in order to collect the laser plasma spectrum. Even then, three of the lines were still saturated. Figure 7-3b is a recording of the laser induced spectrum. Note how remarkably different the two spectra look. The laser plasma is marked by very strong emission from singly charged ions. Many weak emission lines are visible, while copper atom emission which dominated the dc spectrum, is hardly detected. The laser plasma is energetic enough to populate other high lying energy states. Several Cu III lines, which are not seen in GD emission,

are evident in the laser plasma. Figure 7-3c shows a series of Cu II and Cu III lines in the region around 250 nm. The prevalence of ionic species and lack of atomic emission lines was noted.

While the laser produces a very high-energy plasma which emits strongly, there are some limitations which should be considered. Primarily, the plasma generated is so energetic that it acts as continuum source for the first several hundred nanoseconds of its existence. This continuum emission acts as background noise and limits the utility of the laser plasma. Figure 7-4a shows the PMT signal with the monochromator set to a region that does not emit a spectral line. The slit of the monochromator was covered to register the dark current and then uncovered to record the continuum emission. Figure 7-4b illustrates high background from the continuum emission. When the data gate (100 ns integration time) of the boxcar was set to a delay of 40 ns, the spectrum showed a considerably higher background and broad, weak emission from the spectral lines. When a data gate of the same width was moved to a 300 ns delay a very different spectrum was collected. The second spectrum shown in Figure 7-4b, shows that the continuum emission has died away, leaving a spectrum with a much lower spectral background. Some of the high energy species such as the Cu III, 215.73 nm line have disappeared as well. This is most likely due to recombination collisions within the plasma. The spectrum taken at a later delay also shows narrower, more intense lines from both Cu II and even some Cu I lines.

a)



b)

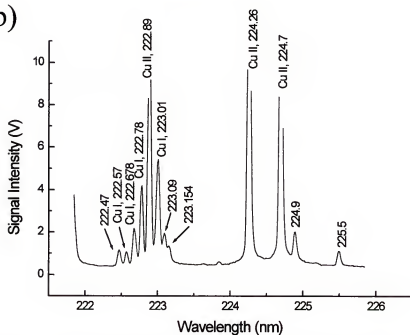


Figure 7-3. Copper emission from dc GD with and without laser.
 Conditions: 900V 1.1 mA, 1 torr. a) Dc: PMT 740 V; b) LEGD:
 PMT 400V.

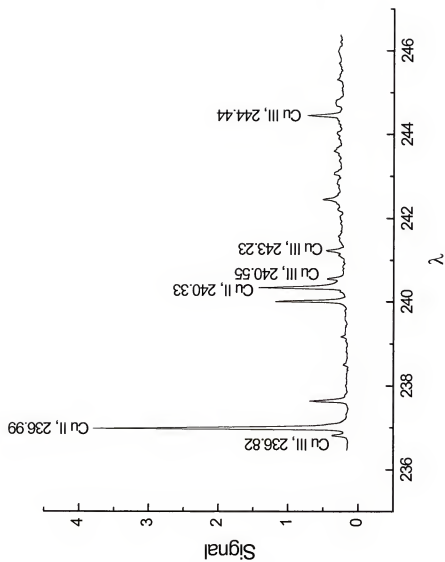


Figure 7-3-continued. c) Laser emission of high energy state lines.

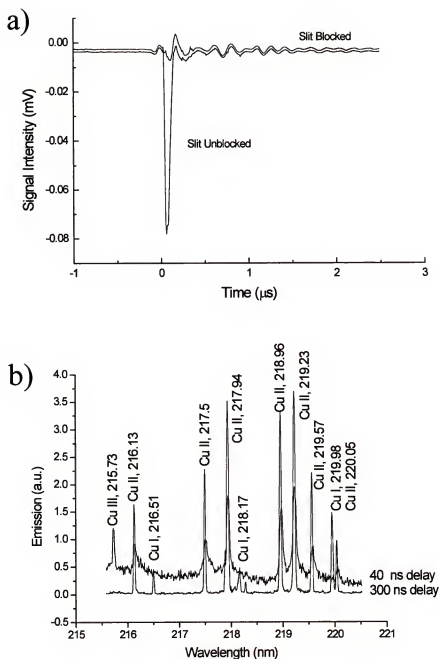


Figure 7-4. Temporal response of laser emission and continuum background. a) Continuum background off-line; b) Laser emission at two delay times: 40 ns and 300 ns.

The temporal profiles of atom and ion lines are indicative of the emerging and decaying plasma. Figure 7-5 shows the temporal profile of several atom and ion lines. The continuum background was measured and subtracted from each of the temporal profiles to sharpen the distinction between the atomic and ionic emission. Unlike the pulsed glow discharge, which first atomizes and then ionizes sample atoms from collisions within the plasma, the laser plasma ionizes 100% of the sample. This is evidenced by the three sharp, narrow Cu II ion lines that are formed immediately in the plasma. There is no atomic emission detected in the early stages of the plasma. Only when electrons and ions begin to recombine within the dense plasma is atomic emission seen. Thus a delay between the peaks of ion and atom emission is seen in the laser spectra.

The total amount of time that the laser plasma emits light is needed to be determined. In many of the studies of the combined laser-GD source, it will be necessary that the emission from the two plasmas does not overlap. Most of the laser plasma emission disappears after 1-2 microseconds. The experimental factor that exhibited the greatest influence on the length of the laser emission was the pressure within the vacuum chamber. Figures 7-6a and 7-6b show the temporal profiles of the background emission and some selected atom and ions lines at two different pressures. To perform this study, the laser plasma emission was viewed from the side, using a lens to form a 1:1 image of the plasma on the monochromator slit. A machining table was used to move the monochromator back and forth precisely, so that different regions within the plasma could be explored. In the data shown, the monochromator sampled the region approximately 1 mm above the sample surface. The lower end of

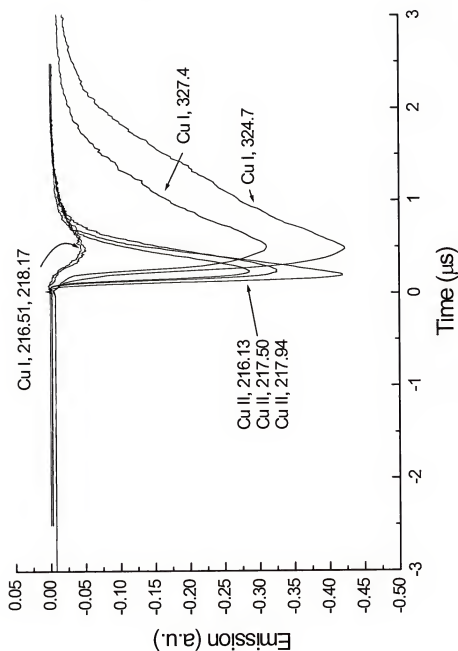


Figure 7-5. Temporal profiles of copper atom and ion lines in the laser plasma.

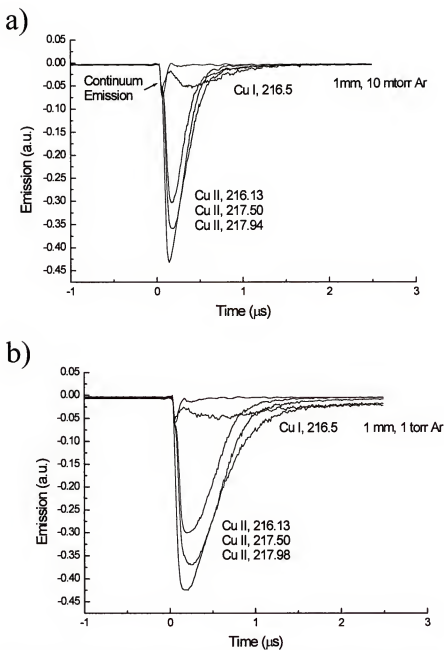


Figure 7-6. Spatial and temporal measurements of laser atom and ion emission. a) 1 mm from cathode, 10 mtorr; b) 1 mm from cathode, 1 torr.

the pressure range studied was 3-10 millitorr, which was the limit of the mechanical vacuum pump. The upper range ended at 10 torr because at that point there was a sufficient density of argon atoms to cause a breakdown within the gas. Figures 7-6a and 7-6b summarize the experimental data for laser emission at 10 mtorr and at 1 torr. One torr is the typical operating pressure of the GD.

The results of this experiment helped to form a more complete picture of the laser plasma, so that it could be matched to the GD in later experiments. It is noted that the continuum emission is relatively unaffected by changes in laser power or pressure. It is unlikely that the extremely high local temperatures and pressures achieved in the initiation of the plasma and responsible for the continuum emission would be affected by such a relatively slight change in the physical surroundings. The pressure also had little effect on the peak intensity of the atomic and ionic lines sampled. The greater number of collisions did cause the temporal profile of the emission peaks to broaden significantly. The area under the peak for the Cu II, 217.94 nm emission line more than doubled. Regardless of the pressure, the emission from the plasma had nearly vanished by 2 microseconds after the laser fired. The temporal profile of the emission and the parameters that affected it would later become quite important when coupling the laser to a GD source.

Not only is the ion emission fairly confined temporally, it is also confined spatially. Figure 7-7 is a graph of the spatial profile of the laser emission collected at a delay of 300 ns after the laser fired. The Cu II, 217.5 nm line is quite intense very close to the surface of the laser target, and more intense than the Cu I resonance line. However, as the plasma is imaged further and further away from the target surface, the

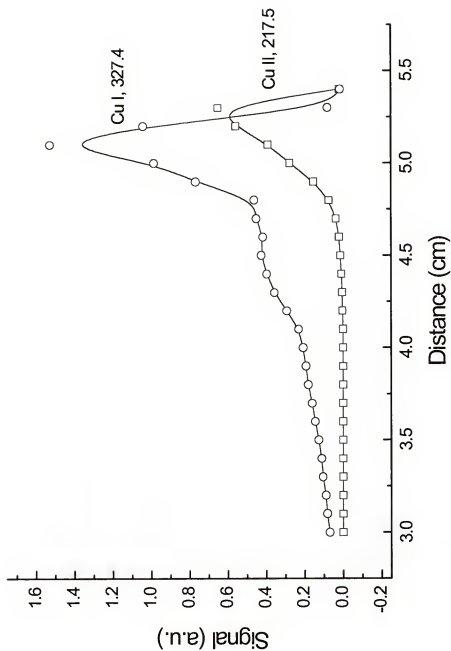


Figure 7-7. Spatial measurements (orthogonal) of laser atom and ion emission. Note: cathode is at 4.9 cm.

ions quickly recombine to form emitting atoms. Because a laser must be fired directly at the target surface, the tight spatial confinement of the ions could cause problems in designing a purely laser based mass spectrometric ion source. On the other hand, when combining the laser with the pulsed glow discharge, the generation of a purely ground state atomic population is desirable.

The relationship between distance and pressure was studied further, trying to characterize the diffusion characteristics of the ablated material. A crude image of the diffusion and excitation processes was formed by measuring atomic and ionic emission at 1mm intervals within the plasma over a range of pressures. Figures 7-8a and 7-8b illustrate the results of this experiment. These graphs show that at the lowest pressure achieved by the vacuum pump, nominally 10 mtorr, the population of the Cu II, 216.13 line is relatively high and tightly focused immediately above the cathode. At 5mm, the ion line has a greatly reduced intensity, but the same temporal profile. Due to the small concentration of particles at low pressure, the mean free path of the ablated particles is relatively high and their collisional cross section low. Therefore, the packet of ions travels out from the surface of the sample with few collisions in a relatively tight orthogonal band. The intensity of the emission line diminishes due to the radial diffusion of the packet.

At higher pressures, more typical of GD operation, the copper ion line shows a very different temporal profile. When the region directly above the surface of the target is imaged onto the entrance slit of the monochromator, only a slight change between 0 torr and 1.2 torr can be seen (Figure 7-8a). Due to the higher pressure, the emission line lasts twice as long. However, a much more dramatic difference is seen

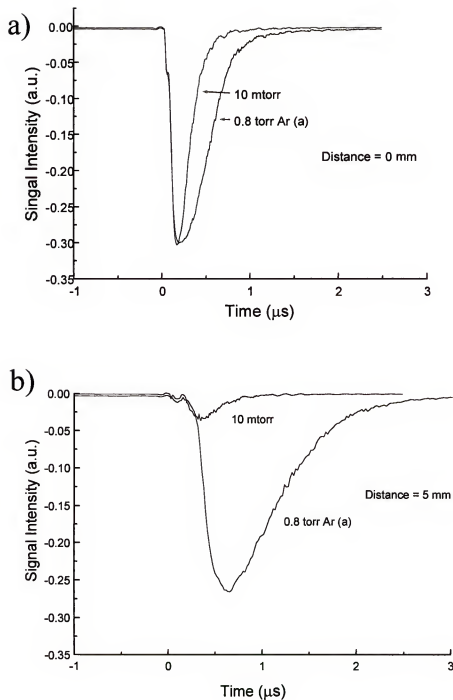


Figure 7-8. Temporal profile of Cu II, 216.13 nm line.

a) Just above cathode surface; b) Centered at 5mm from cathode.

when the region 5 mm from the surface is probed. At very low pressure, the signal had a similar temporal profile (width of 2-300 ns) to the emission scanned at the surface, yet its intensity was greatly diminished. At the increased pressure the emission intensity was only reduced by about 15%. However, the width of the temporal profile increased by a factor of 2.

It is well known that increasing the pressure will both confine the plasma and allow more collisions to take place. A clearer image of the diffusion of the laser ablated atoms will be gained by making absorption measurements within the expanding laser plasma. These measurements will be discussed in a later section.

If the laser is to act as a means of sampling material into the glow discharge, it is important to determine not only the diffusion characteristics, but also the precision of the laser sampling process. Data concerning the reproducibility of the laser were gathered in three ways. First, several individual shots were collected to get an idea of the shot to shot reproducibility. Secondly, the effect of signal degradation due to successive shots impinging upon the surface was measured. Third, the reproducibility of spectra was measured taking into consideration several experimental limitations.

To measure the shot to shot reproducibility of the laser system, the temporal profiles of ten individual laser shots were collected and used to form statistical data. The data was taken by monitoring the Cu I, 324.7 nm line in a 1 torr argon atmosphere. Figure 7-9 shows that the average of the 10 laser pulses showed a 51% relative standard deviation. While the relative standard deviation seems high, this is not unusual. One of the limitations of any pulsed laser technique is the imprecision of laser shot-to-shot reproducibility. A laser was fired into a dc GD to study the

interaction of the two plasmas. Ten individual pulses were collected under the same conditions as the 10 laser-only pulses. The relative standard deviation of the combined plasma was reduced to 8.7%. It seems reasonable that an electric field would serve to focus the ions and electrons formed in the strong plasma and potentially could improve the reproducibility of the plasma initiation. However, even more interesting was that firing the laser into the dc GD increased the emission intensity by a factor of three. If the application of an electric field to a sample was able to significantly improve analysis using laser plasmas by increasing the signal and improving the stability of the plasma, perhaps the sensitivity of the technique could be improved as well, lowering the limits of detection. Another interesting experiment would be to test the establishment of a GD plasma with a non-conductive sample by using repetitive laser pulses to sustain a dc plasma.

One of the benefits of the laser is its ability to remove material from a spatially confined area of a surface. This can also be a disadvantage in the respect that successive shots to the surface will begin to ablate a crater. The removal of material will eventually cause the laser to strike a surface which is no longer in focus. Also, the roughness of the craters bottom and edges serve to diffract some of the laser power. As the number of laser pulses striking the surface grows, the sample removal rate and emission characteristics of the laser plasma will change. Figure 7-10 shows the decrease in emission intensity of the Cu I, 218.17 nm line vs the number of laser shots impinging the surface. Normally, this reduction in emission is managed by rotating or moving the sample with a mechanical stage so the laser rasters across the sample and each shot hits a fresh surface. Lacking this ability on our instrument we

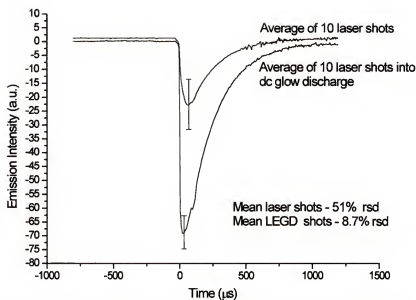


Figure 7-9. Reproducibility of single laser shots and single laser shot into a dc glow discharge. Conditions: 800 V, 1 torr, PMT 400V.

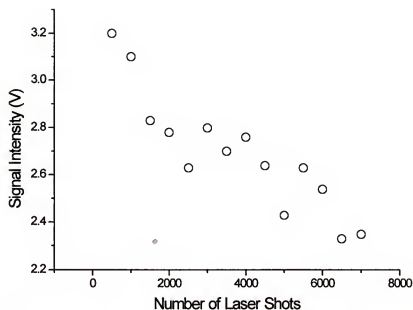


Figure 7-10. Reduction of laser emission intensity with successive number of laser shots. Conditions: Cu I, 218.17 nm line, 20 Hz, 1 torr Ar.

decided to limit the collection of spectral data to between 500 and 1000 laser shots before moving the target manually to allow a fresh surface to be sampled. This should limit the loss of emission due to gradual degradation of the sample surface.

When measuring emission from multi-element, pulsed systems, specifically the pulsed GD and pulsed lasers, the most ideal collection device would be a gated, intensified charge coupled device or photodiode array. These detectors collect the emission from a spectral range simultaneously showing an entire spectral window with each pulse. Alternatively, a PMT can be used while the monochromator scans through a range of wavelengths. Our system was limited to the use of a PMT, which could be a potential problem due to the fact that the laser must fire for each point in the collected spectrum. Normally in pulsed emission sources like the pulsed glow discharge, 100's or even 1000's of emission pulses can be collected and integrated and averaged by a boxcar between each step of the monochromator. Since the laser ablation signal degrades with successive pulses and five hundred pulses are needed to collect a reasonable wavelength range for a spectrum, no averaging could take place.

In order to obtain meaningful results, the following experimental factors needed to be taken into consideration. 1000 points were collected while scanning a 10 nm spectral range. Based on the data shown in Figure 7-10, there should not be a significant reduction in signal from the beginning to the end of any collected spectrum. Without any averaging, the laser shot to shot noise of nearly 50% would result in poor quality spectra. Fortunately, when the laser is operated at a fixed frequency, typically 20 Hz, the precision greatly improved (15%). Ten spectra were collected and averaged to test the reproducibility of the laser induced plasma spectra.

Figure 7-11 shows the relative standard deviation of 7 atom and ion lines that appear between 216 and 225 nm. The rsd was 10% or less, demonstrating that spectra consisting of 1000 individual shots with no averaging would still deliver adequate results. It is noted that the performance of the instrument for both diagnostic and multi-element analysis applications could be greatly enhanced by the addition of a gated diode array, which would allow averaged spectra to be collected. The results of the spectral data from the laser plasma show several interesting characteristics. The energetic nature of the laser ablation plasma and the resulting population of high-lying states, producing mostly Cu II and Cu III emission lines has been previously mentioned. Conspicuously absent from the emission spectra from the laser in a 1 torr argon atmosphere are the argon emission lines. The laser induced plasma emission consists of predominantly ablated atom and ion emission with very little spectral contribution from the argon fill gas. Figure 7-12a shows a dc GD spectrum from 216 to 220 nm. Many of the minor copper lines are seen with a significant number of argon ion lines as well. When the laser is fired, the plasma emission is so intense that the PMT voltage must be turned down to avoid saturation and damage. When the PMT voltage is reduced from 740 V to 400 V, this results in a 1000 fold reduction in sensitivity. Nevertheless, a strong signal from the copper lines is obtained. Figure 7-12b shows the laser induced plasma spectrum covering the same spectral range. The strongest lines are clearly the ion lines with only two Cu atom lines appearing. No emission from the argon lines can be seen.

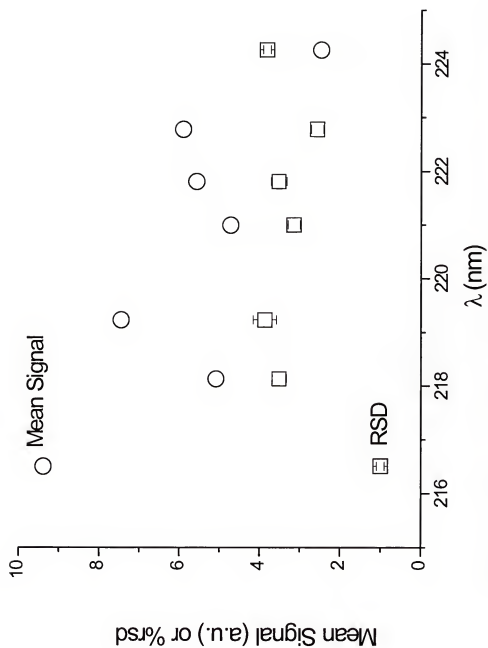


Figure 7-11. Mean and rsd measurements of laser emission for selected copper lines.

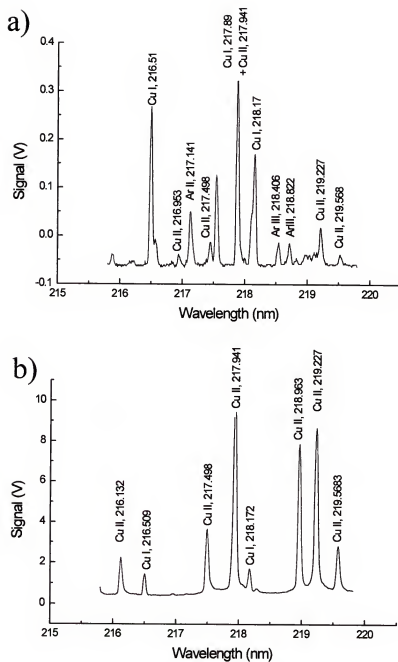


Figure 7-12. Comparison of dc and LEGD emission. Conditions: 900V, 1.1 mA, 1 torr Ar. a) dc discharge, PMT 740 V; b) LEGD, PMT 400V.

To better understand the role of the laser in Cu and Ar ionization, the region between 294 and 298 nm was investigated. Figure 7-13a shows a dc GD spectrum of this region. One copper ion and two argon lines are all clearly seen. Only a weak Cu II, 296.1 nm line can be seen. When the laser is fired into the dc glow discharge the Cu II line becomes strong and the argon lines recede. The ratio of the Cu line to the argon lines is significantly altered as seen in Figure 7-13b. It is interesting to note that the Ar II emission cannot be from the dc discharge alone, because the dc discharge is 3 to 4 orders of magnitude weaker than the laser emission and with the PMT turned down to 400 V, could not be seen. The interaction of the laser with the glow discharge, even in the continuous mode may have some analytical merit by increasing the emission from analyte species while reducing spectral interference from gas species.

Since the emphasis of the laser work was to combine the pulsed GD with the laser, tests were performed to characterize and optimize the new source. These results are contained within the next sections of text. Preliminary results, which connect the work previously reported with the next chapter, are seen in Figure 7-14. The laser induced plasma emission intensity is almost a thousand times greater than the dc discharge emission intensity. The pulsed glow discharge emission intensity falls between the two, being 1-2 orders of magnitude stronger than the dc discharge and still a little over an order of magnitude smaller than the laser emission. Figures 7-14a and 7-14b show the pulsed glow discharge and the laser plasma emission spectra taken at the same conditions, at the reduced PMT voltage of 400V. It is important that the pulsed GD and laser can be run under the same range of pressures, frequency and detector settings if a combined source is to be achieved.

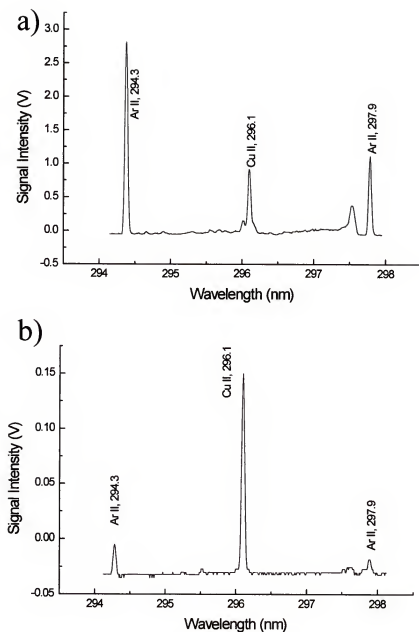


Figure 7-13. Comparison of dc and LEGD emission of Cu II and Ar II lines. Conditions: 900 V, 1.1 mA, 1 torr Ar. a) dc discharge, PMT 740 V; b) LEGD, PMT 400V.

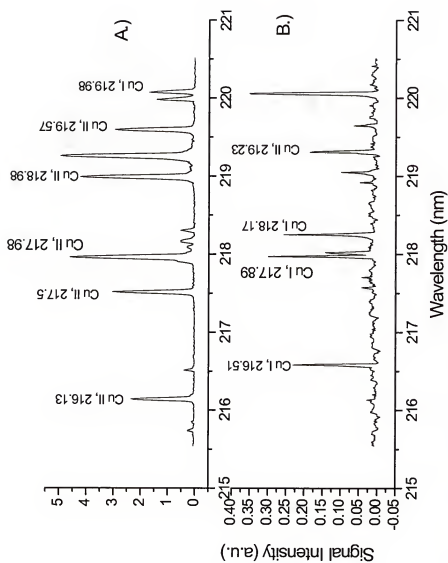


Figure 7-14. Comparison of laser and pulsed glow discharge emission. Conditions: 1 torr, PMT 400V. a) Laser emission; b) Pulsed glow discharge emission, 2 kV.

CHAPTER 8

INTRODUCTION TO THE LASER ABLATION-GLOW DISCHARGE

When a laser with sufficient energy to cause ablation impinges on a target, a bright plasma is formed and material is removed from the surface. The extreme conditions of the initiation of the plasma are quite chaotic, producing even continuum emission. A millisecond later, nearly all the emission has ceased and the only evidence that the laser has fired is a small crater on the surface of the target and a residual population of the ablated atoms in the ground state dispersed throughout the vacuum chamber. When a GD is fired at this time, these ablated atoms are again excited and they emit light characteristic of the atoms involved. The pulsed GD shows an increased amount of emission when the laser target is the GD cathode. Since the pulsed GD emission is enhanced when re-exciting the laser ablated material, the phenomena has been termed the Laser Enhanced Glow Discharge or LEGD. Figure 8-1 shows the temporal profiles of the Cu II, 224.7 nm line when the GD is fired alone and when the GD is fired 0.9 ms after the laser. The signal intensity is enhanced by a factor of 3. This and the subsequent chapters detail the study of the effect and optimization of the experimental factors influencing this phenomenon in addition to applications of the combined laser-GD source.

As mentioned in the last chapter, laser induced plasma emission is between 10 and 100 times greater than the pulsed glow discharge depending on the line being

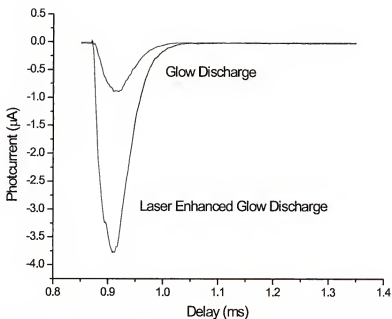


Figure 8-1. Comparison of the pulsed and the laser enhanced glow discharge. Conditions: 1.6 kV, 1 torr, Cu II, 224.7 nm.

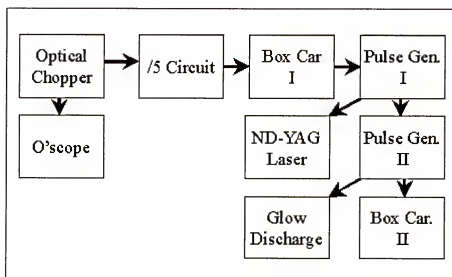


Figure 8-2. Flow chart of timing mechanism for laser ablation-GD studies.

observed. In order to have the greatest sensitivity, it was necessary to make sure that the laser emission did not saturate or hinder the performance of the PMT. To accomplish this, an optical chopper was synchronized with the firing of the laser and glow discharge. Figure 8-2 is a flow chart of the various instruments involved in the timing of the laser and GD pulses. The optical chopper was operated at 100 Hz and was the master trigger. A divide-by-five circuit was used to reduce the frequency of the output trigger of the chopper from 100 Hz to 20 Hz. This trigger was then used to trigger a pulse generator (HP 8003a). The positive output trigger was used to trigger the laser, while the negative output triggered a second HP pulse generator. This second generator triggered the high voltage pulse generator of the glow discharge and was the source of the adjustable delay between the firing of the laser and the GD. Figure 8-3 shows the timing of the various signals involved in the acquisition of the LEGD emission signal. The HP pulse generator sent a trigger signal to the flash lamps of the laser and the Q-switch fired simultaneously with the laser. Between 0 and 0.5 ms, the laser emission was generated and died away. During this period, the optical chopper blocked the entrance to the monochromator slit, eliminating any signal from the laser emission. At 0.5 ms, the back edge of the optical chopper rotated past the slit, allowing the GD emission to be detected. Half a millisecond later the glow discharge was fired. The data gate of the boxcar collected the signal of the re-excited atoms from the PMT.

Figure 8-4 shows a closer view of the timing involved in signal collection. The firing of the GD voltage, the temporal profile of the GD emission, and the LEGD emission are all shown. The GD power supply has a 10 microseconds pulse width.

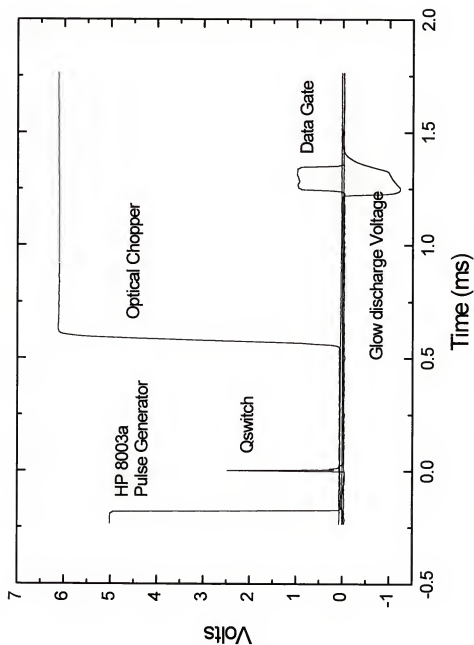


Figure 8-3. Timing of the laser-pulsed glow discharge source.

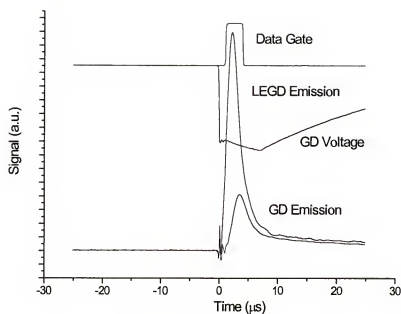


Figure 8-4. Temporal profiles of GD and LEGD emission collection.

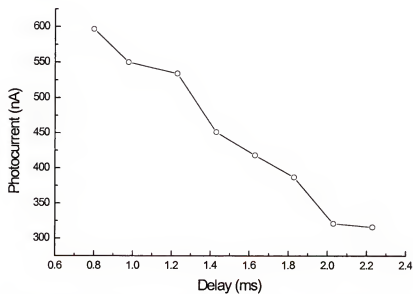


Figure 8-5. Reduction of emission as delay between laser and GD is increased.

The Cu emission from the pulsed GD begins to rise shortly after the initiation of the plasma and reaches a maximum right near the end of the GD voltage pulse. When the laser fires prior to the GD, a significant enhancement is seen in the emission. This enhancement is not due to the laser induced plasma emission, as 100% of the laser emission is blocked by the optical chopper. Instead, it is due to a combination of the sputtered and excited atoms from the glow discharge and the re-excitation of the laser sampled atoms by the GD plasma.

The first parameter to be tested was the delay between the laser and the glow discharge. As the delay between the laser and GD grows, the strength of the signal from the re-excited atoms diminishes. As seen in Figure 8-5, the emission from the Cu I, 216.51 nm line declines as the delay is increased. Due to jitter in the rotation of the optical chopper, a window of 200 microseconds on either side of the rising edge of the optical chopper needed to be maintained if the laser emission was to be blocked completely. Therefore, no results were reported for a delay less than 0.6 ms. Results from experiments without the use of the optical chopper have shown that the emission signal continues to increase until the laser and the GD almost overlap. At 20 Hz, the GD was not very stable and firing the laser directly into the pulsed GD during the pulse-on period started arcing. The GD is both stronger and more stable at higher frequencies and if operated at higher frequencies, perhaps could have been fired simultaneously with the laser. Unfortunately, the laser has a maximum rate of operation of 20Hz.

An enhancement of both Cu atom and ion emission intensity was observed. To understand this phenomenon, the amount of analyte in the chamber needed to be

determined. Ablation rates were measured to determine the amount of material removed by the laser and absorption measurements were taken to describe the transport of the ablated material. Figure 8-6 shows the ablation rate of the laser plotted against the power of the laser. The power of the laser was first measured by using a prism to direct the laser beam into a power meter. The power meter consisted of a head (Scientech model 380101), which was specific for the range covering the 1064nm wavelength of the laser and a power meter (Scientech model 364). It took nearly half a minute for the signal to stabilize, so the average power was read after 30 seconds. To achieve the lower powers it was necessary to attenuate the laser by placing mesh screens in the path of the unfocused laser beam. To measure the ablation rate copper samples were carefully weighed using a microbalance (typical sample weighed 100 mg), attached to the end of a direct insertion probe and then inserted into the vacuum chamber. The number of laser shots was counted using a (Monsanto model 104A) pulse counter. 2,500 shots were allowed to strike the surface and then the sample was removed and reweighed. It was arbitrarily decided that 1.2 W average power would be used for most of the following GD studies. At this power, the ablation rate was 107 ng/pulse. This is 30 times greater than the sputtering rate of the pulsed glow discharge which was 3.47 ng/pulse at the same pressure and normal operating conditions. At first glance, it would appear that the increase in emission was merely due to the presence of more material in the gas phase. The experiments in the next chapter focus on the parametric study of the LEGD plasma and indicate that this is not necessarily the case.

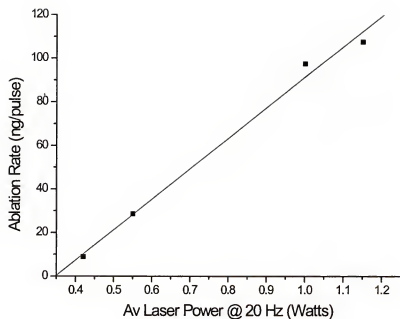


Figure 8-6. Ablation rate of the laser. Conditions: 1 torr argon, copper target.

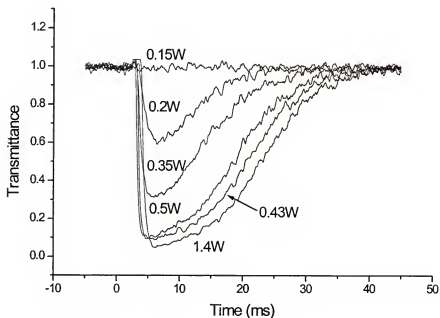


Figure 8-7. Absorption as a function of laser power.

We next consider the diffusion of the ablated material throughout the vacuum chamber. We can estimate the average velocity of an atom in the laser plasma using the Maxwell-boltzmann velocity distribution law:

$$\text{Average } v = (8kT/\pi m)^{1/2}$$

Where k is the Boltzmann constant, T is the temperature of the plasma (about 10,000 K), and m is the atomic weight of the species. For an atom of aluminum with an atomic weight of about 27 amu:

$$\text{Average } v = 2.75 \text{ km/second}$$

This indicates that most of the laser ablated material would hit the walls of the chamber, 2.5 inches away, in about 23 microseconds, leaving little material left in the gas phase. This would suggest there was significantly less ablated material in the gas phase when the GD fired, considering the ablation rate was only 30 times greater than the sputtering rate of the pulsed glow discharge.

To determine the behavior of the laser ablated material, absorption measurements were made. Using configuration 2 of the LEGD instrument, a copper disc was mounted on a direct insertion probe and used as the laser target. The glow discharge probe remained in position, but was not operated. A hollow cathode lamp was focused in a beam of 4 mm diameter centered 2 mm from the surface of the GD cathode. This way, the hollow cathode would only probe the volume directly in front of the GD, where most of the emission due to the glow discharge should take place. A series of absorption measurements at 324.7 nm was used to record the effect of the laser power on the absorption signal of the laser ablated atoms. Figure 8-7 summarizes these results. At 0.15 Watts, no laser plasma was seen and there was no

detectable absorption. As the laser power was increased, the signal increased dramatically and was quickly became completely absorbing.

To determine how material was transported from the laser target to the GD, measurements were taken while placing the laser target at various distances from the axial line of the GD cathode. The effect of pressure on these measurements was recorded as well. The results of these experiments can be seen in Figure 8-8. The most obvious feature of the absorption profiles is that they are nearly completely absorbing. There is little difference in changing the distance from the GD. The slight difference seen at 0 mm for each of the three pressures is most likely due to contamination of the signal by emission from the laser plasma, rather from some fundamental effect. The slight difference in the width of the signals could be used to study the effect of pressure on the diffusion coefficient of the laser ablated material.

One feature of the absorption signal stands out. The width of the absorption signal ranges from 15 to 35 ms. This would indicate that the average velocity of the laser ablated atoms is less than 3 km/second. There are two explanations why the signal would both be saturated and last so long. The first reason would be if the electronics used to measure the signal induced some temporal broadening. The second reason could be that the laser ablated material was being removed as particles rather than atoms. Particles have greater mass and would move much slower than atoms. Also, light from the hollow cathode would scatter or be blocked entirely if a large number of particles were ablated, causing a large absorption signal.

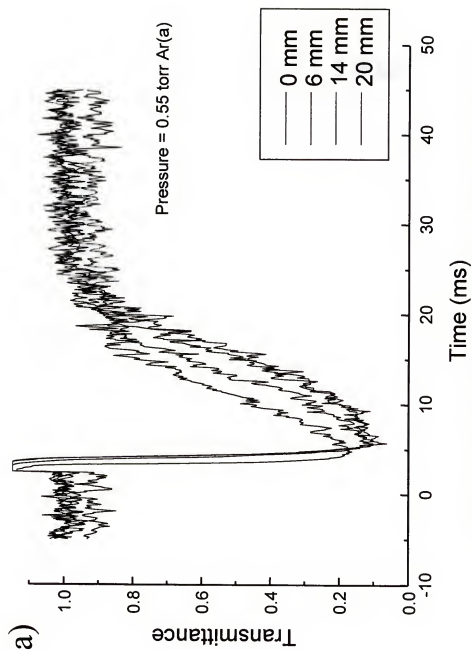


Figure 8-8. Transmittance of laser ablated material. a) 0.55 torr argon.

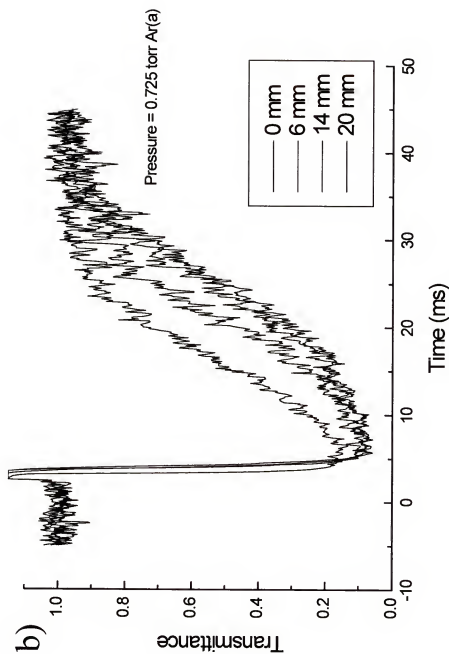


Figure 8-8-continued. b) 0.75 torr argon.

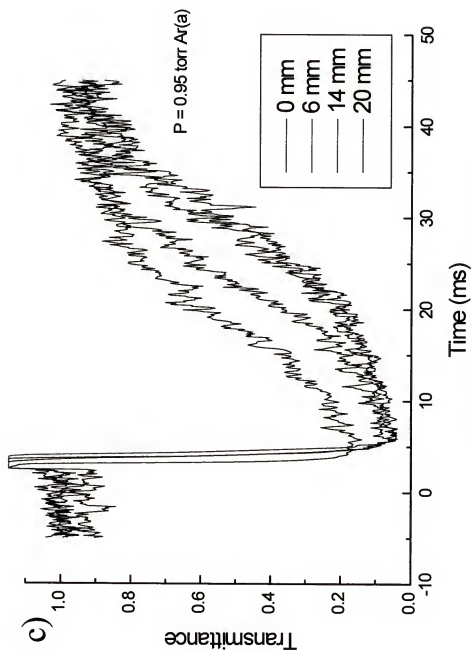


Figure 8-8-continued. c) 0.98 torr argon.

To test the first hypothesis, the level of amplification of the current amplifier (Stanford Research Systems, model SR570) attached to the PMT was changed. The fast pre-amplifier had a time constant of a microsecond indicating that results on the order of ms would not be affected, and no change was noted regardless of the gain used. A second possibility could be that the frequency filter of the pre-amplifier caused the broad signal. The data in Figures 8-7 and 8-8 were taken with no filtering, which corresponds to a 1 MHz measurement bandwidth. Figure 8-9 shows the effect of altering the bandwidth of the pre-amplifier. Only at frequencies 300 Hz and below does temporal broadening begin to show. It was therefore concluded that the pre-amplifier did not distort the broad absorption peaks.

The second possibility for the saturation and broadness of the absorption signal would be the presence of large amounts of ablated particulates. To test for the presence of particulates, the monochromator monitoring the hollow cathode emission was tuned from the Cu I, 324.7 line to the Ne II 332.0 line. The neon ion line was emitted by neon fill gas of the hollow cathode lamp. Since there was no neon in the GD chamber, any decrease in the Ne II line would be due to scattering off particulate matter generated by the laser ablation plasma. Figure 8-10 shows that there was no decrease in the neon line intensity and therefore it is unlikely that the amount of particulates is high enough to cause either of the effects seen in the absorption signal. It was therefore concluded that the absorption profiles accurately reflected the atomic population in the region sampled.

Another test was designed to evaluate the accuracy of the absorption response. If laser ablated material was left in the gas phase up to 20 ms after the laser fired, then

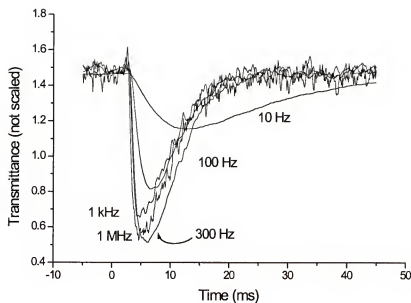


Figure 8-9. Absorption signal vs bandwidth.

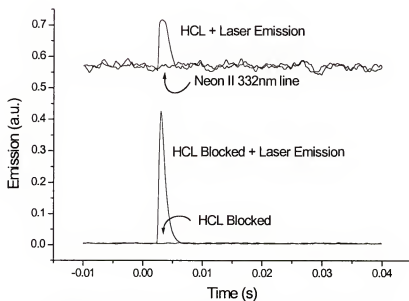


Figure 8-10. Signals showing lack of neon scattering.

it would still be present for excitation at that time. The laser was fired at a secondary target while a continuous dc discharge was in operation. The laser induced plasma emission, dc glow discharge emission, and the emission of the laser fired into the dc discharge was measured and compared to the temporal response of the laser absorption signal at three laser powers. Figures 8-11a and 8-11b show the results of this test. The glow discharge effectively excited the laser material that remained in the glow discharge. Figure 8-12 shows the temporal profiles of the absorption signal and emission overlaid on one another. The fact that they are nearly mirror images of one another indicates the laser ablated material does not diffuse through the chamber as quickly as the Maxwell-Boltzmann equation would predict.

Figure 8-13 serves as a transition to the next chapter. Just as the emission profiles in Figures 8-11 and 8-12, the laser was fired into the dc glow discharge. The boxcar was used to filter out the laser emission and integrate the emission resulting from the increase in the GD emission due to laser material. The laser power and pressure within the chamber were kept constant while the dc GD voltage was increased. Since the amount of material, the sputtered plus the ablated, is the same in each, the resulting increase in emission is mostly due to the efficiency with which the GD re-excites the laser ablated material. The signal intensity was directly proportional to the GD voltage. This suggests that the pulsed GD would be an excellent means of re-exciting the laser sampled material. The pulsed GD operates at higher voltages and much higher peak powers. If the response of the laser ablated material in regard to emission is going to be dependent on the function on the GD, then the pulsed discharge has many promising features.

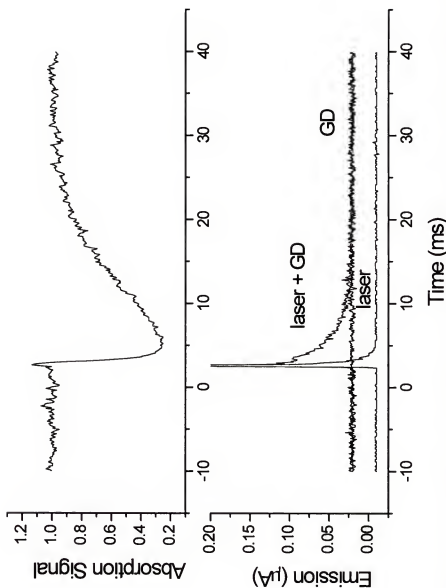


Figure 8-11. Absorption signal of laser ablated material compared to emission of laser sampling into dc discharge. a) Laser absorption, 20Hz, 0.5 W, 800V, 1 torr.

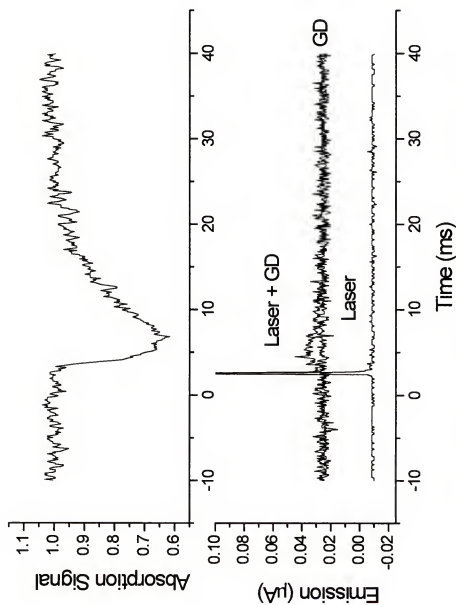


Figure 8-11-continued. b) Laser absorption 20Hz, 0.36W, 800V, 1 torr.

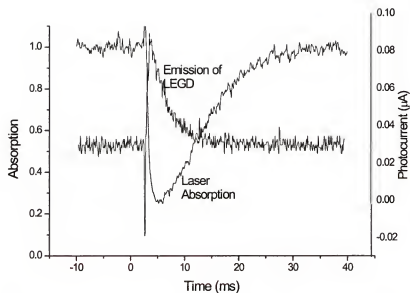


Figure 8-12. Laser absorption signal compared to emission of laser ablated material into the dc discharge.

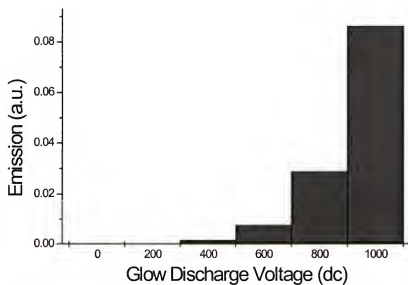


Figure 8-13. Emission from laser ablated material as a function of dc voltage.

CHAPTER 9

PARAMETRIC STUDY AND APPLICATIONS OF THE LASER-ENHANCED GLOW DISCHARGE

The ability of the laser to sample material into the glow discharge has been demonstrated. The impetus of this project was to characterize the laser-glow discharge interactions in order to design an ion source for mass spectrometry and to allow the analysis of non-conductive materials. While an ion source based on this source has not been produced, these studies provide the framework for its design. This chapter will cover several areas of research involving the combined source. Initially, the parametric response of the LEGD will be detailed. Next, some insights into the methods of excitation and ionization within the source will be covered. The configuration of the source will then be discussed. Afterwards, the phenomenon of laser deposition will be explored. Finally, the analysis of non-conductive materials will be described.

Parametric Study of the Laser-Enhanced Glow Discharge

Having characterized the emission of the laser, introduced the LEGD phenomena and studied the laser sampling mechanism, it is time to look at how different experimental parameters affect the laser-GD source. Most often it will be shown that the quality of the signal depends primarily on the ability of the GD to re-excite the laser ablated material and secondly upon the amount of material ablated.

The parametric studies will be divided into three parts. The first section will deal with the parametric effects on the LEGD emission signal of the bulk material. Parameters such as GD voltage, pulse width, and the pressure of the discharge will be examined in addition to others. The second section will deal with the effect of the same parameters on minor and trace levels of elements in a sample. The third section will deal with some details of the LEGD phenomenon and some figures of merit.

Bulk Analysis

As mentioned in the last chapter, the performance of the GD greatly affects the emission of the LEGD. Figure 9-1 shows the effect of increasing the pulsed GD voltage while keeping the other experimental parameters constant. The line marked as GD represents the peak of the pulsed glow discharge intensity, while the line marked as LEGD represents the emission intensity obtained when the laser fires 2 ms prior to the glow discharge. The results indicate that the increased energetics of the pulsed discharge should provide considerable improvement over dc operation. The dc discharge operates at voltages below 1200 volts, whereas the pulsed discharge has been operated at voltages up to 3.5 kV. At normal operating conditions, about 2kV, the emission intensity from the LEGD is an order of magnitude or greater in the pulsed rather than the continuous dc mode. This enhancement in emission intensity includes material that is suspended in the fill gas of the vacuum chamber.

Figure 9-2 is a plot of the effect of the chamber pressure on the LEGD emission intensity. Recalling the material covered in previous chapters, the change in pressure had a small effect on the amount of laser ablated material and on the intensity

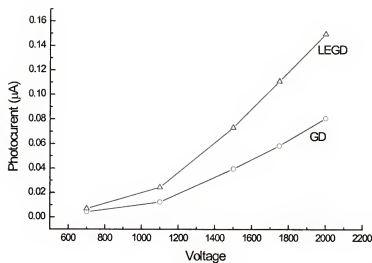


Figure 9-1. Cu I, 216.51 nm emission intensity vs applied voltage.
Conditions: 1 torr.

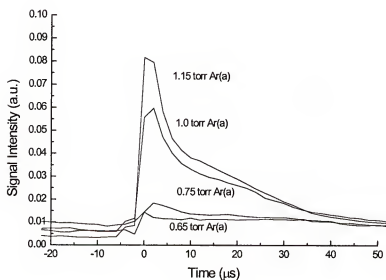


Figure 9-2. Temporal profiles of Cu I, 324.7 nm line from LEGD at varying pressures.

of the laser induced plasma emission. Figure 9-2 shows a clear dependence of the LEGD on pressure. This reflects the graphs of the effect of pressure on the pulsed discharge seen in chapter 4. Not surprisingly, the conditions which favor the GD also favor LEGD emission. The implication of this is that the mechanisms that are responsible for excitation and ionization in the GD are the same within the LEGD. This simplifies the optimization of the LEGD source. Since the many of the parameters of the pulsed discharge have been studied, optimized and reported in this work, the same conditions may be used in conjunction with the laser.

Laser power displayed a great effect on the LEGD emission intensity. The power of the laser controlled how much material was removed per shot. Figure 9-3a shows the enhancement of the LEGD emission when the power of the laser is increased. The pulsed GD emission is shown as a flat line (since laser power will not affect the pulsed GD emission) to show the relative increase in the LEGD signal. The maximum emission intensity shows a six-fold increase. At the conditions of this experiment, 1 torr Ar and 1.5 kV, an average laser power of 1 Watt showed the least enhancement. However, a high laser power is not always desirable. When the laser removes a large amount of material, a deeper crater is formed and the diminishment of the emission vs the number of laser shots is enhanced. Moreover, experiments which varied the pressure, voltage and pulse width have shown that 1 Watt of laser power was most sensitive to these parameters. At 1 Watt power, 1.2 torr Ar, 50 microsecond pulse width and 2kV, the greatest enhancement of the LEGD/pulsed GD was seen.

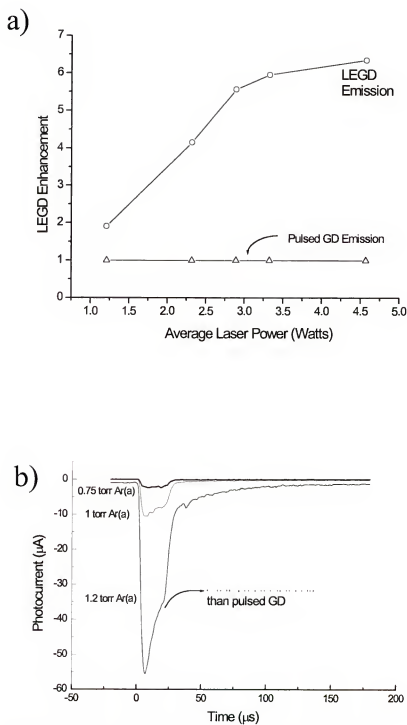


Figure 9-3. Factors affecting signal intensity of the LEGD plasma.
a) Laser power; b) Temporal profiles with respect to pressure.

The LEGD showed emission 9 times more intense than the pulsed glow discharge, surpassing the enhancement due to increased laser power while removing less material from the laser target (Figure 9-3b).

For analytical emission and mass spectral measurements, typically the pulse width of the GD is set to 10 microseconds. It has been mentioned that the GD needed to be fired at a low frequency (20 Hz) in order to be operated in sync with the laser. At 20 Hz, the GD functions adequately by itself, however at this greatly reduced duty cycle, the GD is more sensitive to experimental parameters and less stable than at higher frequencies. To improve the stability of the pulsed discharge while firing the laser, the duty cycle was increased by increasing the pulse width. Figure 9-4 shows the effect of increasing the pulse width on both the GD and LEGD. The emission increases dramatically when the pulse width is increased from 5 to 50 microseconds. After a pulse width of 50 microseconds, little increase is observed. A pulse width of 50 microseconds was chosen because of its increased stability and greater emission intensity. Figure 9-5 shows the emission from 11 LEGD pulses to show the reproducibility of the LEGD phenomenon. The reproducibility of the pulses shown was 10.4 %. The reproducibility of the LEGD ranged between 5% and 18%, varying slightly with pressure, power, voltage, pulse width and emission line used. The stability of the plasma is not only measured by the reproducibility of the emission signal, but also by the robustness of the plasma. Relatively unstable plasma conditions would not operate at higher voltages or at higher pressures without arcing. The more stable plasma conditions will allow the greatest signal enhancement.

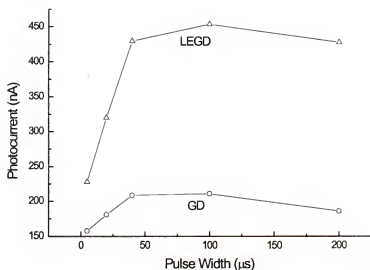


Figure 9-4. Emission intensity of LEGD and GD with respect to pulse width of applied voltage. Conditions: 1.5 ms delay, 1.3 W laser power, 1.5 kV, 1 torr, Cu I, 324.7 nm line from CKD steel.

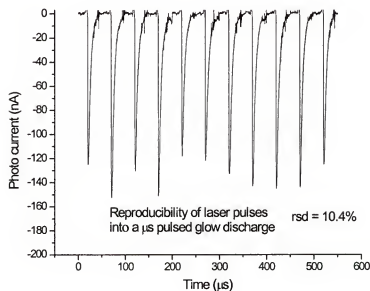


Figure 9-5. Reproducibility of emission due to laser pulses into the pulsed glow discharge.

Minor and Trace Analysis

The above section has summarized the studies which indicate the behavior of the LEGD emission with respect to the bulk sample. This next section will consider the LEGD emission of minor and trace levels of constituents. Figure 9-6. is the temporal profile of the Cu I, 324.7 nm line from NIST 1263 steel containing 0.09% copper. The emission from the LEGD is an order of magnitude greater than that from the pulsed discharge alone. The area under the respective peaks is 30 times greater. The behavior of the minor elements mimicked the bulk elements with regard to voltage, pressure and pulse width.

Looking at the effect of the delay between the laser and GD firing, there seemed to be a slightly different effect. Data from the last section showed an immediate decline in signal when the delay time was increased. Figure 9-7 shows the response of the Cu I line with regard to delay time. A reproducible local maximum occurred between 1 and 1.5 milliseconds. This result indicate that it would be necessary to alter the delay time and the setting of the gated detector when performing trace analysis.

Another deviation from the behavior of the bulk material concerns increasing laser power. In the bulk sample, increasing the power of the laser increased the signal by up to 7 times. When looking at the Cu 324.7 nm line in SRM 1263, the emission is reduced when the power of the laser is increased as seen in Figure 9-8. Reproducing this test under a number of experimental conditions has not revealed a definitive explanation for this behavior. Surface inhomogeneity was ruled out as the cause.

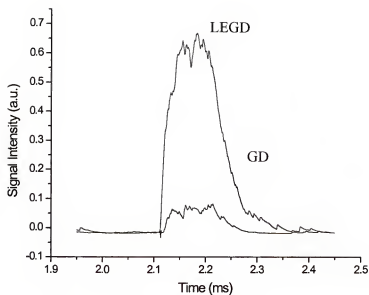


Figure 9-6. Temporal profile of 0.09% Cu in NIST 1263 steel.

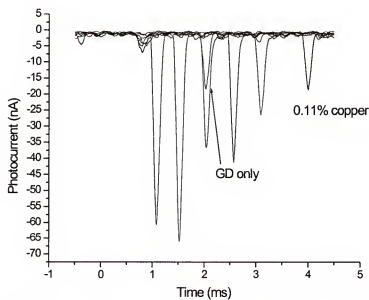


Figure 9-7. LEGD emission from 0.11% copper in steel while varying the delay between the laser and pulsed GD.

However, it is plausible that the larger amounts of material removed at higher powers causes the plasma to become optically thick, and therefore occludes the emission from trace species. A laser power setting of 1 Watt is ideal for laser sampling into the GD for trace analysis.

Figure 9-9 compares the GD and the LEGD plasmas in terms of calibration curves generated from trace Cu levels in NIST steels. The precision of the GD is better than the LEGD, having an average rsd between 4 and 10% whereas the LEGD plasma had rsd's between 10 and 20%. The greater slope of the LEGD response shows that the LEGD has an increased sensitivity.

When the GD plasma ignites and there is atomic material in the gas phase from laser ablation, the emission of both atomic and ionic lines increases. However, the resonance lines show the greatest enhancement. This makes sense, as the material ablated by the laser consists primarily of ground state atoms when the pulsed glow discharge fires. This may have particular analytical utility when performing trace elemental analysis, as it is often the resonance lines of trace materials that are monitored. To illustrate this phenomenon, a GD emission spectrum of SRM 1265 containing 0.0058% Cu was taken. Immediately afterwards, an LEGD spectrum was collected. Figure 9-10 shows the results. The GD spectrum shows the Cu I, 324.7 nm line and a number of iron emission lines. The Cu I 327.4 nm line is not detected. In the LEGD spectrum, the Cu resonance lines are the most dominant features of the spectrum. The Fe lines have a reduced intensity.

While other calibration curves were not examined during this project, a sample of NIST 495 copper containing 147 ppm Fe was analyzed. Figure 9-11 shows two Fe

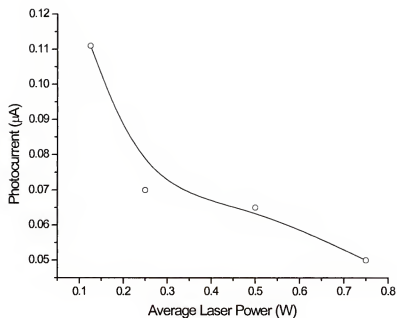


Figure 9-8. LEGD emission from Cu in NIST 1263 steel with respect to average laser power. Conditions: 1.6 kV, 1 torr.

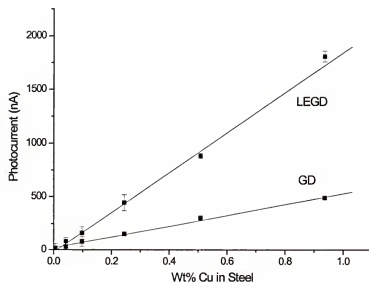


Figure 9-9. Comparison of calibration curves generated from Cu in NIST series steel in the LEGD plasma and GD.

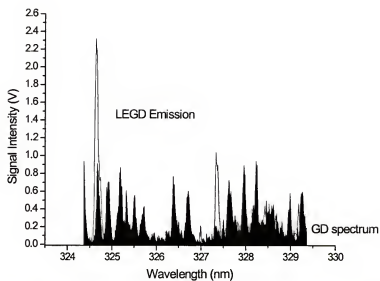


Figure 9-10. Comparison of LEGD and GD spectra showing Cu in SRM 1260.

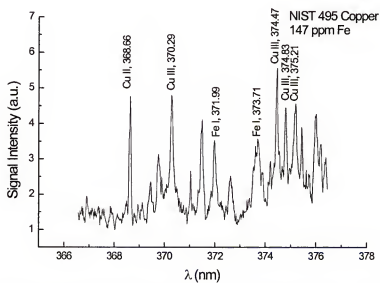


Figure 9-11. Emission from 147 ppm Fe in NIST 495 copper rod in LEGD plasma.

atom lines in the presence of a number of Cu ion lines generated from a LEGD plasma. These two lines were not able to be seen operating the pulsed GD at 20 Hz. This phenomenon of selectively exciting certain lines adds complexity to the LEGD spectrum, but in the case of trace elemental analysis it could prove to be beneficial, improving the sensitivity of the combined plasma. In addition, a study of which lines are enhanced and which are not, will provide a method of determining mechanisms of excitation within the pulsed glow discharge.

Insights into the Method of Excitation in the LEGD

Introduction

One of the goals of combining the glow discharge with a laser was to gain information on how the glow discharge would affect material in the gas phase. What mechanisms of the glow discharge would be responsible for the excitation of this atom population? How effective a secondary excitation and ionization source would the pulsed GD be? The pulsed glow discharge has enough energy to ionize argon. This would indicate that the GD plasma has the energy to excite and ionize the entire periodic table of elements. If a GC column were sampled into the GD, could useful information be obtained? It was decided that the best way to go about answering some of these questions would be to generate an atomic population in the glow discharge chamber. The laser seemed the most effective means of doing so by ablating material from the surface of a secondary target and then waiting until the atomic population returned to the ground state before firing the pulsed discharge.

The last chapter dealt with many of the parameters that affected the LEGD plasma. Most notably, the LEGD functioned much like the pulsed GD, but with increased emission intensity. It was noted that some atomic and ion lines are affected differently. This section will deal with some data that points to certain mechanisms within the GD as possible reasons for this behavior.

Observing atomic emission, most atomic lines show an increase in intensity in the LEGD plasma. Figures 9-12 shows three atom lines of copper both in the GD and the LEGD. All show significant increases in emission when the laser is fired prior to the glow discharge. The most likely explanation for the increased emission involves the higher number density of the analyte in the gas phase. Most atomic emission from the LEGD plasma is due to energetic collisions within the gas phase just as in the GD plasma. A larger analyte atom number density results in more collisions and a higher signal. However, other mechanisms may be effecting the excitation of species as well. For instance, the temporal profiles of Figure 9-12a and Figure 9-12c have a different shape. This difference indicates that there are differences in the mechanisms populating the energy states leading to these emission lines.

Looking closely at Figure 9-12a, It can be seen that the rising edge of the LEGD emission is much sharper than in the GD plasma. Moreover, the peak maximum has shifted to an earlier point in time. Typically within the pulsed GD, the atomic emission intensity reaches a maximum at the point at which the voltage turns off. It is not known what mechanism populates the Cu atom lines depicted in Figures 9-12a and 9-12b. A possible explanation for the forward shift of the peak could be that

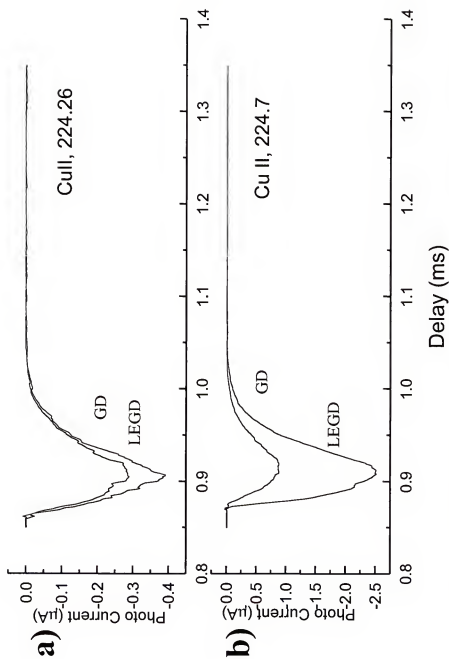


Figure 9-12. Comparison of temporal profiles of ion emission in LEGD and GD plasmas.
 a) Cu I, 224.26 nm ion line; b) Cu II, 224.7 nm ion line.

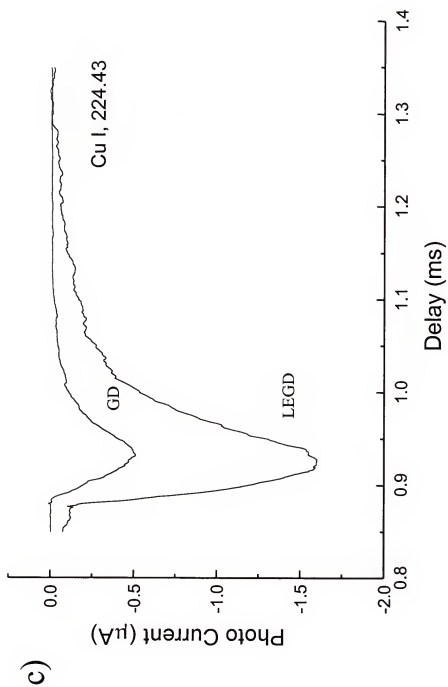


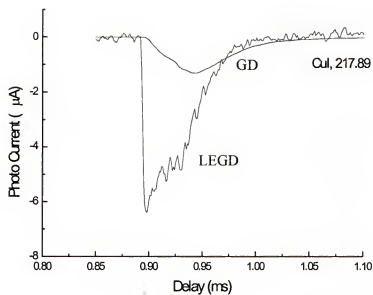
Figure 9-12-continued. c) Temporal profile of Cu I, 224.43 atom line in LEGD and GD plasmas.

electron impact excitation, responsible for ionizing the argon atoms, may play an increased role in exciting ablated atoms within the LEGD plasma. Normally, electron impact ionization is thought to play a minor role in the excitation of analyte species within GD plasmas. Based on the temporal profile of the current in a diode glow discharge, the largest number of electrons is produced at the initiation of the voltage pulse. In the glow discharge, atoms must be sputter removed and diffuse into the gas phase before they can be excited by electrons or by collisions with argon. This delays the peaking of the signal. In the LEGD plasma, a high number density of the analyte is already diffused throughout the GD chamber. Therefore, this population is in position to be excited by electron impact during the initiation of the plasma. However, the sharper rise times and early peaks are not seen for all atom lines, indicating that the mechanism responsible for the temporal responses in Figures 9-12a and 9-12b does not affect all atom emission lines alike. Figure 9-12c stands as evidence to this fact in that the copper atom line is enhanced, but shows a similar temporal profile as in the GD plasma.

Ionization

Unlike the atom lines in the LEGD plasma, which all show some enhancement, only certain ion lines show increased emission. Figure 9-13 shows the GD and LEGD emission of Cu II, 224.7 nm and Cu II, 224.26 nm lines. The Cu II, 224.6 line shows very little change in both intensity or time, yet the Cu II 224.7 nm line shows significantly increased emission. By examining which lines are enhanced and which lines are not, insight into the mechanisms within the GD and LEGD plasmas can be

a)



b)

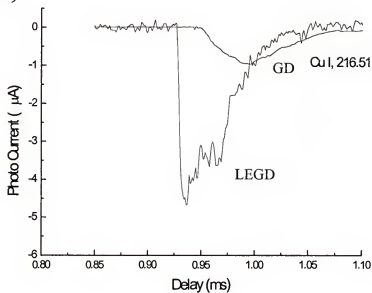


Figure 9-13. Temporal profiles of two copper atom emission lines from the LEGD and GD plasmas. a) Cu I, 217.89; b) 216.51.

obtained. The 224.7 nm line has been linked to asymmetric charge exchange with argon ions within the GD.²¹ The Cu II 224.26 line is expected to be populated *via* Penning ionization by argon metastable atoms within the glow discharge. This indicates that any material sampled into the gas phase of the glow discharge would be subject to significant collisions with argon ions, perhaps even more than if the material were to be sputtered, as in the pulsed discharge. Moreover, since no enhancement is evident in the emission lines that are predominantly ionized *via* Penning ionization, Cu II 224.26 and Cu II, 221.8, it would seem that this process remains unchanged.

Enhancement of ion lines is not limited to these lines. Other ion lines show similar behavior. Figure 9-14 shows the Cu II, 219.23 and Cu II, 217.5 nm lines in both the GD and LEGD plasmas. Again, the 219.23 nm line shows some enhancement while the 217.5 nm line shows very little. The mechanism for the ionization of these two lines has not been suggested, so no tie to electron impact, charge exchange or Penning ionization can be made. It is obvious, however that there is a selective process at work. If the LEGD is to be used as an ion source for mass spectrometry as it was intended, these processes could have a significant effect on its performance. Therefore, it is important that these phenomena be studied.

Introduction to the Analysis of Non-conductors with the LEGD

Many industrially important materials have a non-conductive matrix. The dc discharge, whether continuous or pulsed is not able to analyze non-conductive matrices because a plasma cannot be established. One of the means of analyzing these samples is to power the GD with an rf power supply.⁴ While this practice has become

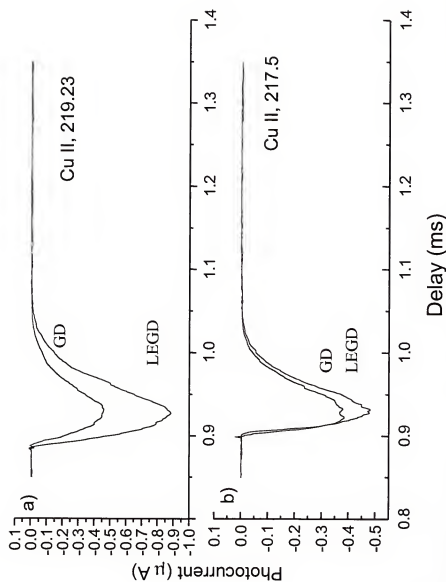


Figure 9-14. Comparison of temporal profiles of two ion emission lines in LEGD and GD plasmas.
 a) Cu II, 219.23 nm ion line; b) Cu II, 217.5 nm ion line.

common in several laboratories, the rf glow discharge emission is weak, generating signals with lower intensity than the continuous dc discharge. A second method of analyzing a non-conductive sample is to grind it and press it into a pellet after adding a conductive matrix such as graphite or copper. This method has been employed successfully, but is subject to contamination just like the other methods of solids analysis that involve grinding and dissolution. Moreover, the conductive matrix could cause a significant spectral background. Yet another method is the use of a secondary cathode, which consists of a conductive ring placed just above the non-conductive material.⁶⁵ It is hoped that sufficient ions and fast atoms will strike the non-conductive matrix and sputter some of the material into the gas phase. The LEGD is also able to analyze non-conductive materials. If the laser is fired at a secondary target, a non-conductor, atoms from the non-conductive matrix will be ablated and available for subsequent excitation by the GD (Figure 9-15). The glow discharge cathode may be a conductive material to facilitate its performance. Thus atomic material from a non-conductor can be excited and ionized by the glow discharge. Moreover, in terms of mass spectrometry, the ions generated should have the low energy and low energy spread characteristic of GD plasmas, which are more easily sampled and focused by ion lenses within the mass spectrometer.

This methodology was first tested using an aluminum target instead of a non-conductor. There were two reasons for delaying the analysis of the non-conductive matrices. First, aluminum is readily available in the laboratory so no important samples would be wasted while testing the system. Secondly, the effect of laser vapor

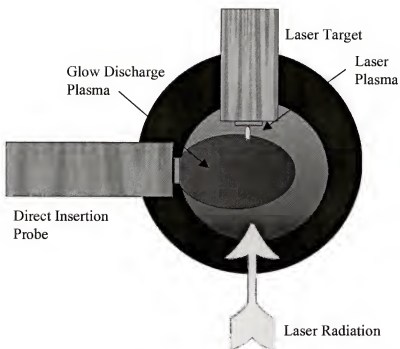


Figure 9-15. Configuration of LEGD instrument employing secondary laser target.

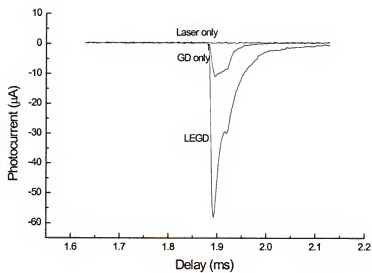


Figure 9-16. Aluminum emission from GD and LEGD. Conditions: Al cathode and laser target. 1 torr, 1.5 kV, 1.2 W laser power, Al I, 369.15 nm.

deposition onto the GD cathode may cause a problem if the deposited layer is a non-conductive material.

Figure 9-16 shows several emission signals resulting from this experimental configuration. First the laser was fired at the aluminum target and the temporal profile of the laser emission was collected. The flat-line signal indicates the optical chopper still blocked all of the laser emission, and there is no residual laser induced plasma emission when the GD is ignited. The temporal profile of an aluminum cathode was measured to serve as a reference for comparison. Next, the aluminum cathode was replaced with a copper cathode and the laser was again fired at an aluminum target. The emission intensity resulting from the LEGD of aluminum was over 5.5 times greater than the GD emission of an aluminum cathode.

To illustrate that the LEGD emission was due solely to the laser sampled material, a spectrum of the GD of the copper cathode and the LEGD which included ablated aluminum, was recorded and compared. Figure 9-17 shows the results of this experiment. In the spectral region between 393 and 399 nm, the glow discharge showed only three argon lines in the region around 394.7 nm and several weak unidentified lines above 396.5 nm. No emission was seen from the two Al lines in this region at 394.3 and 396.152 nm respectively. The Cu cathode was NIST 495 and has a certified Al concentration less than 2 ppm. The conditions of this experiment did not favor the detection of trace concentrations of materials, so it is not surprising that no Al emission was detected. When the laser fired, the same argon and other lines appeared with. However, the most noticeable feature of the LEGD spectrum is the appearance of two strong aluminum emission lines. The optimal parameters of 1 torr

Ar, 100 microsecond pulse width and 1.5kV GD parameters were chosen for this experiment.

When the laser fires at a secondary target, the laser ablated material fills the chamber and may deposit on the surfaces in the vacuum chamber, including the GD cathode. A series of experiments was designed to study laser ablation deposition. Figure 9-18 shows three temporal profiles. The monochromator was set to the Al I, 396.15 nm line. First, the pulsed GD of a copper cathode containing less than 2ppm of Al was taken. No Al emission was detected. Second, the LEGD emission, resulting from the laser striking an aluminum target, was recorded. 200 laser shots were fired when recording the LEGD emission intensity. After the laser ceased firing, aluminum emission continued to be seen. This emission was due to a thin layer of aluminum that was deposited on the GD during the laser ablation events. The deposition of laser ablated material could be viewed in two ways. It could be seen as a disadvantage of the technique as the GD cathode would be contaminated with the material tested. This disadvantage would be minor, as the GD process is self-cleaning through the sputtering process.

An alternative means at looking at the deposition of laser ablated material is regarding it as an opportunity to study thin layer analysis. Comparing the GD emission of an Al cathode in Figure 9-16 with the emission from a laser deposited layer in Figure 9-18, one will notice that the deposited layer gives nearly as much emission as the pure aluminum cathode. It is a fundamental characteristic of the GD process that any layer, even a thin layer that is thick enough not to be sputtered away instantly will yield an emission signal as if it were a pure material made of the layer,

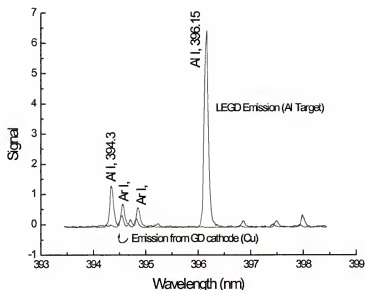


Figure 9-17. Comparison of GD emission of a copper cathode and the same discharge with laser sampled aluminum. Conditions: 0.8 torr, 1.5 kV, 100 μ s pulse, 14 mm cathode distance, 1.2 W laser power.

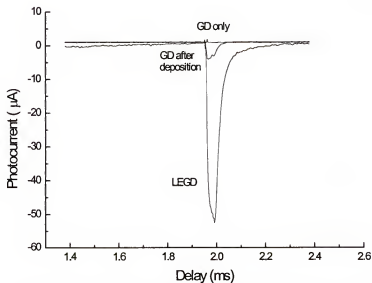


Figure 9-18. Al Emission from laser sampling into copper GD compared to signal resulting from deposition. 1 torr, 1.5 kV, 1.2 laser power, Al I, 369.15 nm.

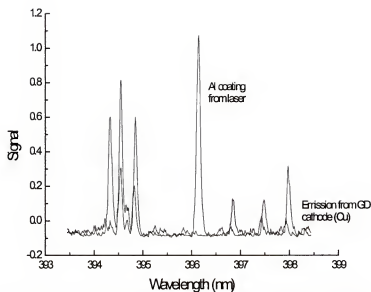


Figure 9-19. GD emission spectra before and after 500 laser shots at aluminum target, 0.8 torr, 1.5kV, 1.21 W laser power.

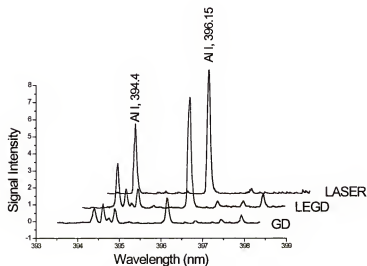


Figure 9-20. Comparison of Al emission from GD, LEGD and laser plasmas in a 1 torr argon atmosphere.

since only the first 1-3 atomic layers are available to the sputtering process. Figure 9-19 shows the spectrum of such a layer compared with a GD spectrum of a copper cathode taken just prior to deposition. The strong aluminum emission displayed in the spectrum is very much like the spectrum obtained from the pulsed GD of a pure aluminum cathode. There is a potential for this method to be used for the analysis of non-conductors by depositing a thin layer of non-conductive material onto the surface of a conductive cathode and then analyzing the sample with the pulsed GD. This potential will be briefly discussed later.

The potential for the laser deposition to be used to study thin layers will be discussed in the next section. In the meantime, some comparisons between the GD and laser emission will be reviewed. Recalling the material from some of the earlier chapters, the emission from the pulsed discharge was 1 to 2 orders of magnitude greater than its dc counterpart. The laser plasma emission intensity was from 1 to 2 orders of magnitude greater than the pulsed GD, depending on the line being measured. The LEGD emission intensity can be 3 to 12 times greater than the pulsed glow discharge emission intensity. Figure 9-20 compares the laser plasma emission intensity from an aluminum target to the emission from both the GD of an aluminum cathode and the LEGD from an aluminum target into a copper discharge.

Thin Layer Deposition

When the laser is fired at a secondary target in close proximity to the pulsed glow discharge, some of the ablated material is deposited onto the GD cathode. Depending upon the experiment this could be seen as a detriment or an advantage. In

this section we shall explore the laser deposition of aluminum on a copper cathode in more detail.

If the laser deposition is viewed as a contamination there are several factors that need to be considered. To begin with, the glow discharge is self-cleaning and will eventually remove any deposited material. However, when the GD is fired in sync with the laser, its maximum repetition rate is 20 Hz. A low duty cycle corresponds to an equally low sputtering rate. At this frequency, even with a 100 microsecond pulse width, the duty cycle is very low. Under the conditions used in a typical experiment, even a thin layer could take quite some time to remove. Figure 9-21 shows a spectrum from a copper cathode 2 minutes after being subjected to 600 laser shots. The aluminum originating from the deposited layer is clearly seen. It is obvious from this spectrum that it would take a long time for this material to be completely removed at the current GD parameters. To clean off the surface more quickly, a cleaning cycle involving a higher repetition rate would be advised. Increasing the frequency of the GD between LEGD analysis from 20 Hz to 100 or even 800 Hz will reduce the time needed to clean the cathode.

To examine the laser deposition phenomenon further, the GD was turned off and a secondary aluminum laser target subjected to 100 laser pulses. The glow discharge was then ignited and the emission signal monitored until no Al emission could be seen. Figure 9-22 shows that it took a little over 400 seconds to remove the deposited material.

There is an acute difference between the emission seen when the GD excites material ablated in the gas phase and the emission from a deposited layer. To

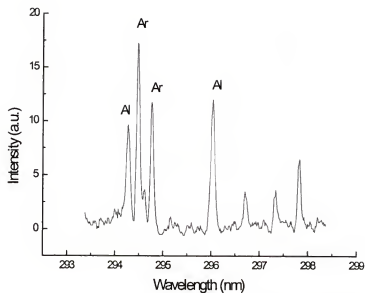


Figure 9-21. Emission spectrum of copper cathode showing the existence of laser deposited aluminum 2 minutes after 600 laser shots.

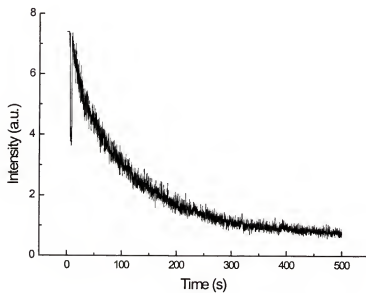


Figure 9-22. Removal of Al layer from 100 laser shots deposited onto a Cu cathode.

illustrate the difference between the GD of the cathode, LEGD plasma and the emission from a deposited layer the data shown in Figure 9-23 was taken. The monochromator was set to monitor the Al I, 396.152 nm line during the three emission events. Between 0 and 5 seconds, the pulsed glow discharge was fired at 20 Hz. No emission is seen due to the very low levels of aluminum in the copper cathode. At five seconds, the laser was allowed to fire in sync with the glow discharge for 20 pulses. When the two pulses were fired in sync, the strong LEGD emission was observed. After the 20th pulse, the laser is turned off. Immediately (on the time scale of seconds) the emission is decreased to a little under a volt. Since it has been demonstrated that the copper cathode showed no appreciable Al emission, this reduced emission must be due to Al that is either in the gas phase or that has been deposited on the cathode surface. The absorption measurements, shown previously, in addition to the very sharp decline in the emission indicate that this residual emission is due to deposition on the GD cathode. For the next 70 seconds, the emission from the deposited layer can be seen to decay until no deposited material is left on the cathode. Moreover, the emission from the deposited layer is nearly equal to the emission from a solid aluminum cathode. The pulsed glow discharge will give the same emission spectrum from a layer consisting of a few monolayers as from several hundred monolayers. This has some unique applications in the area of thin film analysis.

To explore the nature of thin layer analysis by the pulsed glow discharge, an experiment was set up to first determine the amount of material ablated by the laser. This number was then used to estimate how much material could be deposited onto the surface. Finally, a thin layer was deposited onto the GD cathode and its temporal

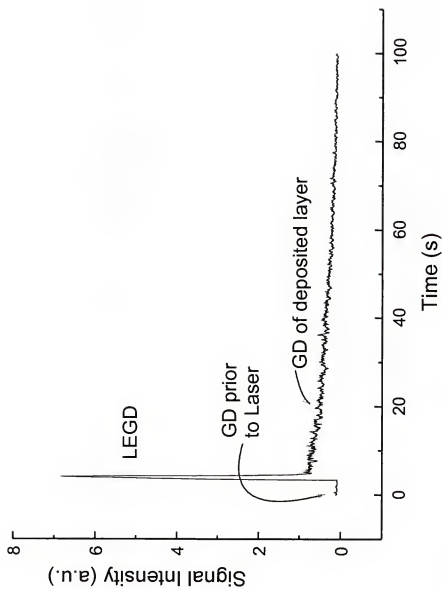


Figure 9-23. Comparison of Al emission in the GD plasma: from a copper cathode, during laser ablation of Al, and due to a deposited layer.

profile measured. A triplicate measurement of the ablation rate of the laser, fired at 20 Hz and having an average power of 0.36 Watts, when fired at an aluminum target, gave a value of 105 ng per shot. This corresponds to 2.38×10^{15} atoms per pulse. The trigger to the pulsed GD power supply was interrupted so that the power supply remained warm, but would not fire. With the discharge turned off, 137 laser shots were fired, removing approximately 3×10^{17} atoms. A crude approximation of the efficiency was made to estimate how much material would be deposited on the surface of the GD cathode. Figure 9-24 shows a schematic of the laser ablation-GD source. The laser center of the laser target was 1.3 cm from the surface of the GD cathode and was placed 2.0 cm off its axis. To approximate the amount of deposition on the cathode it was assumed that the laser ablated material would distribute itself evenly throughout the chamber. If we also assume that the particles removed stick to the first object that they come in contact with, we can ratio the surface area of the chamber to the surface area of the cathode. Comparing the surface area of the 4 mm copper cathode to a sphere that is 20 mm in diameter, the ratio of the two is 0.0039. So, our approximation would set an upper limit for the efficiency of the deposition at 0.5%. In reality, we would expect this number to be much lower. When material is ablated from the surface, it has an initial velocity retracing the path of the laser beam. Therefore, the greatest amount of deposition would be seen opposite the surface of the laser target, and not on the cathode which sits at 90° to the surface. Secondly, the surface of a 2.75 in 6-way cross is much larger than the volume of a 20 mm sphere. Taking this into account, we would expect no more than 0.5% of the material to be deposited on the cathode surface and perhaps even an order of magnitude less.

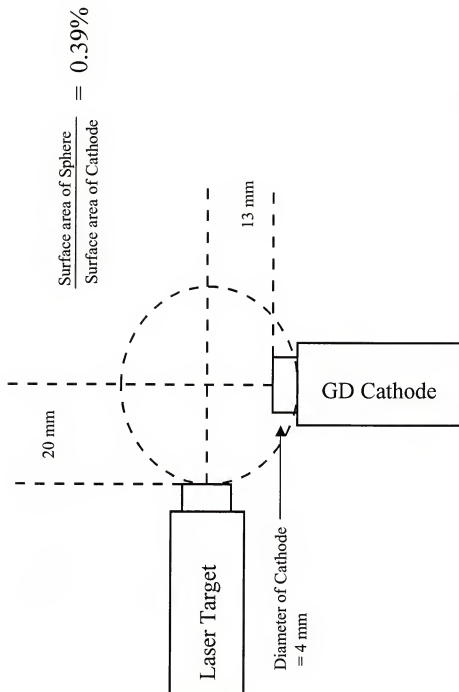


Figure 9-24. Estimations of amount of aluminum deposition during laser ablation events.

Assuming an efficiency of 0.5%, no more than 1.606×10^{15} atoms or 8 monolayers of aluminum should be deposited. 8 monolayers corresponds to 1.5 nm of material. Having deposited 8 monolayers (or less) of aluminum onto the copper cathode, the pulsed discharge was now ignited and ran at 1.5 kV, and 100 Hz. Figure 9-25 shows that it takes nearly 2 minutes to remove this layer entirely. This indicates that two full minutes are available to interrogate the composition of 1.5 nm of material. In addition to this, the emission resulting from this analysis would be much greater than in the conventional, continuous dc mode. This promises significant results in terms of layer analysis using the GD. The frequency and pulse width of the discharge give the spectroscopist control of the sputtering rate of the discharge while the power of the discharge results in high emission intensity. Thus, thicker layers (10's of microns) to very thin layers (monolayers) can be analyzed for their bulk, and possibly even trace composition. As a further test, the GD was run at 1.5kV, 50 microsecond pulse-width, 1 torr argon and 20 Hz. Under these conditions, a single laser shot was fired, asynchronously, into the GD plasma. Because the laser and GD were not fired in sync, the LEGD plasma was not seen. However, Figure 9-26 shows that even the deposition from a single laser shot can be detected and monitored for 20 seconds before being completely sputtered away. Thus the pulsed glow discharge has shown some promise in the analysis of thin layers and perhaps particle analysis as well. It might also prove useful in monitoring and controlling laser plasma vapor deposition processes.

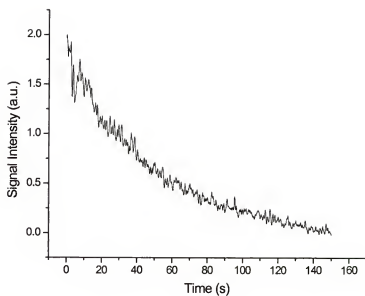


Figure 9-25. Emission from Al I, 396.15 nm layer deposited by 137 laser shots. Conditions: 1.5 kV, 1 torr, 2 W laser power.

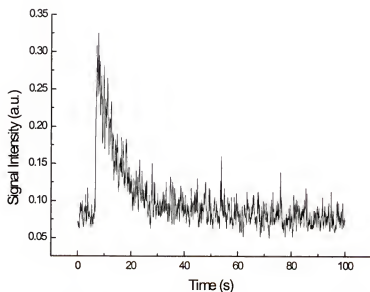


Figure 9-26. Temporal profile of Al emission due to 1 laser shot into Cu discharge. Conditions: 1 torr, 1.5 kV, 3 W laser power.

Laser Sampling of Non-conductive Materials into a Pulsed Glow Discharge

The final goal of the experiments involving sampling laser ablated material into the pulsed glow discharge was to evaluate its ability to analyze non-conductive materials. The importance of analysis of these materials is underlined by the sheer number of sample types that exist. Glasses, ceramics, soils, and polymers are just a few types of non-conductive matrices that are of importance in a number of commercial, environmental and research industries. Due their insolubility, solution-based, analytical methods are hard pressed to analyze these samples. Likewise, dc methods such as the continuous and pulsed discharge cannot establish a plasma with a non-conductor unless mixed with a conductive material.

To determine the effectiveness of the laser sampling method, a number of different samples were ablated into a pulsed glow discharge. It was thought that a simple, uniform matrix would be the most appropriate material to begin our study. Quartz consists entirely of SiO_2 and is readily available in the analytical laboratory. In our early experiments, a fragment of a quartz glass slide was mounted on a direct insertion probe and positioned within the vacuum chamber. A disc cut from NIST 495 copper rod consisting of less than 2 ppm of both Si and Al was used as the GD cathode. Copper was chosen on the basis of its availability, purity and ability to produce a strong, stable GD plasma. Also, familiarity with the copper matrix, which has been well researched, allows windows of matrix and interference free emission to be quickly identified. The region between 250 and 255 nm proved suitable for the analysis of several silicon lines. Figure 9-27 shows the emission spectrum resulting

from material sampled by the laser and excited by the pulsed glow discharge. Strong emission is clearly evident from several spectral lines of silicon.

Work with quartz and soft, borosilicate glass was used to explore the effect of the different experimental parameters. Figure 9-28 shows a spectrum of borosilicate glass which contains between 70-80% SiO_2 and 7-13% B_2O_3 . It was quickly determined that the GD plasma could not run at the same range of conditions as when Al was used as the laser target. In this mode of sampling, the pulsed GD was more sensitive to experimental conditions and was not quite as stable as when the laser target was conductive. Periodic arcing was evidenced when the pressure was increased above 1 torr. This complicated studies involving the response to pressure as higher pressure often results in higher emission. Likewise, the higher ranges of glow discharge operating voltage could not be used. When the discharge was operated above 1.75 kV, there was also an increased chance of arcing. Finally, the GD was also sensitive to the amount of material that was deposited on the surface of the cathode. The pulsed GD operated well as long as the continuous number of shots was not more than 2000 shots. Above 1500 - 2000 shots, there was an increased chance of arcing. Above 2000 shots, there was always some amount of arcing within the discharge. This slowed down the collection of data slightly, as after every several thousand shots, the GD was left running for several minutes to clean itself off. With these limitations in mind, the parametric studies of the laser enhanced plasma of non-conductive materials performed quite similarly to the studies using copper and aluminum. Increases in voltage and pressure showed expected increases in emission.

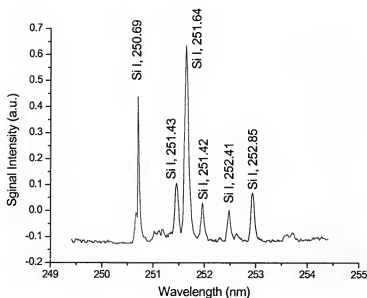


Figure 9-27. Emission from a quartz slide consisting of 100% SiO_2 .

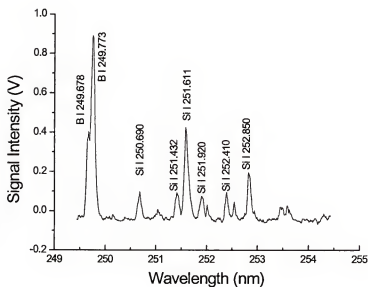


Figure 9-28. LEGD emission spectrum of borosilicate glass. Conditions: 1.2 W laser power, 1.7 kV, 1 torr. 80 % SiO_2 , 7% B_2O_3 .

Since the conditions for the LEGD source had been optimized using aluminum, it was decided to continue studies using non-conductive materials using the same parameters, with the aforementioned limits taken into consideration. For the analysis of non-conductive materials, the pressure was 1 torr for most experiments. Analyses were held to less than 1000 laser shots with 0.36 Watts average power. Between experiments, the discharge was allowed to run so as to clean off the cathode. The delay between the laser and GD was between 1 and 2 ms for most experiments. The GD fired at 20 Hz in sync with the laser with a voltage of 1.5 kV and a 100 microsecond pulse width. During the initial studies of the borosilicate glass, the smallest amount of material detected was the aluminum line which corresponded to 2-7% Al_2O_3 (Figure 9-29).

Besides solid samples such as glasses, non-conductive materials come in a number of different forms, such as powders and even quick drying liquids such as polymers and epoxies. To meet the need to analyze such samples, any technique has to be able to sample the diverse forms available.

Many non-conductive samples come in powder form with varying grain size. To test the LEGD system, a powdered sample of aluminum oxide G (Al_2O_3 G, for thin layer chromatography consisting of 15% CaSO_4 , Brinkman Instruments, NY, USA) was pressed into a solid pellet. Figure 9-30 shows the two aluminum spectral lines. A spectrum of the copper disc revealed no aluminum signal. Therefore, this strong emission was due to the re-excited atoms sampled by the laser. Many powdered samples cannot be pressed into a pellet without the use of some kind of binding agent.

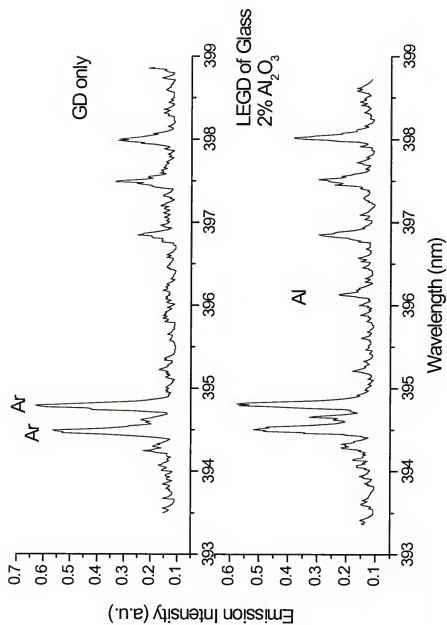


Figure 9-29. Comparison of copper discharge with a copper discharge including laser sampling of glass.

A small addition, less than 10%, of reagent grade cellulose allows a uniform, cohesive pellet to be formed with little dilution and chance for contamination. Also, the cellulose causes few interferences in the emission spectra.

The ablation of non-conductive materials is quite different than the ablation of metals. The strong, uniform lattice of most conductive matrices serves to confine the ablation to the point of irradiance and its immediate surroundings. The laser ablation craters of non-conductive materials are considerably larger and less uniform. They were also marked by excessive erosion of the sample material. A Dusty sediment was also found on the floor of the vacuum chamber, indicating that material was removed as particulate matter as well as being atomized.

Figure 9-30 showed the ability to analyze a powder sample for its bulk composition. To prevent excess sample erosion the samples were alternatively coated with a drop of epoxy (Duro Brand Quick Set epoxy, Loctite Corporation, CT, USA) or mixed in a 50% weight-to-weight ratio. Both types of samples seemed to produce effective results without massive trauma to the sample surface. A sample of phosphate rock was used to test the system's ability to analyze minor constituents within a non-conductive sample. Phosphate rock No. 56 (NIST) consists of 31.33% P_2O_5 , 3.3% Fe_2O_3 , 3.07% Al_2O_3 , and 44.83% CaO . Figure 9-31 is a spectrum from 394 to 399 nm of a 50/50 mixture of the epoxy-rock sample. Both Al atom lines in this region are clearly visible. It is suspected however, that the Al I, 394.40 nm line may have some spectral interferent since its ratio to the Al I, 369.15 is drastically different than expected. The 396.15 nm line seems to be free of interference and corresponds to an

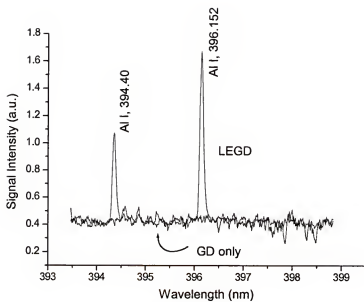


Figure 9-30. Emission from laser sampling of pressed pellet of Al_2O_3 G. Conditions: 1.5 kV, 1 torr, 700 μs delay.

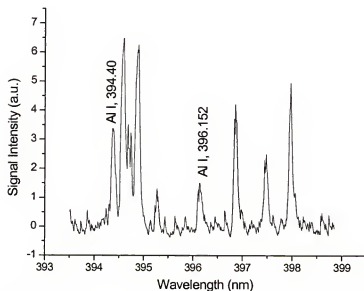


Figure 9-31. LEGD of Phosphate rock No. 56. 3.07% Al_2O_3 .

aluminum content of 1.63%. Because the sample was mixed with epoxy (50% by weight), the percentage of the sample ablated into the discharge would be even less than one percent.

Many non-conductive samples that are of analytical interest take the form of thin layers and coatings. Protective and decorative coatings such as paints are one example of this sample type. A drop of flat, white, latex wall paint (ACE seven star No. 16492, 183A100 white) was placed on a copper disc and allowed to dry.

The contents of 183A100 white are listed as: water, butyl acrylate/vinyl acetate copolymer, titanium dioxide, aluminum silicate and amorphous silicate. While the amount of aluminum silicate is not indicated, a strong aluminum signal was observed when the laser struck the surface of the sample. Figure 9-32 shows the aluminum signal from the paint. When lower laser powers (0.35 W) are used to analyze non-conductors, even the thin layer of paint could sustain over 250 shots before burrowing into the copper below. Thus, the laser sampling method allows a vast number of sample types such as solids, powders and even thin coatings such as paints to be analyzed for their elemental composition.

Figure 9-33 is a spectrum of Macor, a machinable ceramic. Macor has the following nominal composition: 8.47% Al, 2.17 % B, 8.3% K, 10.3% Mg, 45.3 % O, and 21.5% Si. Macor is used as general example for the analysis of non-conductive materials. Macor is very difficult to analyze via solution based techniques.⁴ Figure 9-33 shows the strong emission resulting from laser sampling. Several silicon atom lines and a pair of boron lines are dominant in this area. The emission from the Macor sample was lower intensity than the LEGD emission of an aluminum target.

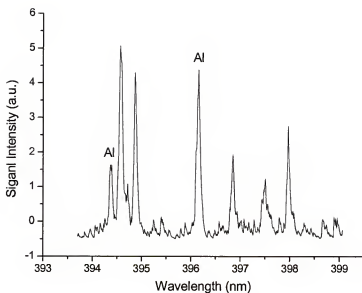


Figure 9-32. LEGD emission of spectrum of paint containing aluminum silicate.

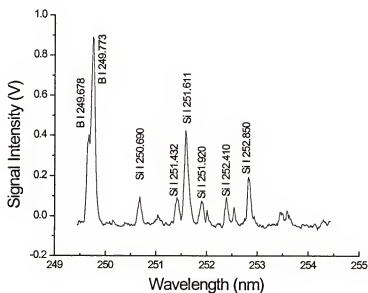


Figure 9-33. Laser sampling of Macor (2.17% B, 21.5% Si) into pulsed GD of NIST Cu 495 (<2ppm Si).

It is on the same order of magnitude as the pulsed glow discharge. This reduction in intensity is most likely due to the lower operating conditions while performing the non-conductive work due to the less robust plasma. The voltage and pressure, which both result in higher intensities were reduced to increase the stability of the discharge. The lesser intensity could also be due to a number other conditions both fundamental and experimental. Rationale considering fundamental aspects include lower transition probabilities of the lines monitored, higher excitation energies of the species and different collisional cross-sections. Not to mention that an excessive amount of oxygen is released in atomizing Macor (43% oxygen). Vacuum leaks, even slight ones, consist mostly of nitrogen and oxygen and have been known to reduce the emission intensity of plasmas.⁶⁶

The spectral lines of the different elements of Macor were all analyzed. Some of the emission results point to the potential of mass spectrometry for greatly improved analysis. For instance, only two weak lines of potassium could be seen in the wavelength range of the grating used. Figure 9-34 shows the potassium lines when compared to the background of copper. The two weak lines can just be seen above the background, despite that the sample consisted of 8.3% K. The more uniform response of mass spectrometry would be but one advantage of a LEGD-TOFMS instrument.

The deposition of laser ablated material onto the glow discharge cathode was reported. The pulsed discharge was relatively intolerant of excessive deposition of non-conductive material, due to the potential of arcing. However, one method of analyzing a non-conductive sample would be to fire the laser in order to allow a thin coat of non-conductive material to be deposited on the surface of the cathode. Figure

9-35 shows that this method could be effective. Fifty laser shots were fired in the absence of a glow discharge. The pulsed GD was then ignited, and a spectrum taken. The figure shows the fairly strong aluminum peak that resulted. Thus, non-conductive materials could be analyzed by their deposition onto a conductive cathode of known composition.

Since re-deposition could be a problem for some analyses, a method of reducing the deposition was implemented. A Macor sheath, typically used to shield the glow discharge was attached to the direct insertion probe, which held the laser sample. The Macor shield was 20 mm long tube with a 12.7 mm diameter and a wall thickness of 1mm. The use of the tube reduced the time needed to clean the cathode between runs by 60%.

While work with the Macor sheath was being performed, a curious plasma phenomenon was noticed. A stream of small sparks retraced the path of the laser from the target. This phenomenon is referred to as a micro-breakdown and occurs when the laser beam impinges upon a particle with sufficient energy to cause a breakdown. Figure 9-36 shows both the Macor sheath and the micro-breakdown phenomenon. This indicated the presence of particles in the discharge.

To test for the presence of particulate matter produced by the laser ablation of a non-conductive matrix, the neon line from the hollow cathode lamp was used to check for scatter. Figure 9-37 shows the reduction in transmittance of the neon line during laser ablation. Thus, non-conductive samples form a considerably larger amount of particles than conductive samples. This is most likely a result of the differences between the lattice structures of the conductive and non-conductive

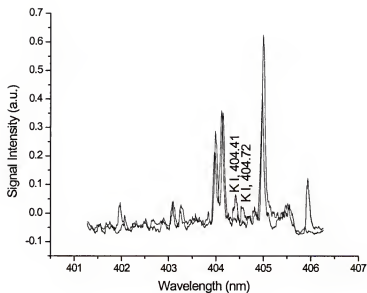


Figure 9-34. LEGD of Macor ceramic containing 8.3% potassium.

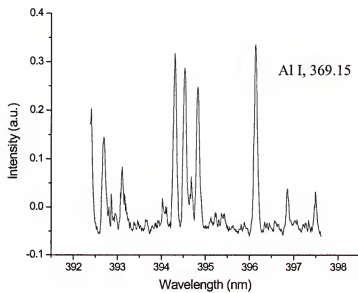


Figure 9-35. Aluminum emission from deposited layer of Macor.

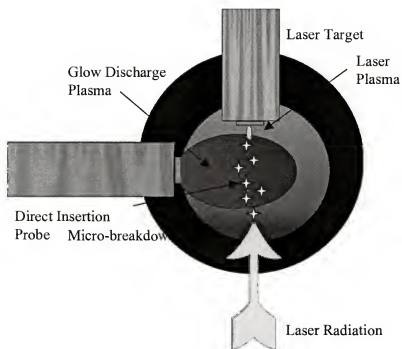


Figure 9-36. Illustration of micro-breakdown events due to laser ablated particulates.

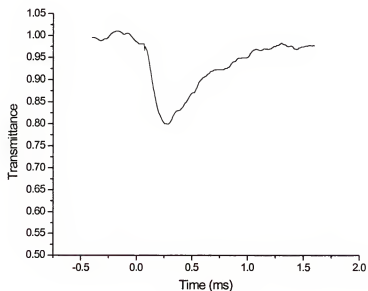


Figure 9-37. Dip in transmittance of Ne line from a hollow cathode into LEGD of Macor.

matrices. The non-conductor, not having a tightly packed, strongly held matrix, in addition to lacking the ability to dissipate heat as quickly or as uniformly as a conductor, shows a much higher and irregular ablation process.

The effect of the diverse species within the LEGD plasma upon the operation of the glow discharge was undetermined. Spectra of the glow discharge was taken before and during the ablation of a Macor target. This was done in order to determine the effect of the laser ablated material on the glow discharge. Earlier, it was stated that the emission from the non-conductive material was weaker than expected. Figure 9-38 shows that the emission from the copper cathode is relatively unaffected by the presence of the other atoms and particles. This phenomena could prove useful for mass spectrometry in that a pure glow discharge cathode could act as a steady reference for normalizing mass spectral analyses. Alternatively, a tantalum cathode could acts as both the means of ionizing the non-conductive material, but also as a getter for the plasma. In mass spectrometry, the interference from the GD cathode would be considerably less. Instead of several to several hundred emission lines, the mass isotopes would only interfere with an analysis of the element composition when the element of interest is the same as the cathode.

The results of the experiments with the LEGD have show that there is much work still to be done in understanding both the laser and glow discharge plasmas, as well as their interaction. The LEGD has produced a considerable increase in both atomic and ion emission. This has shown a greater sensitivity when performing trace analysis in copper and steel. Analysis of the interaction of the two plasmas has also indicated that mechanisms within the discharge may be studied. Finally, the pulsed

glow discharge has demonstrated the ability to act as an effect secondary excitation source. Work with non-conductive matrices has shown that the bulk and minor composition of a non-conductive material can be performed quickly, easily, and effectively. This adds functionality to the pulsed discharge which is unable to analyze non-conductors otherwise. Also, the intensity of the laser sampled atoms has been on the same level as the pulsed glow discharge emission. Therefore, the LEGD system produces signals as strong as if it was the cathode material. This is significant since the rf discharge, which is the primary means of determining the composition of a non-conductor by the glow discharge, shows very weak emission. The continuous dc mode shows greater emission than the rf 9-38 discharge and the pulsed glow discharge is greater than an order of magnitude more intense than the dc mode. Figure 9-39 and Figure 9-40 Thus, the LEGD plasma shows the potential for improved performance for the analysis of non-conductive matrices. Application of the LEGD source to the determination of trace analysis has yet to be proven. Regardless, the results all indicate that the next step in the LEGD work should include modifications that will enable it to act as an ion source for a mass spectrometer. The pulsed glow discharge, when compared to its dc counterpart, has shown considerable advantages as an ion source. The sensitivity of the mass spectrometer and the spectral simplicity of the data generated will likely open up even more areas of research.

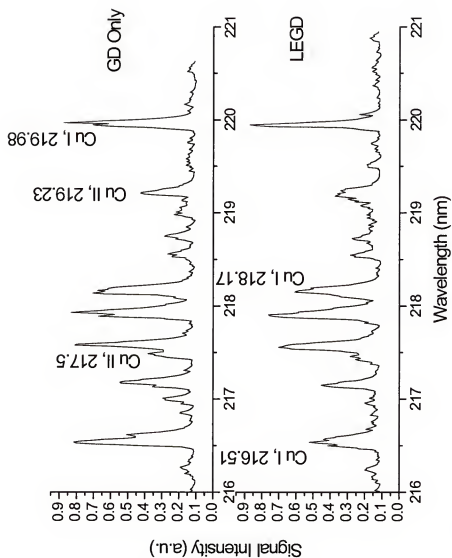


Figure 9-38. Comparison of copper spectral lines in pulsed glow discharge only and with laser sampling of Macor.

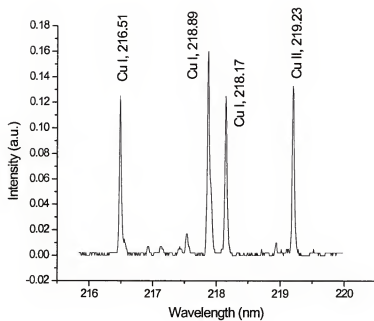


Figure 9-39. Radio frequency glow discharge of copper sample.
Conditions: 100W, 6 torr.

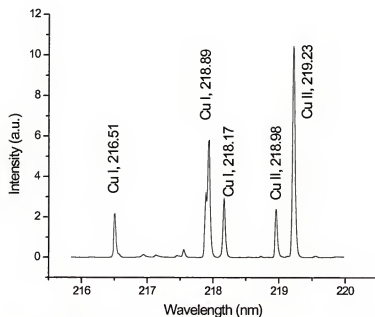


Figure 9-40. Pulsed glow discharge of a copper sample. Conditions:
1.4 kV, 6 torr.

CHAPTER 10

SUMMARY

The main focus of the dissertation research was the characterization of the microsecond pulsed glow discharge. The pulsed discharge creates an intense, time-dependent signal that is useful for both fundamental studies and analytical applications. The pulsed discharge has also shown great potential as an ion source for atomic mass spectrometry and a photon source for atomic emission spectroscopy.

A renewed interest in emission spectroscopy was developed during our studies due to its ability to provide a wide range of diagnostic information about the plasma behavior. Parametric studies were used to characterize the response of the pulsed plasma to the range of experimental conditions. The applied voltage and pressure were the two most important experimental parameters, influencing both the shape and intensity of emission. Pulse width and frequency were also performed. The parametric studies, coupled with sputtering rate and absorption data have characterized the removal of material by the pulsed discharge. Control of material removal is critical for thin layer analysis.

The temporal nature of the pulsed discharge has resulted in several analytical advantages. The higher voltages and currents applied to the discharge have transformed the relatively low power discharge into a highly energetic plasma with up to kilowatts of power. This energetic plasma has resulted in orders of magnitude

greater emission signal intensity. Resultant signal to noise and signal to background measurements have displayed considerable (up to three orders of magnitude) improvements as well. The temporal nature also allowed kinetic mechanisms of the discharge to be studied. Trends in the temporal profiles of atoms and ions of the sputtered and fill gas were linked to fundamental processes such as electron impact ionization and Penning ionization. The role of these fundamental processes could be further investigated based on the understanding gained from the parametric studies. Plasma diagnostic techniques were also employed to study the temperature of the plasma.

Though not in local thermal equilibrium, the plasma temperature measurements were used to probe fundamental processes. Results from using an electrostatic probe compared and contrasted the electron temperature and electron density in the dc and pulsed discharges. Rotational temperatures indicated a relationship between temperature and duty cycle in the μs pulsed, ms pulsed, and continuous operation of the discharge.

The μs pulsed glow discharge was also investigated as an ion source for mass spectrometry. The highly energetic pulsed plasma produced ion signals that were an order of magnitude or greater than when the discharge was operated in the continuous mode. The background and noise did not change between the two power modes, indicating the increased sensitivity of the pulsed source. In addition to greater signal intensity, a temporal separation between isobaric gas interferences and analyte signal was effected. Parametric studies were used to optimize this temporal separation and to determine the diffusion of ionic species within the discharge.

A laser was incorporated into a standard pulsed glow discharge in order to study laser – pulsed GD interactions. The ability of a focused laser to atomize a solid sample into a glow discharge for subsequent excitation by the pulsed discharge was demonstrated. This method was shown to be an effective means of determining the composition of a series of non-conductive materials. While the analytical utility of the combined source was not proven, results indicated that the signals obtained would be orders of magnitude more intense than if analyzed by employing an rf glow discharge. As a secondary excitation source, emission spectroscopy studies indicated the importance of asymmetric charge transfer in the pulsed discharge. Laser deposition experiments also indicated the sensitivity of pulsed discharge for very thin, nanometers to several atomic layers, layer analysis.

Glow discharges, while simple in appearance and easy to generate, are actually the result of complex plasma processes. Detailed parametric studies of the microsecond pulsed discharge have served to unravel some of the mysteries of this novel spectroscopic source. Characterization of the pulsed discharge with respect to emission spectroscopy, mass spectrometry, and laser interactions, has proven its capability as an atomization, excitation and ionization source for analytical spectroscopic analysis. The temporal nature of the pulsed discharge is important to study plasma mechanisms. Glow discharges, specifically high-power pulsed glow discharges, will continue to be a rich area of further research.

REFERENCES

1. Thompson, J.J. "Rays of Positive Electricity and Their Application to Chemical Analysis"; Longmans, Green: London, 1913.
2. Duan, Y.; Chamberlin, E. P.; Olivares, J. A. *Internat. J. Mass Spectr. Ion Proc.* **1997**, *161*, 27.
3. Westwood, W.D. *Progress in Surface Science* **1972**, *7*, 71.
4. Chapman, B. "Glow Discharge Processes"; Wiley: New York, 1980.
5. Marcus, R.K.; Harrison, W.W. *Anal. Chem.* **1987**, *59*, 236.
6. Stirling, A.J.; Westwood, W.D. *J. Phys. D.* **1971**, *4*, 246.
7. Chakrabarti, C.L. *Surf. Interf. Anal.* **1992**, *19*, 638.
8. Omenetto, N.; Smith, B.W.; Winefordner, J.D. *Spectrochim. Acta* **1988**, *43*, 1111.
9. Bengtson, A. *Spectrochim. Acta* **1991**, *40B*, 631.
10. Harrison, W.W.; Loving, J. *Anal. Chem.* **1983**, *54*, 1523.
11. Hess, K.R.; Marcus, K.R. *Spectroscopy* **1987**, *2*, 24.
12. Harrison, W.W.; Hang, W.; Yan, X.; Ingeneri, K.; Schilling, C. *J. Anal. At. Spectrom.* **1997**, *12*, 891.
13. "Glow Discharge Spectroscopies"; Marcus, R.K., Ed.; Plenum Press: New York, **1993**.
14. Bogaerts, A.; Gijbels, R.; Carman, R.J. *Spectrochim. Acta B* **1998**, *53*, 437.
15. Bogaerts, A.; Gijbels, R. *Phys. Rev. A* **1995**, *52*, 3743.

16. Laegreid, N.; Wehner, G.K. *J. Appl. Phys.* **1961**, 32, 365.
17. Bogaerts, A.; Gijbels, R. *Spectrochim. Acta B* **1998**, 53, 1.
18. Vriens, L. *Phys. Lett.* **1964**, 8, 260.
19. Penning, F.M. "Electrical Discharges in Gases"; Macmillan, New York, 1957.
20. Levy, M.K.; Serxner, D.; Angstadt, A.D.; Smith, R.L.; Hess, K.R. *Spectrochim. Acta B* **1991**, 46, 253.
21. Steers, E.B.M.; Fielding, R.J. *J. Anal. At. Spectrom.* **1987**, 2, 239.
22. Steers, E.B.M.; Leis, F. *Spectrochim. Acta B* **1991**, 46, 527.
23. Steers, E.B.M.; Thorne, A.P. *J. Anal. At. Spectrom.* **1993**, 8, 309.
24. Carman, R.J. *J. Phys. D* **1989**, 22, 55.
25. Hyman, H.A. *Phys. Rev. A* **1979**, 855.
26. Harrison, W.W.; Hang, W. *Fresenius J. Anal. Chem.* **1996**, 355, 803.
27. Westwood, W.D. *Prog. Surf. Sci.* **1976**, 71, 7.
28. Smith, B.W.; Womack, J.B.; Omenetto, N.; Winefordner, J.D. *Appl. Spec.* **1989**, 43(5), 873.
29. "Glow Discharge Optical Emission Spectrometry"; Payling, R.; Jones, D.; Bengtson, A., Eds; Wiley: West Sussex, 1997.
30. Watson, C.H.; Wronka, J.; Laukien, F.H.; Barshick, C.M.; Eyler, J.R. *Anal. Chem.* **1993**, 65, 2801.
31. Bogaerts, A.; Wagner, E.; Smith, B.W.; Winefordner, J.D.; Pollman, D.; Harrison, W.W.; Gijbels, R. *Spectrochim. Acta B* **1998**, 52, 205.
32. Dogan, M.; Laqua, K.; Massmann, H. *Spectrochim. Acta B* **1972**, 27, 65.
33. Milton, D.; Hutton, J.C. *Spectrochim. Acta B* **1993**, 48, 39.
34. Bogaerts, A.; Gijbels, R. *J. Anal. At. Spectrom.* **1996**, 11, 841.
35. Piepmeier, E.H.; de Galan, L. *Spectrochim. Acta B* **1975**, 30, 263.


36. Yang, C.; Ingeneri, K.; Harrison, W.W. *J. Anal. At. Spectrom.* **1999**, *14*, 693.
37. Mei, Y.; Harrison, W.W. *Spectrochim. Acta B* **1991**, *46*, 175.
38. Mei, Y.; Harrison, W.W. *Anal. Chem.* **1993**, *65*, 3337.
39. Hang, W.; Baker, C.; Smith, B.W.; Winefordner, J.D.; Harrison, W.W. *J. Anal. At. Spectrom.* **1997**, *12*, 143.
40. Yan, X.; Hang, W.; Smith, B.W.; Winefordner, J.D.; Harrison, W.W. *J. Anal. At. Spectrom.* **1998**, *13*, 1033.
41. Weide, J.O.; Parsons, M.L. *Anal. Lett.* **1972**, *5*, 363.
42. "Gaseous Conductors Theory and Engineering Applications"; Cobine, J.D., Ed.; Dover Publications: New York, 1941.
43. Harrison, W.W. "Treatise on Analytical Chemistry" Pt. 1, 2ed., *11*, Ch 3; Wiley: New York, 1989.
44. Pollmann, D.; Ingeneri, K.; Harrison, W.W. *J. Anal. At. Spectrom.* **1996**, *11*, 849.
45. Work in conjunction with Yan, X. Unpublished results, University of Florida, Gainesville, FL, 1997.
46. Work in conjunction with Yang, C. Unpublished results, University of Florida, Gainesville, FL, 1999.
47. Yang, C.; Ingeneri, K.; Mohill, M.; Harrison, W.W. *Anal. Chem.* **1999**, *71*, 5328.
48. Yan, X.; Harrison, W.W. *1998 Winter Plasma Conference on Plasma Spectrochemistry*, **1988**, Scottsdale, AZ.
49. Yan, X. Unpublished results, University of Florida, Gainesville, FL, 1997.
50. Walden, W.O. "Novel Spectroscopic Techniques Using the Pulsed Glow Discharge"; Dissertation, University of Florida, **1995**, 103.
51. Klingler, J.A.; Barshick, C.M.; Harrison, W.W. *Anal. Chem.* **1991**, *63*, 2571.
52. Oxley, E. Unpublished results, University of Florida, Gainesville, FL, 1999.
53. Harrison, W.W.; Magee, C.W. *Anal. Chem.* **1974**, *46*, 461.
54. Hieftje, G. *J. Anal. At. Spectrom.* **1980**, *11*, 613.

55. Hang, W.; Harrison, W.W. *J. Anal. At. Spectrom.* **1996**, *11*, 835.
56. Hang, W.; Yan, X.; Ingeneri, K.; Harrison, W.W. *Relative Sensitivity Factors of dc, rf, and Pulsed Glow Discharge Mass Spectrometry*, in preparation.
57. Vieth, W.; Huneke, J.C. *Spectrochim. Acta B* **1991**, *46*, 137.
58. King, F.L.; Harrison, W.W. "Glow Discharge Spectroscopies"; Marcus, R.K., Ed.; Plenum Press: New York, **1993**.
59. Rusak, D.A.; Castle, B.C.; Smith, B.W.; Winefordner, J.D. *Crit. Rev. Anal. Chem.* **1997**, *27(4)*, 257.
60. Bryden, W.A.; Benson, R.C.; Ecelberger, S.A.; Philips, T.E.; Cotter, R.J.; Feselau, C. *Johns Hopkins APL Technical Digest* **1995**, *16(3)*, 296.
61. Russo, R.E. *Appl. Spec.* **1995**, *49(9)*, 14A.
62. van Deijcke, W.; Balhe, J.; Maesser, F.J.M. *Spectrochim. Acta B* **1979**, *24*, 359.
63. Mitchell, P.G.; Sneddon J.; Radziemski, L.J. *Appl. Spec.* **1989**, *40*, 274.
64. Hess, K.; Harrison, W. W. "Lasers and Mass Spectrometry" Ch.. 9, Lubman, Ed.; Oxford University Press: New York, 1990.
65. Schelles, W.; DeGendt, S.; Muller, V.; Van Grieken, R. *Appl. Spec.* **1995**, *49*, 939.
66. Harville, T. "Glow Discharge Optical Emission Spectrometry" Ch. 11.8, Payling, Ed.; Wiley: New York, 1997.

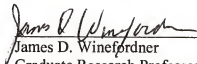
BIOGRAPHICAL SKETCH

Kristofor Ingeneri was born in Natick, MA, on March 26, 1972. As a resident of FL, he attended Keswick Christian High School, actively pursuing interests in science, art, philosophy, and athletics. In August, 1990, he enrolled at the University of South Florida, in Tampa, FL as a chemistry major. In May 1995 he received a bachelor of science degree with honors in chemistry. He continued his education in chemistry as part of the analytical chemistry division of the graduate program at the University of Florida, Gainesville. Under the direction of Dr. W. W. Harrison, he obtained the degree doctor of philosophy. After graduate school he accepted a postdoctoral position at Oak Ridge National Laboratory, Oak Ridge, TN.

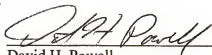
I certify that I have read this study and that in my opinion it conforms to acceptable standards of scholarly presentation and is fully adequate, in scope and quality, as a dissertation for the degree of Doctor of Philosophy.


Willard W. Harrison, Chair
Professor of Chemistry

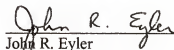
I certify that I have read this study and that in my opinion it conforms to acceptable standards of scholarly presentation and is fully adequate, in scope and quality, as a dissertation for the degree of Doctor of Philosophy.


James D. Winefordner
Graduate Research Professor of
Chemistry

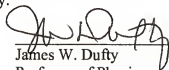
I certify that I have read this study and that in my opinion it conforms to acceptable standards of scholarly presentation and is fully adequate, in scope and quality, as a dissertation for the degree of Doctor of Philosophy.


David H. Powell
Scientist in Chemistry

I certify that I have read this study and that in my opinion it conforms to acceptable standards of scholarly presentation and is fully adequate, in scope and quality, as a dissertation for the degree of Doctor of Philosophy.


John R. Eyler
Professor of Chemistry

I certify that I have read this study and that in my opinion it conforms to acceptable standards of scholarly presentation and is fully adequate, in scope and quality, as a dissertation for the degree of Doctor of Philosophy.


James W. Dufty
Professor of Physics

This dissertation was submitted to the Graduate Faculty of the Department of Chemistry in the College of Liberal Arts and Sciences and to the Graduate School and was accepted as partial fulfillment of the requirements for the degree of Doctor of Philosophy.

May 2000

Dean, Graduate School